Rockefeller University
Digital Commons @ RU

Student Theses and Dissertations

1970

Variability in the Firing of Nerve Impulses in Eccentric Cells of the Limulus Eye

Robert Shapley

Follow this and additional works at: http://digitalcommons.rockefeller.edu/student_theses_and_dissertations

 Part of the Life Sciences Commons

Recommended Citation

Shapley, Robert, "Variability in the Firing of Nerve Impulses in Eccentric Cells of the Limulus Eye" (1970). *Student Theses and Dissertations.* Paper 41.

This Thesis is brought to you for free and open access by Digital Commons @ RU. It has been accepted for inclusion in Student Theses and Dissertations by an authorized administrator of Digital Commons @ RU. For more information, please contact mcsweej@mail.rockefeller.edu.

Variability in the Firing of Nerve Impulses in Eccentric Cells of the Limulus Eye

A thesis submitted to the Faculty of The Rockefeller University
in partial fulfillment of the requirements
for the degree of Doctor of Philosophy

by

Robert Shapley, A.B.
III

June 1970
The Rockefeller University
New York

PREFACE

In these troubled times I have been sustained in the conduct of my research by the friendship and commitment to excellence of many people at Rockefeller University. I am especially grateful to the members of the Hartline-Ratliff laboratory. H.K. Hartline and Floyd Ratliff contributed greatly to my development as a scientist, by example and instruction. Bruce Knight and Frederick Dodge inspired my thesis research and continuously aided its progress.

Maintenance of my rationality and enthusiasm would have been impossible without the care and affection of my wife Laurie.

Finally, I am grateful to Teresa Colaco for her expert help in the preparation of this thesis.

154923

SUMMARY

This thesis is concerned with the source and characteristics of variability in the discharge of impulses by neurons. The neuron in which variability was studied is the eccentric cell in the compound eye of the horseshoe crab, Limulus polyphemus.

In Part I a theory is presented which accounts for the variability in the response of an eccentric cell to light. The main idea of this theory is that the source of randomness in the impulse rate is "noise" in the generator potential. Another essential aspect of the theory is the view that the process which codes the generator potential into the impulse rate may be treated as a linear filter.

These ideas lead directly to Fourier analysis of the fluctuations of the generator potential and fluctuations of the impulse rate. Experimental verification of theoretical predictions was obtained by measurement of the fluctuations and calculation of their variance spectrum. The variance spectrum (or power spectrum) of the impulse rate is shown to be the filtered variance spectrum of the generator potential. Another verification of the theory is the finding that in many cells the signal-to-noise ratio is constant for responses to sinusoidally modulated light, at all modulation frequencies.

Inhibition from neighboring eccentric cells will have an effect on the variability of firing of a given eccentric cell. The effects of inhibition are discussed in Part II.

The reduction in the average impulse rate which is caused by inhibition decreases the variance of the impulse rate. However, this reduction of the average impulse rate increases the coefficient of variation of the impulse rate.

Inhibitory synaptic noise adds to the low frequency portion of the variance spectrum of the impulse rate. This occurs because of the

slow time course of the inhibitory synaptic potentials. As a consequence, inhibition decreases the signal-to-noise ratio for low frequency modulated stimuli.

The net effect of inhibition is to increase the coefficient of variation of the impulse rate. This effect is predicted by the linear model of the eccentric cell. The same qualitative effect is predicted by other theories of neuronal variability, although its importance is stressed here for the first time.

TABLE OF CONTENTS

Page

Page

Page

Chapter 1
INTRODUCTORY REVIEW

Variability of neuronal firing has been a subject of interest for neurophysiologists. Some degree of randomness in the maintained response of a neuron to steady stimulation is characteristic of all sensory neurons and neurons of vertebrate and invertebrate central nervous systems. Therefore, neural variability must affect the accuracy of signal transmission between neurons (Burns, 1968). Intermittent and irregular discharge of neurons when they are not being stimulated, so-called "spontaneous" activity, is also a common trait of many neuron types. The ubiquity of a random component in neuronal activity has led many investigators to propose models for neurons and neural networks based on the statistical characteristics of the variability in neural discharge. Thus, the study of neuronal fluctuations is significant because these fluctuations are widespread, may provide clues to the performance of an entire nervous system, and may also provide detailed understanding of the function of single neurons.

My dissertation is concerned with the random component of the maintained response of a type of sensory neuron, the eccentric cell in the eye of the horseshoe crab. An eccentric cell is a good neuron in which to study the source and characteristics of variability because there already exists a model for the activity of these cells based not on the fluctuations in the steady state but rather on the response of the neuron to time-varying stimulation. Instead of developing an _ad hoc_ model for variability, I am attempting to extend a theory which accounts for the dynamic response of the neuron. While in some systems this may not be a fruitful approach, it is useful in studying these _Limulus_ visual neurons. It focusses attention on the fact that the random component of the response is determined by the same mechanisms which affect neuronal response to time-varying stimuli.

The existence of several component mechanisms, and the possibility of measurement and control of their effects, is another feature of the

Limulus eye preparation which enhances its usefulness. For instance, it is possible to study how variability arises in a single sensory neuron, with the use of appropriate stimuli. By altering stimulus conditions, one can also investigate the effects of neural interaction, specifically lateral inhibition, on the variability of neural response. Thus, in a single neuron type, I have been able to probe two separate causes of neural variability and study their characteristics.

The details of the anatomy and physiology of the compound eye of the horseshoe crab have been extensively reviewed recently (Ratliff, 1965; Wolbarsht and Yeandle, 1967; Dodge, 1968). Rather than restate these reviews in summary form, I will refer them to the reader's attention and proceed to a more pertinent topic, namely a review of theories for neuronal randomness which have been proposed by other investigators. The latter topic has also been the subject of recent review (see Moore et al., 1966; Harmon and Lewis, 1966). However, consideration of these ideas about neuronal function may help to clarify what is different about my approach to the subject.

Models for Neuronal Variability: General Features

Whatever the specific details of a model for neuronal variability, it must possess a minimum number of features just to begin to account for the observed phenomena: a mechanism for the repetitive discharge of nerve impulses and a mechanism for the introduction of randomness into the discharge. The usual test of adequacy for these stochastic neural models is the degree of fit of model predictions with statistical measures of neural activity, e.g. the interval histogram. Rarely considered is the fact that the detailed characteristics of two models may be different yet they may both fit the same neural data. This would not be the case if there were sufficient experimental evidence to decide between theories, or if we understood the mechanism for repetitive neuronal discharge. In my work on Limulus eccentric cells I seek to overcome this difficulty by making measurements on the response of the cell to dynamic electrical stimulation. This measurement provides a fairly rigorous test of the theory for the

variability in the response of this cell, a subject discussed extensively in Part I.

Most models for neural variability propose that neurons possess a threshold for firing. According to such theories, a neuron discharges whenever the membrane potential of the neuron (or some function derived from the membrane potential) exceeds the level of the threshold. In these models the threshold need not be constant; for example, in the model of Geisler and Goldberg (1966) the threshold is a decaying function of time with an infinite initial value immediately after discharge of an impulse, and with a steady state value. Such a model is designed to account for the effect of refractoriness on the discharge of nerve impulses. Another feature which is present in many models is some assumption about a source of random fluctuation in the membrane potential. A common assumption about the source of noise is that it is caused by the summation of unit postsynaptic potentials which occur in a random, or quasi-random, manner. An example is Stein's so-called "exponential decay" model (Stein, 1967; the term "exponential decay" refers to the shape of postsynaptic potentials in Stein's theory). Opposed to this view are theories of neural variability which propose that variability results, not from random fluctuations of membrane potential, but from some degree of randomness within the mechanism which fires impulses (cf. table I in the review of Moore et al. (1966)).

The situation in the field of stochastic neural models is similar, in many ways, to the state of theories about neural excitability before the work of Hodgkin and Huxley. The "two factor" models of Rashevsky, Monnier and Hill were proposed to explain temporal summation of subthreshold stimuli, strength-duration curves, and accommodation in the axons of peripheral nerve (these theories are discussed and criticized in the monograph by Katz, 1939). These models involve a few simple variables like threshold, "local potential", and time constants for threshold and "local potential". While such theories are more primitive and less widely applicable than the later, well known formulation of Hodgkin and Huxley, they relate a wide range of observations on excitability to a small set of physiologically meaningful, theoretical parameters.

There is a striking formal similarity between these models for excitability in peripheral nerve axons and models for neuronal variability. Nevertheless, there are large differences in time scale, and also in the introduction of noise sources, in the latter class of models. The similarity exists because the present state of ignorance about details of the mechanisms which underlie repetitive neural activity is analogous to the ignorance in 1939 concerning the ionic mechanisms underlying neural excitability. The differences in time scale are introduced to account for phenomena in the repetitive discharge of impulses which last ten to a hundred times longer than the characteristic times of mechanisms underlying excitability in peripheral nerve.

Before concluding this overview of neuronal models, I will mention one idea about neuronal randomness which may be particularly significant. As mentioned before, several theorists propose that the ultimate source of fluctuations in neuronal activity is the random occurrence of synaptic potentials. These certainly cause the membrane potential of a neuron to vary in a more or less random manner. The random component of the membrane potential causes most of the variability of neuronal discharge, according to this view. My observations on Limulus eccentric cells support this idea. In eccentric cells, discrete potentials sum together to produce a fluctuating membrane potential. The discrete potentials are probably not synaptic in origin, but their random occurrence and temporal summation strongly resemble the process which causes "synaptic noise". As shown in Part I, there is good evidence that the fluctuations in membrane potential, caused by the summation of these randomly occurring discrete events, does cause the variability in the discharge of the eccentric cell.

The view of neuronal randomness as resulting from "synaptic noise" is significant for several reasons. First, it places the theory of neuronal variability within the larger framework of the theory of shot noise (shot noise is any stochastic process caused by superposition of randomly occurring discrete events, e.g. the voltage fluctuation in vacuum tubes;

cf. Rice, 1944). Second, it assigns an important role to the characteristics of unit synaptic potentials -- the statistics of their arrival, their magnitude and time course. The importance of "synaptic noise" also implies that variability is designed into a nervous system, because pulse frequency coding, convergence, and synaptic transmission have as a consequence the production of some amount of "synaptic noise".

Models for Neuronal Variability: Examples

This section is a discussion of specific neuronal models which illustrate the general points mentioned in the previous section. The reader may want to skip this material and proceed directly to the presentation of my own research in Part I.

Gerstein-Mandelbrot Model. The Gerstein-Mandelbrot model is one representative of that class of models which propose that "synaptic noise" causes neuronal variability (Gerstein and Mandelbrot, 1964). Actually, in their paper Gerstein and Mandelbrot present a few different models, but the one which they stress is their one-dimensional random walk model for a neuron. The other formulations they present are either too simple, being purely descriptive, or are unproductively complex considering the data they are seeking to explain.

The one dimensional random walk model includes the following assumptions. The electrical state of a neuron can be specified by a number, the state point. The state point moves from one value, the resting potential, to another value, the threshold. When the state point reaches the threshold an impulse is discharged. An excitatory or inhibitory synaptic potential moves the state point one step toward or away from threshold, respectively. After it reaches threshold the state point returns to the resting potential. In addition, the Gerstein-Mandelbrot model includes the assumption that each of the steps produced by a synaptic potential is small compared to the difference between threshold and resting potential; this allows treatment of the random walk as a diffusion process.

Gerstein and Mandelbrot devote some effort to the case in which the

rates of excitatory and inhibitory steps are equal. This is because, in this case, the impulse intervals possess a stable density function, i.e. a probability density function which does not change shape when convolved with itself. This may be a point of mathematical significance, but one with marginal physiological significance, since the particular stable distribution derived in this manner has infinite moments of all orders. The more realistic case is the one in which there is net excitation, so that the state point drifts towards threshold, on the average. This random walk with drift does not generate a stable interval density function (as defined above), but does provide a density function with finite moments which can be fit to physiological data. As in the random walk without drift, the interval density function is calculated in the diffusion limit in which the synaptic potentials are small compared to the difference between resting potential and threshold.

The Gerstein-Mandelbrot model yields an interval density function which does fit interval histograms obtained from neurons in the cat auditory pathway. The density function is characterized by two parameters: one corresponds to the difference between resting potential and threshold, the other is a measure of the net rate of drift of the state point, i.e. the difference between the rates of arrival of excitatory unit potentials and inhibitory unit potentials.

Some aspects of the Gerstein-Mandelbrot model have aroused criticism. For instance, Stevens (1964) criticized the allegedly unphysiological assumption in the model that the effect of a synaptic potential could persist indefinitely long while the state point returned instantaneously to the resting potential after reaching threshold. This objection is not so serious. It can be answered with the argument that the state point is not a measure of the membrane potential but rather corresponds to a quantity like the electric charge transported through the membrane. In other words the state point might be the integral of electric current flowing through the membrane. The latter idea corresponds to the model of impulse initiation

I employ to explain eccentric cell firing; it is discussed in the Theoretical Background chapters of Parts I and II.

A limitation of the Gerstein-Mandelbrot model is its restriction to the case of small synaptic potentials relative to threshold. In the case of larger synaptic potential/threshold ratios, the random walk model for purely excitatory input becomes simply a scaler for Poisson pulses (Barlow and Levick, 1969). The interval density function for a Poisson scaler is the gamma density function, a two parameter distribution of the form $\frac{1}{\tau S!}\left(\frac{t}{\tau}\right)^{S} e^{-t/\tau}$ with a time constant τ set by the rate of arrival of excitatory potentials, and a numerical parameter S equal to the ratio of the number of input synaptic potentials to the number of impulses fired. The extension of the Gerstein-Mandelbrot model to relatively larger synaptic potentials can also include the pooling models of ten Hoopen (1968) and Bishop et al. (1964), although in these latter models the statistics of synaptic potential arrivals are not Poisson statistics as they are for the Gerstein-Mandelbrot model or the Poisson scaler. Instead, the arrival rates are rather complex superpositions of many periodic processes or periodic processes superposed with Poisson processes. Nevertheless, although rather different in detail, they share with the Gerstein-Mandelbrot model a common attitude to the sources of neuronal variability. All these models assign a major role to "synaptic noise" as a determinant of neuronal variability.

The Geisler-Goldberg Model. This model is a modern version of models previously proposed by others, one with a noisy membrane potential and a time dependent threshold. The membrane potential is assumed to be a Gaussian process (of undetermined origin) with a bandwidth of 500 hz, a fixed variance, and a non-zero (but adjustable) average value. The threshold is a complicated function of time, being infinite after an impulse is discharged, and decaying to zero. At long times the decay of the threshold to zero is approximately exponential. Other very similar models propose that the threshold has the noise in it, and the membrane potential is constant (for instance, cf. Verveen and Derksen, 1961). The

predictions of Verveen and Derksen resemble those of Geisler and Goldberg, but would have different physiological implications since Verveen's model puts the noise in the impulse mechanism while Geisler places it in the membrane potential. Both are adequate models for the statistical characteristics they seek to explain.

A very significant finding from this type of model is that a single parameter is sufficient to describe the variance and shape of the interval density function over all states of excitatory drive, for some sensory neurons. Geisler and Goldberg show this by fitting the parameters of the model to the statistics of the response to one stimulus, and then merely varying the constant value of the membrane potential to fit the statistics of responses to all other stimuli. They perform this for neurons of the superior olivary complex (third or fourth order auditory neurons). They can also match the relation between standard deviation of impulse intervals and mean interval, for data from chemoreceptor neurons and muscle spindle afferents, with adjustment of the same parameter, the average level of the membrane potential. While a very important finding, such a model would not be adequate to explain the behavior of variability in all sensory neurons. For instance, in the Limulus eccentric cell, among other features which differ from the predictions of this model, the standard deviation of its membrane potential depends on the intensity of the light stimulus (Dodge, Knight and Toyoda, 1968b). Therefore, in these cells, not just the mean level of the membrane potential changes with intensity of stimulus. Also, as shown extensively in Part I, the spectral character of the noise in the model of Geisler and Goldberg is not correct for eccentric cells and the effect of the difference in the spectrum is not negligible. Nevertheless, the model of Geisler and Goldberg is widely applicable to other sensory neurons.

Geisler and Goldberg also extend their model to explain negative serial correlation of intervals. They do this by introducing into their model a prolonged hyperpolarization of the membrane following each impulse discharge. The resemblance of this feature in their extended model to self-inhibition in the Limulus eccentric cell model is very striking; I will return to this topic in the Discussion of Part I.

Calvin-Stevens Model. Although it is not very different from the previously mentioned theories of neuronal variability, the model of Calvin and Stevens (1968) is important because of its correlation with detailed intracellular measurements of neuronal properties. Calvin and Stevens recorded the membrane potential of motoneurons in the spinal cord of the cat. They observed and measured the statistics of spontaneous or electrically driven discharge. Then they attempted to explain the observed impulse interval variability in terms of the properties of the recorded "synaptic noise" and observed properties of the impulse firing mechanism.

The Calvin-Stevens model is basically the same as a model Stevens suggested as a more physiological replacement for the Gerstein-Mandelbrot model (Stevens, 1964). In Stevens' formulation one part of the membrane potential is the integral of the constant component of the excitatory current. This accounts for the ramp-like climb of the membrane potential to the firing threshold. Added to the ramp component of the membrane potential is the "synaptic noise" component of the excitatory current. Calvin and Stevens do not explicitly attempt to justify the completely different treatment of the constant and noisy components of input to the neuron, although it is not clear why they should be different.

In the experiments of Calvin and Stevens, the cats were spinal or anesthetized. With these conditions, the "synaptic noise" in motoneurons was a Gaussian process with a bandwidth of approximately 40 hz. Different experimental conditions might easily change the statistics of the "synaptic noise".

The Calvin-Stevens model adequately predicts the shape (Gaussian) and parameters (mean, variance) of the interval distribution functions in most cases. This is a rigorous fit of prediction to data, to an extent that the previously mentioned models could not reach. The reason is the greater detail of experimental measurement rather than any novelty in the theoretical method.

Junge-Moore Model. Junge and Moore (1966) also have tried to augment theories of neuronal variability with the greater detail of intracellular measurement. They recorded the fluctuations of impulse firing in

Aplysia giant neurons and correlated the observations with a new model of variability. Although this model includes the standard features of a membrane potential climbing to an asymptotic level, and causing an impulse to fire when it reaches a threshold level, it includes a novel source of randomness which sets it apart from the other theories of neuronal variability. Junge and Moore propose that the important feature in variability is the discrete resetting of the asymptotic level towards which the membrane climbs after each action potential. They propose that the reset value is a random variable, and that it is reset independently of the previous history of the neuron. They base this model on observations from some Aplysia neurons. By adjustment of the statistics of the reset value they can fit the interval histograms measured in several Aplysia giant neurons.

The Junge-Moore model places the source of neuronal variability in the resetting of the membrane potential; this emphasizes the role of the impulse firing mechanism rather than membrane potential fluctuations. The emphasis on the impulse firing mechanism may be appropriate for the Aplysia neurons they studied, since their published records reveal negligible fluctuations of the membrane potential. However, such a theory probably is not appropriate for all Aplysia neurons (cf. records of Aplysia neurons in Bullock and Horridge, 1965) or for many other neuron types. To take just one example, it certainly is not pertinent to mammalian motoneurons, as Calvin and Stevens (1968) have shown.

The introduction of variability at each impulse in the Junge-Moore model suggests another model for neuronal variability as an extension of the theory of Junge and Moore. This would be a discrete Markov process, where the length of each interval influenced the probable length of the next interval, independent of the previous history of the neuron. Such a model, also known as a discrete first-order autoregressive process (Jenkins and Watts, 1968, p. 162) would predict a set of monotonically decreasing positive correlation-coefficients if intervals were positively correlated, and a set of alternately negative and positive correlation coefficients, decreasing in magnitude, if adjacent intervals were negatively correlated. This would be the case because, for such a process, the nth correlation coefficient would be the first correlation coefficient

raised to the nth power. The interval histogram could be fit as in the model of Junge and Moore, by choice of a distribution for the asymptotic value of the membrane potential.

The autoregressive process has been proposed, but not shown to be adequate to explain neural variability in any neuron type (Wallø, 1968); it is mentioned again in the Discussion of Part I. Another weakness of this model is that it is purely phenomenological -- no mechanism has been suggested to account for the correlation of adjacent intervals independent of all others. The same weakness applies to the Junge-Moore model and, to some extent, to models of the Geisler-Goldberg type, since these models propose sources of variability which are not explained by any mechanism intrinsic to the model.

PART I

VARIABILITY IN A SINGLE SENSORY NEURON, THE ECCENTRIC CELL

PART I

INTRODUCTION

Randomness is an outstanding aspect of the activity of many neurons. Neurons in central nervous systems of vertebrates and invertebrates often fire impulses spontaneously and, to some extent, randomly. When they are driven by sensory nerves or other cells of the central nervous system, their activity remains variable, although it reflects net average excitation or inhibition. Fluctuations in activity or responsiveness are not confined to cells in the central nervous system. Numerous investigators have studied fluctuations in the maintained response of primary sensory neurons -- cells which do not receive convergent input from other neurons (frog muscle spindle, Buller et al., 1953; Limulus visual cells, Ratliff et al., 1968; cat auditory nerve, Kiang, 1965; mammalian cutaneous mechanoreceptors, Werner and Mountcastle, 1965; cat muscle spindle, Stein and Matthews, 1965; cat chemoreceptors, Biscoe and Taylor, 1963). The sources of variability in primary sensory nerve cells may not be the same, in detail, as those causing variability in the firing of neurons in the central nervous system. However, because such neurons are more susceptible to experimental control, they are more suitable for quantitative study than the richly interconnected central neurons. It is widely believed that fluctuations of a neuron's membrane potential causes variability in its impulse firing. In sensory neurons the source of fluctuation in the membrane potential is probably not the same as it is in central neurons. However, the coding of stochastic voltage into fluctuating impulse firing can be studied in peripheral neurons and the results generalized to nerve cells of the central nervous system where the sources of voltage fluctuations are different but the coding itself is likely to be similar.

I have studied the way randomness arises in the maintained response to light of eccentric cells in the compound eye of the horseshoe crab. The axons of the eccentric cells gather to form the Limulus optic nerve. As far as we know, these are the only cells in the compound eye

which respond to light by firing nerve impulses (Waterman and Wiersma, 1954; Purple, 1964; Behrens and Wulff, 1965). Hartline and his colleagues have attempted to understand the physiology of these cells in quantitative terms: the intensity-response function, dark adaptation as a function of time, the steady state interaction of excitation and lateral inhibition, the generator potential underlying nerve impulse firing, and the transient responses to increments of excitation or inhibition (Hartline and Graham, 1932; Hartline and McDonald, 1947; Hartline and Ratliff, 1957; Hartline, Wagner and MacNichol, 1952; Lange, Hartline and Ratliff, 1965). Intrinsic to this approach is a desire to understand cellular mechanisms which are the basis for visual sensitivity and the shaping effects of inhibition.

Recently, study of the frequency response to modulated stimuli has provided a more detailed picture of cellular mechanisms in the Limulus eye (Dodge, Knight and Toyoda, 1968b). Particularly relevant to the present study is the use of linear systems analysis by Dodge et al. to study the impulse firing mechanism of the eccentric cell.

Because the impulse firing mechanism can be treated as a linear filter for modulated stimuli, I have used the theory for the linear filtering of stochastic processes to explain steady state fluctuations in the impulse rate. I wanted to show that the randomness in the generator potential, ultimately the result of randomness in photon arrival and absorption, was responsible for the impulse rate fluctuations. This hypothesis was based on the experiments of Ratliff, Hartline and Lange (1968). Their work implied that the impulse firing mechanism itself does not add much randomness to the firing rate. They found that the variance in the steady state firing rate in response to electrical stimulation is about an order of magnitude smaller than the variance of the response to stimulation by light.

Part I of this thesis deals with maintained responses to illumination of single ommatidia. This enables the study of effects due to excitation alone. In Part II I will report what happens to variability in nerve firing when light stimuli excite many interacting nerve cells in

the Limulus eye. Under the latter, more complicated conditions, lateral inhibition produces changes in the pattern of firing rate fluctuations. However, in order to understand the effects of interaction, you must consider first the simpler problem of purely excitatory stimuli.

Chapter 2

EXPERIMENTAL METHODS: MEASUREMENTS

The experiments required diverse electrophysiological techniques and a significant amount of data processing. I used methods of nerve fiber recording and intracellular recording from cells in the horseshoe crab compound eye, techniques of measurement used by others who were interested in different questions (for example, Ratliff, Hartline and Miller, 1963; Fuortes, 1959; Lange, 1965; Dodge, Knight and Toyoda, 1968a; Ratliff, Hartline and Lange, 1968).

The study of fluctuations in firing rate required innovations in analysis of the data -- specifically, relating the voltage input noise to the variations in neuronal firing rate. There were also the usual problems of statistical analysis: departures from stationarity, and slow trends in the data (discussed in Appendix I). In this chapter I will discuss the experimental methods, and then data processing. In the next chapter I will present the methods of analysis with some reference to the technique of spectral analysis applied to random processes.

The Biological Preparation

This work was done on excised lateral eyes of the horseshoe crab Limulus polyphemus. For intracellular recording, the eye was sliced in half with a razor blade. The slice was parallel to the long axis of the eye and perpendicular to the surface of the eye. The sliced eye formed the fourth wall of a three sided plexiglass chamber; it was sealed into place with beeswax. The chamber was filled with artificial sea water. For experiments on generator potentials, the impulse firing mechanism was poisoned by adding 10^{-6} M tetrodotoxin to the sea water.

The fundamental experiment of this dissertation was performed with a micropipette as intracellular recording probe and current stimulator. The methods of this experiment were pioneered by Hartline, Wagner

and MacNichol (1952) and MacNichol (1956). Micropipettes were made from glass capillary tubing which had been heated to melting and then pulled strongly to produce a fine point of diameter 500 nm. more or less. Micropipettes were filled with a conducting solution, 3 molar potassium chloride in most of these experiments. Such micropipettes were high impedance devices; they had a resistance of 10-20 Megohms measured in sea water.

Signals were passed from the micropipette probe to a unity gain negative capacitance bridge amplifier designed by Mr. John Hervey and built by the Rockefeller University Electronics Shop. This amplifier has been described by Purple (1964). Some of its features were particularly useful in these experiments. First, the intrinsic noise of the amplifier is low, about forty microvolts r.m.s. noise with short-circuited input and 5 KC bandwidth. Second, the bridge circuit allows resistance measurement and current stimulation with imposed external waveforms. Third, the amplifier itself can act as a constant current source. Finally, calibration and bucking voltage controls make it convenient for accurate resting membrane potential and generator potential measurements.

Nerve fiber recording was done using standard techniques. Bundles of nerve fibers were teased from the Limulus optic nerve with glass needles and dissected until a single active fiber was present on the recording electrode. A preamplifier (Tektronix 122) provided a gain of one thousand. In the experiments on nerve fiber responses, the eye was removed from the animal with one to five centimeters of optic nerve, and mounted as above.

Action potentials and/or slow potentials were fed to a Tektronix 502A oscilloscope. The vertical signal output from the oscilloscope was monitored on a loudspeaker. The output of the oscilloscope was fed into a CDC 160-A digital computer in a manner described below. When on-line acquisition was impractical, impulses and slow potentials were recorded on a 7-channel FM tape recorder (Sanborn Division, Hewlett Packard, Model 2000). At a later time tape recorded data were played back into the oscilloscope and passed to the computer.

Stimulus and Stimulus Control

Two sets of stimulus conditions were established. First, different time-varying waveforms were used to modulate the light intensity illuminating an eccentric cell or the current that was directly driving the cell. Second, under conditions of steady stimulation the interval between stimuli had to be the same throughout the experiment. The second stimulus regime was required because statistical measures were obtained by averaging several responses to identical stimuli. The responses would be statistically the same only if the cell were in the same adaptation state at the onset of each stimulus presentation. In addition, the computer required signals to mark the start of an experimental run and its termination, and the computer also needed a clock so that it could count clock cycles between nerve impulses.

In order to do these things I used an experimental set-up developed by and for Dr. Frederick Dodge for previous experiments. The stimulus waveform was generated by adding together constant voltages with time-varying voltages generated by a waveform generator (Hewlett-Packard 3300A or, Wavetek). The various stimulus options are shown in Figure 2-1. For current stimulation the summed voltage was led directly to the bridge stimulus input of the bridge amplifier. For light stimulation, the summed voltage was first fed to a voltage-to-frequency converter with center frequency adjusted to 400 hz.

The output of the voltage-to-frequency converter triggered a pulse generator (Tektronix 161) which then triggered a glow modulator driver, designed by Mr. Michael Rosetto of the Rockefeller University Electronics Shop. The glow modulator driver provided pulses of constant current, adjustable from 8 to 30 ma., to drive a glow modulator tube (Sylvania R1131C). Since the color of the glow tube is set by the current, driving it with pulse frequency modulation of constant current pulses enables you to obtain large modulation depths without color changes in the tube output.

The light stimulus was brought to single ommatidia of the compound eye via light guides. The light guides (American Optical Co.) were made from glass fibers with a diameter of 30 , strengthened and protected by hypodermic tubing. The use of light guides for isolated optical stimulation of single photoreceptors was developed by Robert Barlow (1966, 1969). The single light guide was mounted on a mechanical

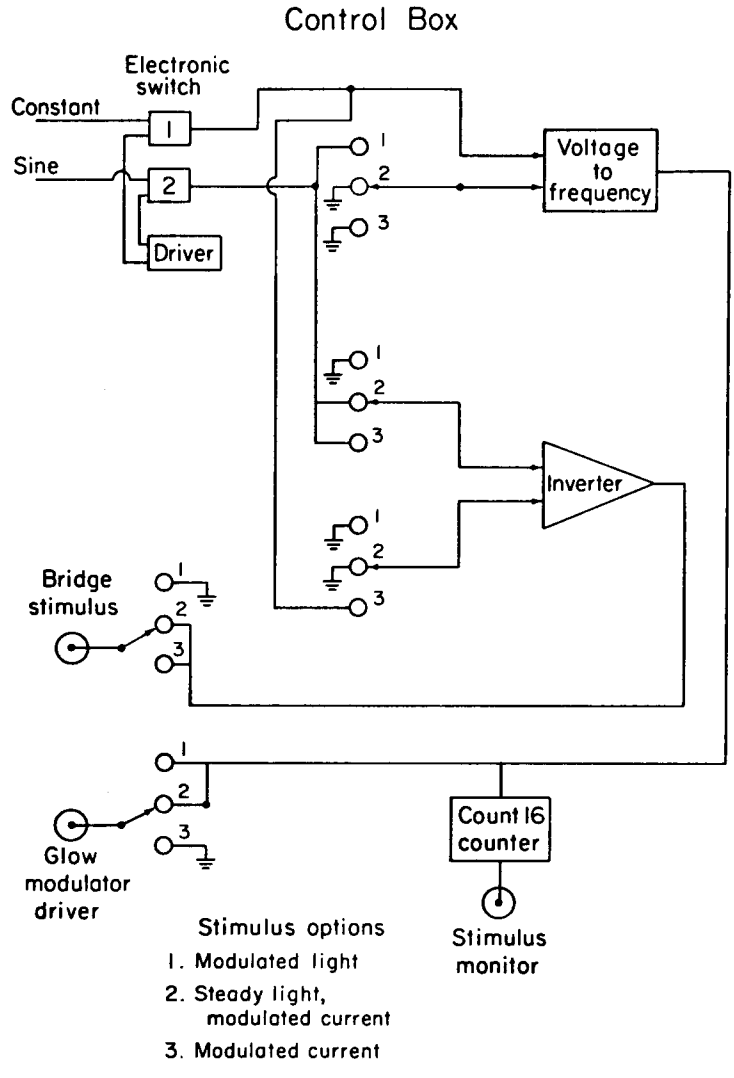

Figure 2-1. Control Box. This device controls the type of stimulus applied to the neuron. Two electronic switches, numbered 1 and 2, apply a constant voltage and a sine (or some other modulated input) to other points in the circuit. An external switch allows selections of three stimulus options, numbered 1, 2, 3 in the figure. In position 1, the control box will cause the glow modulator tube to produce modulated light. In switch position 2, the glow tube will produce steady light, while a sinusoidal current is passed to the bridge amplifier and thence to the neuron through an intracellular micropipette. In switch position 3, the current led to the pipette is the sum of the constant voltage and the sinusoidal voltage, and no light stimulus is produced.

pantagraph manipulator (R. Barlow, 1969) which enabled accurate location of the optimal stimulus direction and position.

In some experiments a steady light and a sinusoidal current were applied simultaneously to the same cell in order to modulate the activity of the cell around a level of excitation produced by the natural stimulus. For such experiments a constant voltage was passed through the voltage-to-frequency converter and via the pathway described above to the glow modulator light source. A time-varying voltage, typically a sine-wave, was led to the bridge amplifier stimulus input (cf. Figure 2-1), and thence to the microelectrode.

In order to control the timing of experimental runs and provide electronic gating and clock signals for on-line computer data acquisition, I used a programmed timer built by Mr. Willard Friedman and Mr. Norman Milkman in the Rockefeller University Electronics Laboratory. This device is a modified version of the programmed timer which was constructed by Milkman and the Rockefeller University Electronics Laboratory for Hartline's laboratory (Lange, 1965; Schoenfeld and Milkman, 1964). The programmed timer provided an input/output (I/O) gate signal which is used to alert the computer. The I/O gate was programmable, i.e. its time of onset and duration could be determined by the experimenter. The timer also provided the 5 KC clock rate the computer used in the data acquisition program.

Seven additional programmable gates were available in the programmed timer to turn stimuli on and off in a prescribed sequence. The I/O gate and stimulus gates were each controlled by two three-decade switches which determined the beginning and end of each particular gate. Each gate was assigned a set of output lines by means of a matrix plugboard (like the one discussed in Schoenfeld and Milkman, 1964).

An example of gate length control and output line assignments is illustrated in Figure 2-2. Here Gate 1 is eighteen seconds long, begins two seconds after the I/O Gate and terminates at the same time as the I/O Gate. Gates 2 through 7 are unused. Gate 1 is connected to output lines 3 and 5 through the plugboard so both these output lines are on for ten seconds starting two seconds after the I/O Gate.

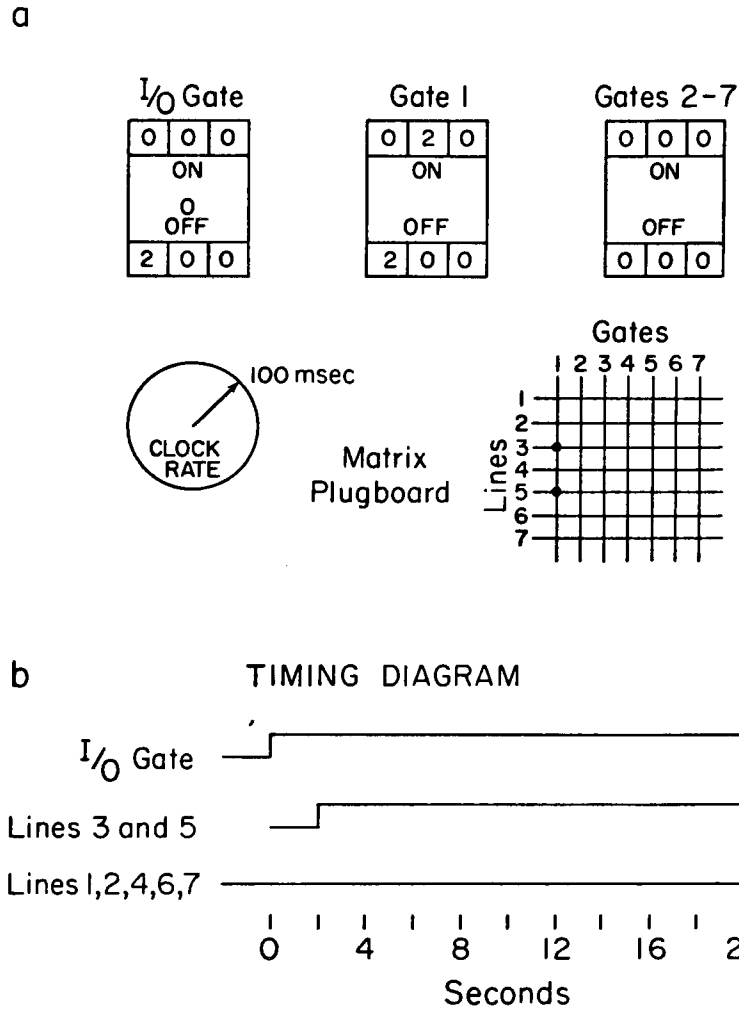

Figure 2-2. Programmed Timer. (a) The three decade switches control onset and ending of the gate signals connected to those switches. The numbers are in terms of the unit clock cycle, which is set by the "clock rate" switch. The programmable gates control output lines by means of linkage through the matrix plugboard. As indicated in the figure, output lines 3 and 5 go on and off at the times indicated for GATE 1, because they are connected to it through the matrix plugboard. The I/O Gate goes directly out on a special line and is not controlled by the matrix plugboard. (b) The sequence of control signals determined by the timer configuration in (a). Deflection up denotes "on".

The programmed timer also controlled the repetition rate of stimulus presentations. This was done by setting the experimental episode length to some value and running the timer in Continuous mode. In this mode of action, the timer repeated the experimental episode again and again. A fraction of the experimental episode was occupied by the stimulus and during the remaining portion of the episode the preparation recovered from the effects of stimulation. The eye was thus kept at a constant adaptation level. In this way I sought to preserve stationarity of response from one stimulus presentation to the next.

Data Processing

Having described the experimental probes and stimuli, I will now discuss data acquisition and analysis which are essential to the investigation of impulse firing statistics. The general data acquisition program, written for the CDC 160A computer by H.K. Hartline, Norman Milkman and David Lange, performed four functionswhich were particularly important for my experiments. First, the program measured time between pulse events on three separate data channels. Second, it sampled one voltage channel by means of an analogue to digital converter and stored the values of the voltage in memory. These two functions performed on line took, on the average, a little less than 0.2 milliseconds. Third, at the end of each experimental run the program stored time interval data and voltage data on magnetic tape in a format compatible with FORTRAN magnetic tape subroutines (so that they would be accessible to analysis programs written in FORTRAN). Fourth, the program typed an experimental protocol and plotted one channel of pulse rate data and the single voltage channel data on a digital plotter (CalComp). The experimental plots were graphs of the data stored on tape and were valuable for monitoring an experiment in progress.

Because the storage capacity of the computer is not infinite, some compromises had to be adopted in the data acquisition program. It was decided that the experimental run should be twenty seconds long and the sampling rate for the voltage channel was 50 hz. These values were chosen because a twenty second stimulus is sufficiently long for a Limulus visual cell to reach steady state, and the voltage fluctuation spectrum is contained within a 25 hz bandwidth.

Measurement of time intervals on three parallel channels was accomplished by means of external electronic logic which is interfaced to the computer. Nerve impulses triggered discriminators which produced standard shaped pulses of controllable width. The electronic logic produced a twelve digit binary number synchronized with each clock cycle of the programmed timer. The appearance of a 1 in each bit position of this number was contingent on whether a discriminator pulse had occurred during that clock cycle on the channel assigned to that bit position. The computer sensed whether the number produced by the above device was non-zero, i.e. whether a pulse had occurred on any channel; if it was non-zero the number was stored in the computer memory. During every clock cycle the program incremented a running counter by one and each time an event; i.e. a non-zero word, occurred, the accumulated count was stored in memory. This procedure produced two lists in the computer memory, one of event types and another of event times. From these two lists it was possible to unravel the list of time intervals between events on each of many channels. The data acquisition program and hardware used in these experiments could handle three channels simultaneously. In my experiments one channel was the nerve impulse channel. The second channel carried phasing pulses to monitor phase of modulated stimuli. The third channel was used to measure relative modulation of the stimulus.

The resolution of this measurement of time intervals was 0.2 msec, the length of the clock cycle. This was one per cent accuracy for a firing rate of fifty impulses/sec, one half per cent accuracy for a firing rate of twenty five impulses/sec.

Chapter 3

ANALYTICAL METHODS

Impulse Rate

The primary data for the experiments on impulse firing are intervals between impulses. These time intervals were measured on-line with a digital computer, as previously described. Since the neurons under study fire fairly regularly, nerve impulses were separated by approximately evenly spaced intervals of time. All the information about fluctuations is contained in the departure from strictly regular firing.

One way to study the characteristics of these fluctuations is to convert the list of pulse intervals into a list of instantaneous impulse rate samples. As shown below, in the case of regularly firing neurons, important statistical parameters for the impulse rate variable are the same as for the impulse intervals. The reason for using the pulse rate, rather than interpulse interval, as a measure of neural activity is that the rate is a more direct measure of the level of excitation of the neuron than the interval. Subsequent analysis and results will reveal that the choice of pulse rate allows us to connect membrane potential with neural activity in a straightforward way.

The first method that requires explanation is the construction of "instantaneous" pulse rate from pulse intervals. The algorithm is illustrated in Figure 3-1. For any particular interval between pulses, the reciprocal of the time interval, the impulse rate, is assigned to all the time between the beginning and end of the interval. In effect, in constructing the impulse rate, one is transforming a frequency modulation into an amplitude modulation. The reciprocal of the time interval, the instantaneous pulse rate, is larger when the firing is faster and smaller when firing is slower. In fact, as MacNichol (1956) showed, impulse rate is proportional to cell membrane depolarization in Limulus eccentric cells.

If the instantaneous impulse rate is sampled at equi-spaced inter-

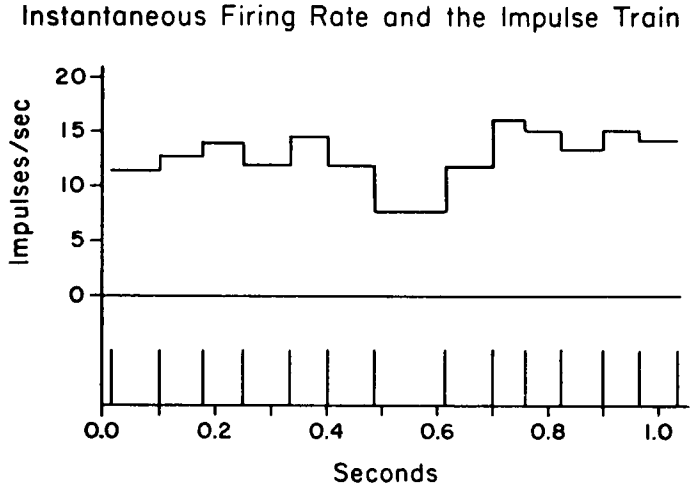

Figure 3-1. Instantaneous Firing Rate and the Impulse Train. The computation of impulse rate is demonstrated in this picture. During the interval between two pulses the impulse rate equals the reciprocal of that interval. The pulse train and the firing rate are plotted on the same time scale. The pulse train in this picture is from an eccentric cell.

vals of time, one obtains a list of pulse rate samples which can be mathematically manipulated in the same way as periodically sampled continuous functions (one might expect discontinuities in the firing rate at instants when impulses are fired; discontinuities are eliminated by averaging the instantaneous rate before and after an impulse discharge, to obtain a value of the impulse rate for those sampling intervals in which an impulse has occurred). If the "sampling" intervals are a fine enough time mesh, a negligible amount of information about the statistics of the pulse train will be lost. To be fine enough the sampling time increment ought to be less than half the length of the average interspike interval, a limit consistent with the sampling theorem (see Shannon and Weaver, 1949, p. 53 for a discussion of the sampling theorem).

The method for instantaneous pulse rate calculation was developed by Hartline and Ratliff, originally for averaging responses to similar stimuli over identical time periods. In cases where fluctuation in the maintained impulse rate is not relevant to the problem, the rate of sampling can be slower; averaging experimental runs with the choice of a sampling rate slow compared to the average impulse rate corresponds to the construction of a post-stimulus time histogram (cf. Moore et al., 1966) but with greater accuracy in that fractions of a pulse interval are included in the bin count. The usefulness of this method is discussed by Lange (1965) and Bicking (1965).

I wish to propose the introduction of a new unit to replace "impulses per second". This should be done in order to clarify the conception of modulation frequency of the impulse rate, which arises in the Fourier analysis of neuronal firing. The unit is named after E.D. Adrian, who discovered neural pulse frequency coding. One adrian equals one impulse/second. I shall use this unit in some of my figures, principally those illustrating spectral analysis of the impulse rate.

Spectral Analysis

Spectral analysis is an analytical tool developed to help understanding of the filtering of signals by linear, time invariant devices. It has been applied in communication theory to the problem of filtering of stochastic processes (Parzen, 1962).

A linear filter is a device which obeys the law of superposition. This means that if the filter produces an output $y_1(t)$ for an input $x_1(t)$, and an output $y_2(t)$ for an input of $x_2(t)$, then it will produce the output $a y_1(t) + b y_2(t)$ when the input is $a x_1(t) + b x_2(t)$. A linear filter is time invariant if translating the input signal in time merely results in a translation of the output signal by the same amount in time, i.e. if input $x(t)$ elicits an output $y(t)$, then the input $x(t+\tau)$ will elicit the output $y(t+\tau)$.

Sines and cosines are merely changed in amplitude and phase when passed through a linear time invariant filter. This scaling property can be shown most easily using the complex exponential $e^{i\omega t}$ which is the linear combination $\cos \omega t + i \sin \omega t$; after it is shown that the complex exponential has this property you can prove it for sine and cosine functions by taking the difference and sum of positive and negative complex exponentials.

Suppose an input to a linear filter is $x(t) = e^{i\omega t}$. Then the time translated input is $x(t+\tau) = e^{i\omega(t+\tau)} = e^{i\omega\tau} x(t)$; this can be written $a\,x(t)$ where $a = e^{i\omega\tau}$ is independent of t. The output $y(t+\tau)$ must obey the equation $y(t+\tau) = a\,y(t)$ because the filter is linear. To show that the functional form of the output $y(t)$ is a complex exponential, the same as the input, you then set $t = 0$, implying $y(\tau) = y(0) e^{i\omega\tau}$. Thus, the output function is merely the input function multiplied by a constant (a complex number). If an input function has this property, it is called a characteristic function of the filter. Sine functions, complex exponentials and real exponentials are the characteristic functions of time invariant linear filters.

Given any time-invariant linear filter, you can characterize it by specifying the response to a unit amplitude sinusoidal signal at each frequency. The function which relates the amplitude and phase of the output to the modulation frequency is called the frequency response. As an example, one can measure the amplitude filter characteristics of an optical filter by measuring its frequency response with many different monochromatic lights.

It is possible to express any continuous, deterministic function of time as a weighted sum of sinusoidal functions of time. This is shown in Figure 3-2. The decomposition of a function into its sinusoidal components is called Fourier analysis or spectral analysis of the function. The operation of a filter on an input function can be expressed as the separate multiplication of each of the weighted sines in the sum, which represents the input function, by the appropriate value of the frequency response.

For random processes a similar theory can be developed (cf. Bartlett, 1955; Parzen, 1962). A stochastic process is an ensemble of time functions which have some average properties in common but which cannot be determined exactly as a function of time. In an experimental context, this ensemble is composed of the group of noisy records which are measurements of the stochastic process.

One average property of a stochastic process is its autocovariance. The autocovariance is defined as the average product of the deviation of a random variable from its mean, multiplied by the value of the deviation later in time. For the stochastic process $n(t)$ with mean value $\bar{n}$, the autocovariance is defined as $\overline{(n(t)-\bar{n})(n(t+\tau)-\bar{n})}$. The autocovariance is a continuous, deterministic function of time; it depends on the time lag τ, the lag between the two random variables in the product. The autocovariance is a measure of how rapidly the stochastic process fluctuates around its average value. The value of the autocovariance at zero time lag is the variance of the stochastic process, i.e. $\overline{(n(t)-\bar{n})^2}$.

The autocovariance of a stochastic process can be represented as a weighted sum of sinusoidal functions, since it is a deterministic function of time. The value of the weighting factors in the sum representing the autocovariance is what I call the variance spectrum. This name is appropriate because the value of the variance spectrum at a particular frequency represents the contribution of that frequency to the total variance of the stochastic process. Spectral analysis of stochastic processes was applied first to electrical signals for which variance means power, and so what I call the variance spectrum is more commonly referred

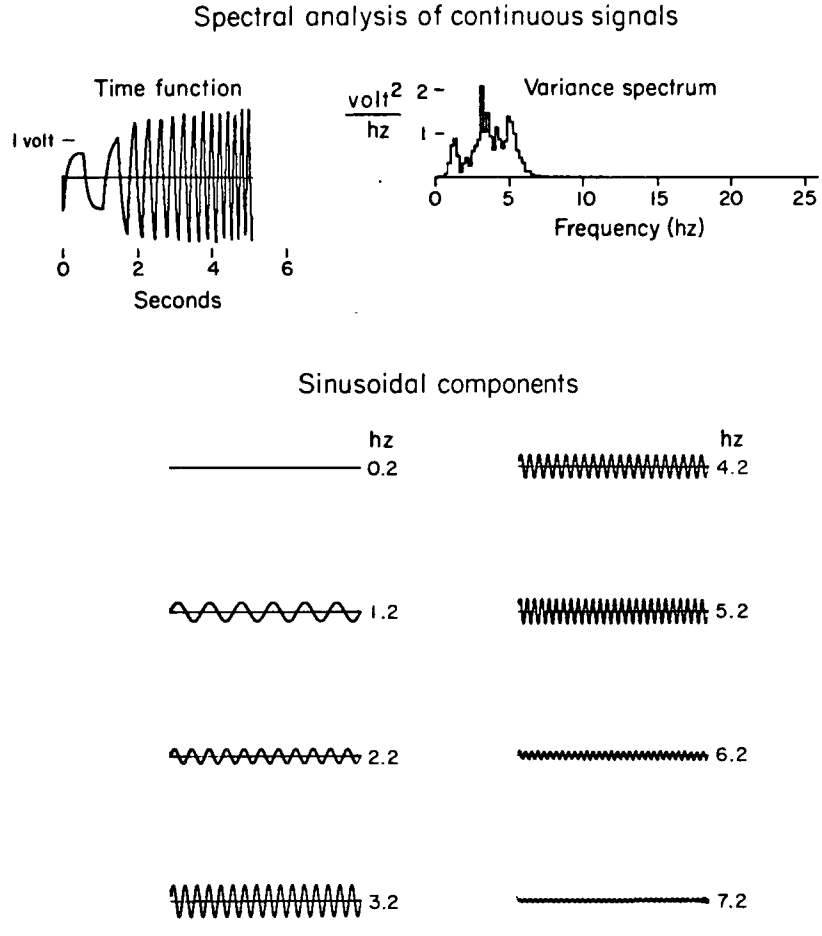

Figure 3-2. Spectral Analysis of Continuous Signals. An arbitrary deterministic signal is shown with the sine waves which sum to form it. The relative strength of each sine wave in the sum is shown in the variance spectrum. The variance spectrum is the squared amplitude of each sinusoidal component, as a function of frequency.

to as the power spectrum.

The variance spectrum of a stochastic process can also be calculated from direct Fourier analysis of the individual time functions which are members of the ensemble of functions which constitute the stochastic process. The squared amplitudes of the sinusoidal components must be averaged from many members of the ensemble to obtain the variance spectrum. It is a theorem that the variance spectrum computed in this manner is equal to the variance spectrum calculated from Fourier analysis of the autocovariance (Bartlett, 1955, pp. 159-166).

The function which relates the variance (power) spectrum of a stochastic process put into a linear filter to the spectrum of the output stochastic process is usually called the power transfer function of the filter (using my terminology it ought to be called the variance transfer function). It is the squared absolute value of the frequency response of the filter.

Spectral analysis is often performed on continuous functions of time which have been sampled at equally spaced points in time (Cooley, Lewis and Welch, 1967). This procedure generates a list of numbers which are the values of the continuous function at the sample times. You compute the variance spectrum of this list of numbers in the following way. First you perform a Fourier analysis of the list; this is done by digital computer with subroutines incorporating the Fast Fourier Transform algorithm (Cooley, Lewis and Welch, 1967). The Fourier transform is a list of complex numbers, each number associated with a particular frequency. One calculates the amplitude, or absolute value, of each of these numbers and squares it. The resulting list, of squared amplitudes at a number of evenly spaced points in the frequency domain, is the variance (power) spectrum, of the original list representing the time function. The bandwidth of the variance spectrum is set by the frequency of sampling of the continuous signal. The bandwidth is one half the sampling frequency. In my experiments the sampling frequency was 50 hz,

so the bandwidth of the spectrum was 25 hz. The lowest frequency in the spectrum, and the frequency resolution, are the reciprocal of the record length. The record length was 5.12 seconds so that the lowest frequency and frequency resolution were about 0.2 hz.

If the original list is from evenly spaced time samples of a stochastic process, the sample spectrum from one record is not adequate to allow accurate estimation of the spectrum of the stochastic process. You must average several independent spectral estimates from a group of realizations of the stochastic process (cf. Jenkins and Watts, 1968, for details). What this means in a neurophysiological application is that one averages spectral estimates from several experimental runs which have identical stimulus conditions. In order to obtain smooth spectral estimates for stochastic processes I used Welch's method of averaging overlapping sample spectra (Welch, 1967), the method shown in Figure 3-3.

Autocorrelation

The variance (power) spectrum of any stochastic process is related to the autocorrelation of the process. The autocorrelation is defined as the autocovariance divided by the variance. Thus the autocorrelation is unity at zero time lag and varies with time lag, typically becoming zero as the time lag becomes large.

The autocorrelation of the impulse rate has a very definite relationship with the serial correlation coefficients of the impulse intervals. The autocorrelation of the impulse rate, $n(t)$ is

$$\overline{(n(t)-\bar{n})(n(t+\tau)-\bar{n})} \Big/ \overline{(n(t)-\bar{n})^2}$$

The impulse rate n and pulse interval S are related by the equation $n = \frac{1}{S}$. In fairly regularly firing nerve cells, where deviations from the mean are not large, for deviations from the mean in pulse rate Δn; $\Delta n(t) = n(t) - \bar{n}$ and deviations in pulse intervals ΔS, we can write $\frac{\Delta n}{n} = -\frac{\Delta S}{S}$. In particular, for the coefficient of variation, $\frac{\sigma_n}{\bar{n}} = \frac{\sigma_S}{\bar{S}}$. Using the same argument you can show that

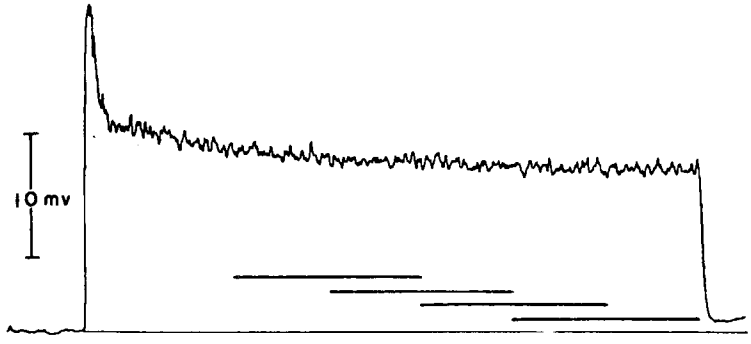

SEGMENTATION OF DATA RECORD

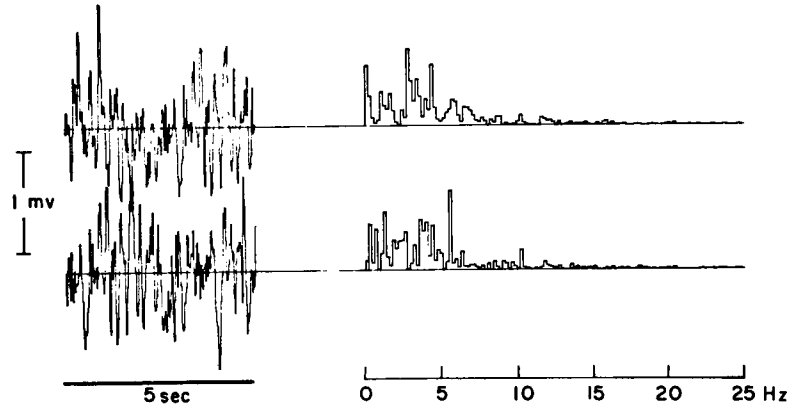

DATA SEGMENT AND ESTIMATE OF POWER SPECTRUM

Figure 3-3. Welch's Method of Spectral Estimation Applied to Limulus Generator Potential. A record of light-evoked generator potential is shown. Overlapping segments of data are used for single estimation of spectra. Several of these single estimates will be averaged to obtain a smoothed spectral estimate. Welch's method of using overlapping data segments allows a more economical use of data. Fewer data are required for the same smoothness of estimate.

$\frac{\overline{\Delta n(t)\,\Delta n(t+\tau)}}{\overline{\Delta n(t)^2}} = \frac{\overline{\Delta S_k\,\Delta S_{k+m}}}{\overline{\Delta S_k{}^2}}$ when $\tau = m\bar{S}$, where $\bar{S}$ is the mean pulse interval and $m = 1,2,3\ldots$ In words, the autocorrelation of the impulse rate equals the interval serial correlation coefficients at time lags which equal an appropriate integral multiple of the mean interval. For example, the autocorrelation of the firing rate at time lag $\tau = 2\bar{S}$ equals the second interval serial correlation coefficient.

This is shown for some electronically generated pulse interval data in Figure 3-4.

As is clear from the graph in Figure 3-4, the autocorrelation of the impulse rate is a smooth interpolation between the serial correlation coefficients of the intervals. The entire analysis procedure produces a smooth function which interpolates between those autocorrelation points fixed by the data. It is important for the relation between autocorrelation of spike rate and correlation coefficients of interspike intervals that the firing be fairly regular, i.e. coefficient of variation less than 0.25, say. It is the regularity of the firing which enables us to make an identification of a time function, the impulse rate autocorrelation, with a discrete function which measures serial dependence, the serial correlation coefficient of all orders.

I would like to refer to the nomenclatural fog surrounding the subject of autocorrelation in neurophysiology. (The renewal density or renewal intensity is defined as the average rate of pulse occurrence between time t and $t+\Delta t$ after a given pulse; it is discussed in Cox and Lewis, 1966). Moore et al. (1966) call the renewal density of a nerve impulse train the autocorrelation of the impulse train. I agree with the nomenclature of Moore et al. if it is made clear what variable is being correlated with itself. In their case it is a (stochastic) function of time which is a delta function at each time a nerve impulse occurs and zero elsewhere, i.e. the pulse train. In my case the function is impulse rate as defined before. As shown above the autocorrelation of the impulse rate is an interpolated estimate of serial correlation of the pulse intervals; the autocorrelation of the pulse train is a measure of the periodicity (regularity) in a pulse train. One final point -- while the autocorrelation of the impulse rate as I have defined it is normalized and goes to zero as time lags approach infinity, the renewal density (which is what Moore et al. call

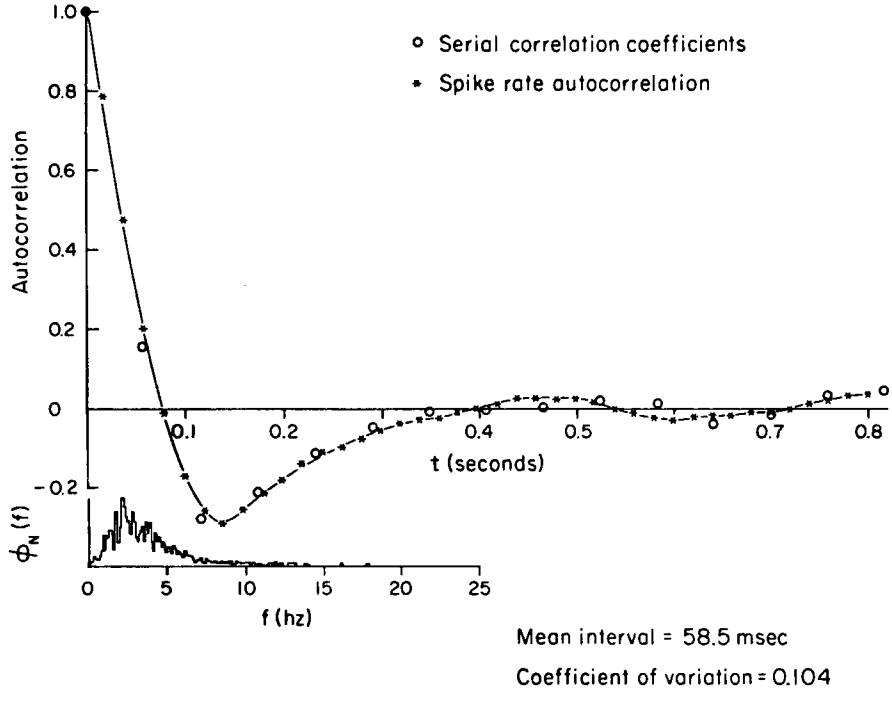

Figure 3-4. Autocorrelation of the Impulse Rate and the Serial Correlation Coefficients of Pulse Intervals. The autocorrelation is plotted as a continuous curve and as X's. The serial correlation coefficients are plotted as open circles at times equal to integral multiples of the mean pulse interval. At the lower left is shown the spectrum of the impulse rate, from which the autocorrelation of the impulse rate was calculated by Fourier transformation.

the autocorrelation of the pulse train) is not normalized at time zero, and converges to a constant (the mean pulse rate) at long time lags, contrary to the conventional definition of autocorrelation.

Probability Distributions

Interspike interval distributions are the routine measures applied to impulse trains by previous workers. Such distributions are usually displayed as an interval histogram in which the ordinate is number of intervals and the abscissa is the magnitude of an interval. I constructed interval histograms and also firing-rate histograms for Limulus nerve fiber and eccentric cell data. Cursory inspection indicates that the firing rate distribution is a normal distribution for Limulus cells. Statistical tests were applied to the impulse interval data to ascertain how much the interval density function departed from a Gaussian function. These statistical tests involved the moments of the distribution.

The moments around the mean are average values of power of a random variable around its mean, e.g. the second moment around the mean, otherwise known as the variance, of the spike intervals ζ is $\overline{(\zeta - \bar{\zeta})^2}$. For a Gaussian density function, which is symmetric around the mean, all odd moments around the mean are zero. The third moment, the lowest order odd moment around the mean which might be non-zero, is used to measure skewness; the parameter that is tabulated in statistical tables is the third moment squared divided by the variance cubed (in order to get a dimensionless measure of skewness). Another more stringent test for a normal density function is the size of the fourth moment; this is a measure of the peakedness of the density function. I used statistical tests on the third and fourth moments around the mean to test departures from a Gaussian density function.

I measured the variance spectrum and probability density function of the impulse rate, in order to characterize the randomness in nerve impulse firing. Because I sought to link voltage fluctuations and spike firing variability, I performed the same spectral and probability distri-

bution calculations on the stochastic generator potential in those experiments where generator potential measurements were made.

Chapter 4

THEORETICAL BACKGROUND

The Eccentric Cell: Components of its Response

The Generator Potential. An eccentric cell responds to light by firing nerve impulses steadily while the light is on. The events leading up to this response consist of three stages. The first stage is the generator potential. This probably results from light-dependent ionic permeability changes in the photoreceptor membrane (for recent evidence on this point, see Millecchia and Mauro, 1969a, b). Such permeability changes cause depolarization of the membrane. The depolarization induced by light appears to be quantized, as if each effectively absorbed photon triggered a unit slow potential fluctuation. The discrete slow potentials have a half width of approximately one hundred milliseconds, a slow rise time and decay. They are not uniform in size, but have a mean amplitude with a distribution of amplitudes around this average value. At very low light intensities the discrete potentials can be easily resolved, but at higher light intensities they occur more frequently and superimpose on one another. Over the range of light intensity that they can be resolved, their rate of occurrence is proportional to the intensity. The size of the discrete slow potentials depends on the past history and present level of illumination (Yeandle, 1957; Adolph, 1964; Dodge, Knight and Toyoda, 1968a). Dodge et al. (1968a) showed that the characteristics of the generator potential could be accounted for by the summation of the discrete potentials.

The occurrence of the discrete potentials is a random process, presumably reflecting the randomness in the arrival and absorption of photons. The generator potential is therefore the summation of randomly occurring, similarly shaped discrete events. This phenomenon is analogous to the shot noise observed in vacuum tubes and photomultipliers (the analogy is quite important and will be referred to later in this chapter). At all light intensities, the generator potential has an inherent noisy component, provided by the summation of the discrete potentials.

The variance of the generator potential is determined by the effective duration, size and arrival rate of the discrete potentials. Dodge, Knight and Toyoda (1968a) showed that the effective duration of the discrete slow potentials is reciprocal to the logarithm of light intensity, while their average size is proportional to the inverse square root of light intensity. This means that the eye of the horseshoe crab adapts to brighter light by reducing the size, and reducing the duration of its discrete responses to single photons.

Voltage-To-Frequency Converter. The second component of the neuronal response is the encoding of depolarizations into the impulse discharge. The average rate of impulse firing is proportional to the amount of depolarization. In addition, the impulse rate in these cells will follow time-varying depolarizations in a linear manner as long as the depth of modulation is not too great.

An integrate-and-fire device is a model for such an impulse firing mechanism. In this model, membrane potential (or perhaps current through the membrane) is integrated until the integral reaches a threshold and then an impulse is fired and the integral is reset to zero (this model is discussed further in Lange, 1965; Knight, 1969). This device functions as a voltage-to-frequency converter.

Self Inhibition. There is also a stage of neuronal adaptation, or self-inhibition, in the Limulus eccentric cell. Stevens (1963) and Purple (1964) first studied this phenomenon and showed it had the characteristics of synaptic inhibition. Purple showed that each nerve impulse triggers a long lasting hyperpolarization of the eccentric cell, a hyperpolarization which is associated with an increase in the conductance of the membrane. The time course of the hyperpolarization is a decaying exponential with a time constant of about half a second. Self inhibition will therefore prevent the cell from making large, slow excursions in impulse rate, but will not prevent abrupt transients in the impulse rate due to rapid changes in excitation or inhibition.

The Linear Model for Dynamic Responses Of The Eccentric Cell

The components of stimulus-response coding -- sensory transduction, temporal summation and neuronal adaptation -- are present in other sensory neurons, but can be isolated and studied in detail in the eccentric cell. A model for an eccentric cell is shown in Figure 4-1. The stages in sensory coding are labeled GENERATOR POTENTIAL, FM for the integrate-and-fire device, and SELF INHIBITION. The analytic model, which is diagrammed in Figure 4-1, includes the following ideas. The firing of nerve impulses by the FM mechanism depends on the level of the summing point, labeled Σ in Figure 4-1. External influences which can change the value of the summing point are light, acting through the GENERATOR POTENTIAL mechanism, and electric current injected into a cell through a microelectrode. Each nerve impulse acts to reduce the level of the summing point through the SELF INHIBITION mechanism. The summing point corresponds to the membrane potential (or current through the membrane) at the critical site in the cell which drives the impulse firing mechanism.

The model also includes the assumption that the overall dynamics of the response of the cell to time-varying illumination can be broken up into the dynamic response of each of the stages in sensory coding. If we consider that the input to the neuron is light, and the output is the impulse rate, the stages in sensory coding can be dissected into two sequential mechanisms. The first is the mechanism transducing light into generator potential. The second is the mechanism which produces the impulse rate from depolarization of the cell membrane. The properties of the latter mechanism can be measured by injecting modulated current into the cell and observing the modulation of the firing rate thus produced. There is evidence (MacNichol, 1956) that injected current acts like the current produced by the photoreceptor in causing impulses to be fired.

Dodge, Knight and Toyoda (1968b) studied the response of these pro-

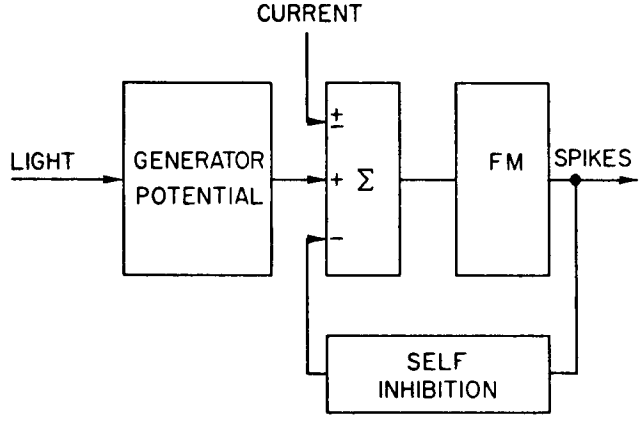

Figure 4-1. Model for the Eccentric Cell. This is a schematic diagram of the linear model of an eccentric cell. The summing point Σ can receive signals from three sources: from external CURRENT injection, from the GENERATOR POTENTIAL produced by light, and from SELF INHIBITION. The net value of the sum is coded by a voltage-to-frequency converter, FM, into the "spikes" or nerve impulses which propagate down the optic nerve. GENERATOR POTENTIAL, FM and SELF INHIBITION each have their own specific dynamic responses which determine the overall dynamic response, and fluctuations, of the eccentric cell. This figure is from Dodge, Knight and Toyoda (1968b).

cesses to time-varying stimuli. From the response of the neuron to small stimuli modulated around a steady stimulus level, they demonstrated that the neuron could be approximated by a time-invariant, linear filter. This conclusion followed from the findings that superposition of responses occurs for stimuli which are added to one another, and that sinusoidally modulated stimuli evoke sinusoidally modulated responses. They also showed that the light-to-generator potential process and the current-to-firing rate process are like filters connected in series. The generator potential varies sinusoidally in response to sinusoidally modulated light intensity. A sinusoidally modulated membrane depolarization causes the impulse rate to vary sinusoidally also. The frequency response of the complete process, from modulated light to modulated firing rate, is the product of the separate frequency responses for the two component mechanisms: the light-to-generator potential, and current-to-firing rate. Let us call the frequency response of the light-to-generator potential process $G(f)$, the frequency response of the current-to-firing rate process $S(f)$, and the frequency response of the light-to-impulse rate process $N(f)$. Then the conclusion of Dodge et al. (1968b) can be written $N(f) = S(f) \cdot G(f)$

Frequency Response of the Current-to-Firing Rate Process

The essential theoretical problem of this thesis is the relation between noise in the membrane potential and variability of the impulse rate. The important mechanism to understand, in connection with this problem, is the process which produces the impulse rate from depolarization. It can be characterized by the way it affects the response of the cell to time-varying stimuli, as indicated by its frequency response, $S(f)$.

As Knight (1969) has shown, the frequency response of an integrate-and-fire device is

$$B(f) = \frac{1 - e^{-2\pi i f/f_0}}{2\pi i f/f_0}$$

where f_0 is the average impulse rate and f is the modulation frequency. This expression was first used in a neurophysiological application by Borsellino (Borsellino et al., 1965).

The integrate-and-fire device can exhibit sidebands. Sidebands become especially apparent at modulation frequencies which are greater than half the mean impulse rate. For such modulation frequencies, the difference frequency ($f_0 - f$) component is larger than the modulation frequency component, and so the firing rate appears to be modulated at a frequency $f_0 - f$. Nevertheless, $B(f)$ gives the amplitude and phase of the impulse rate modulation at the stimulus modulation frequency. The linear model for the integrate-and-fire device works adequately as long as modulation frequencies are kept low enough. This is the expected behavior for a frequency modulation system.

The integrate-and-fire mechanism with self-inhibitory feedback has a more complicated transfer function. The self-inhibitory hyperpolarization has the time course of a simple exponential. As a consequence, a system with self-inhibitory negative feedback, but without the discreteness imposed by pulse rate coding, would have the frequency response,

$$I(f) = \frac{1 + K_S}{1 + \frac{K_S}{1 + 2\pi i f \tau_S}}$$

where K_S is the self-inhibitory coefficient and τ_S is the self-inhibitory time constant. $I(f)$ is the often encountered frequency response of a linear negative feedback network in which the feedback loop has an exponential impulse response. The frequency response $I(f)$ has an amplitude of 1 at very low frequencies of modulation, and an amplitude approaching $1 + K_S$ at high frequencies. This can be seen by computing $I(0)$ and $I(\infty)$.

However, self-inhibitory potentials are triggered by, and therefore phased to, the occurrence of nerve impulses. Therefore, the exact expression for the frequency response of the current-to-firing rate mechanism is more complicated than $I(f)$ or $B(f)$. Knight (1969) has shown

that the frequency response for the coupled system is

$$S(f) = \frac{(1 + K_s)(B(f))}{\left\{1 + K_s\left[1 - \frac{(1/\tau_s f_o)(1 - e^{-2\pi i f/f_o})}{(e^{1/\tau_s f_c} - 1)(1 - e^{-(1/\tau_s + 2\pi i f)/f_o})}\right]\right\}}$$

The current-to-firing rate frequency response $S(f)$ possesses a low frequency cutoff with a shape roughly the same as $I(f)$, the frequency response of a continuous negative feedback network discussed above. The high frequency behavior of $S(f)$ is like that of $B(f)$, the frequency response of an integrate-and-fire device. The latter has nulls at multiples of the average impulse rate and attenuation of frequencies approaching the average impulse rate and all frequencies above it. These features result in a peak amplitude of $S(f)$ in the region of the spectrum between zero frequency and the frequency equal to the average impulse rate. This peak is a consistent characteristic of the current-to-firing rate mechanism of eccentric cells. Dodge (1968) shows several examples of how well the analytic expression for $S(f)$ fits experimental measurements; in chapter 5 of this thesis, Figure 5-5 illustrates the characteristic features of $S(f)$ (peak frequency, low and high frequency cutoffs) and the degree of agreement between theory and experimental measurement.

Neuronal Variability as Filtered Fluctuations Of the Generator Potential

Since the current-to-firing rate process acts like a linear filter, the theory of spectral analysis outlined in chapter 3 can be applied usefully to the problem of relating generator potential fluctuations to variability in the impulse rate. The spectral characteristics of the impulse rate fluctuations can be predicted from the variance spectrum of the input, the generator potential "noise", filtered by the current-to-firing rate process.

I have called the generator potential variance spectrum $\phi_G(f)$, the impulse rate spectrum $\phi_N(f)$. The variance spectra are real-valued functions of frequency. A frequency response is a complex-valued function of frequency. Thus, $S(f)$, the frequency response of the current-to-firing rate process, has an amplitude $|S(f)|$ and a phase. According to the theory for filtering of stochastic processes, the variance spectrum of the output process is the product of the variance spectrum of the input multiplied by the squared amplitude of the frequency response of the filter (Parzen, 1962; see also chapter 3). In this case, this leads to the equation

$$\phi_N(f) = \phi_G(f) \cdot |S(f)|^2 \qquad (1)$$

This equation is correct if ϕ_N and ϕ_G are in the same units. ϕ_G is expressed in the units of millivolts^2/hertz (mv^2/hz). ϕ_N is expressed in the units adrian^2/hz; an adrian has been previously defined as 1 impulse/second. A scale factor with units (adrian/mv)^2 must be used to convert ϕ_G from the units of a voltage spectrum to the units of an impulse rate spectrum. This factor is in the range 1 - 25 (adrian/mv)^2 (cf. Fuortes, 1959).

As mentioned previously in chapter 3, a correct prediction for the variance spectrum of the impulse rate according to equation (1) implies a correct prediction for the serial correlation coefficients of impulse intervals. Equation (1) also enables you to derive the variance of the impulse rate from the variance spectrum of the generator potential. This is because the integral of the variance (power) spectrum with respect to frequency is the variance, i.e.

$$\int_0^\infty \phi_N(f)\,df = \sigma_N^2 = \overline{(n(t) - \bar{n})^2}$$

Steady State Fluctuations And The Frequency Response, N(f)

There is another way to predict the shape of the variance spectrum of the impulse rate. It is based on the finding (Dodge et al., 1968a) that

for steady state fluctuation of the generator potential,

$$\phi_G(f) = \alpha |G(f)|^2 \qquad (2)$$

As stated before, $G(f)$ is the frequency response for the transduction from light to generator potential. If we multiply both sides of equation (2) by $|S(f)|^2$ we get the equation

$$|S(f)|^2 \cdot \phi_G(f) = \alpha |S(f)|^2 \cdot |G(f)|^2$$

As discussed before, Dodge et al. (1968b) have shown that $N(f) = S(f) \cdot G(f)$ where $N(f)$ is the frequency response of the overall process, light-to-impulse rate. Substituting in the previous equation, and also using equation (1), we obtain

$$\phi_N(f) = \beta |N(f)|^2 \qquad (3)$$

In words, what equation (3) says is that the variance spectrum of steady state fluctuations is proportional to the squared amplitude of the frequency response, for the total process which transduces light intensity into the impulse rate. This is an important theoretical prediction. It emphasizes that, according to the model of the eccentric cell presented here, dynamics and fluctuations of the impulse rate are very closely related.

Equation (2), the proportionality of the generator potential spectrum to its frequency response, is a general equation which describes the relation between the frequency response of a filter and the variance spectrum of the output noise produced from white noise input; a particularly pertinent example is the case of shot noise (see Rice, 1944; Parzen, 1962). The equation applies to the generator potential of Limulus eccentric cells even though the discrete potentials which constitute the generator potential are not simply uniformly shaped shots, but adapt in

size to changes in light intensity (Dodge et al., 1968a). The extra stage of linear filtering by the current-to-firing rate mechanism carries over to the impulse rate the relation between frequency response and variance spectrum. Thus, equation (2) becomes equation (3).

Impulse Rate Distribution And The Interval Distribution

While I have concentrated on spectral analysis of the impulse rate and generator potential, there are also interesting theoretical and experimental findings to report concerning the probability distributions of the impulse rate and generator potential. The theoretical arguments are based on the idea that if a Gaussian stochastic process is passed through a linear filter, the output is a Gaussian process. A Gaussian process is rigorously defined as a stochastic process whose density function, and all of whose higher order joint probability density functions, are Gaussian in form. I have not attempted to show that, rigorously speaking, the generator potential is a Gaussian process. However, it is a shot noise process whose probability density function is Gaussian; unless it is unusual, such a process ought to have joint distributions which are Gaussian in form. With this plausible assumption, we can conclude that the generator potential is a Gaussian process.

If one accepts the plausibility of this argument, it follows that the probability density function for the impulse rate is derivable from that for the generator potential. Since my experiments were performed with light stimuli bright enough that deviations around the mean of the generator potential had a Gaussian probability density, the impulse rate fluctuations should also have a Gaussian distribution (the variance of the distribution can be calculated, as previously described, using the techniques of spectral analysis). Departures from a Gaussian distribution for fluctuations of the impulse rate might imply inadequacy of the working hypothesis that fluctuations of the impulse rate can be treated as generator potential "noise" filtered through the impulse firing mechanism.

The interval probability density function will not be a Gaussian function if the probability density of the rate is Gaussian. The interval is the reciprocal of the impulse rate. From the functional relation between the two variables, you can derive an expression for the interval distribution based on the assumption that the distribution of the firing rate is Gaussian. This expression is,

$$P(s) = \left(\frac{\bar{s}}{s}\right)^2 \frac{1}{\sigma\sqrt{\pi}} \exp\left\{-\frac{1}{2}\left(\frac{\bar{s}}{\sigma}\right)^2\left(\frac{s-\bar{s}}{s}\right)^2\right\}$$

where s is the length of a pulse interval.

Chapter 5

RESULTS

Variability in the Responses to Light and Electric Current

The starting point for this work was the finding that the impulse rate in an eccentric cell was more variable when the cell was stimulated by light than when it was stimulated by electric current (Ratliff, Hartline and Lange, 1968). This result is illustrated in Figures 5-1 and 5-2, where two sample records from the same eccentric cell are exhibited. Figure 5-1 is the graph of a response to steady light; Figure 5-2 is the response to steady current in a light adapted cell. The variance of the response to light is about seven times that for the response to current stimulation.

The variance (power) spectra of the impulse rate strikingly illustrate the difference in variance under these two conditions. This is shown in Figure 5-3 for spectra computed from the data shown in Figures 5-1 and 5-2. Not only are the variances obviously different, but the variance spectra are also different in shape. The variance spectrum for the response to electric current is flatter, with less of a low frequency cutoff and no peak at four hz where the spectrum of the light response peaks. Of course, all the spectral components are smaller for the response to electric current reflecting the overall difference in variance.

The variance spectra show that both the amount and the temporal pattern of variability differ in the two cases. The source of fluctuations in the activity stimulated by electric current is as yet unexplained, although it may reflect low frequency fluctuations of membrane potential, or membrane permeability, in the dark. If this should prove to be correct, it would reinforce even more the working hypothesis of chapter 4 that the impulse firing mechanism itself is not very random and contributes little to the observed variability.

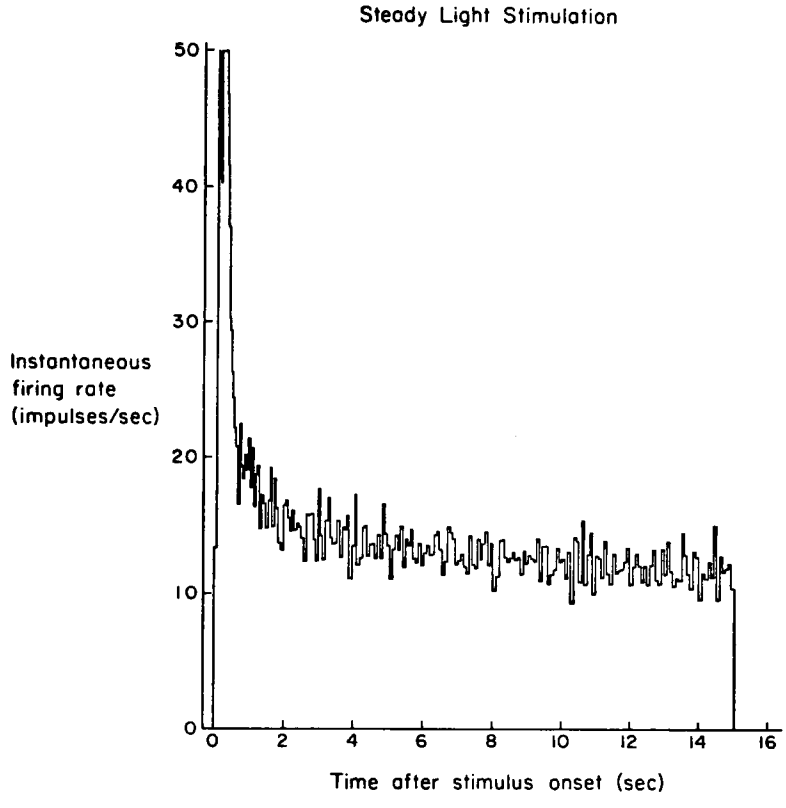

Figure 5-1. Impulse Rate in Response to Stimulation by Light. This is a typical response to a light one thousand times more intense than the threshold for maintained firing. The variance of the maintained firing is approximately 1 adrian^2.

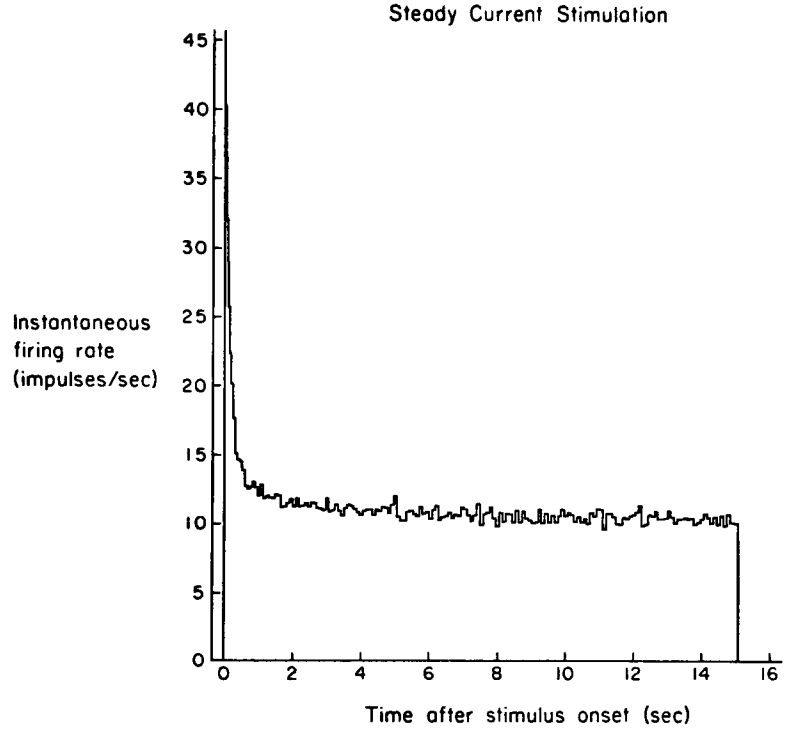

Figure 5-2. Response to Electrical Stimulation. Response of same cell as in Figure 5-1 to a maintained electric current stimulus which is injected through an intracellular micropipette. The variance of the maintained firing is approximately 0.15 adrian^2.

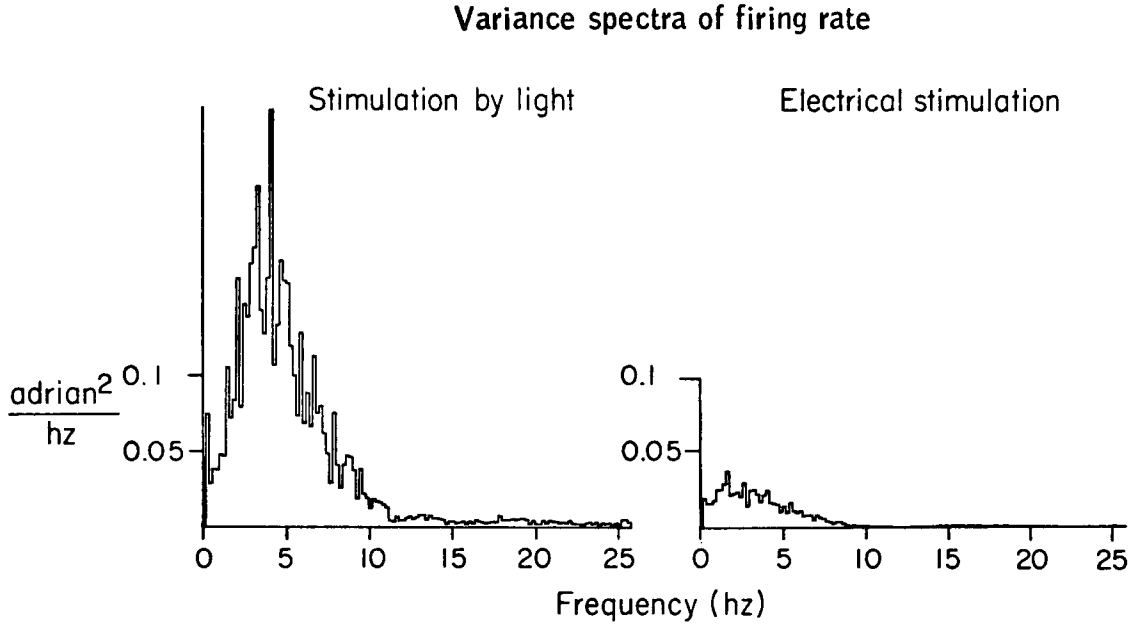

Figure 5-3. Variance Spectra of the Response to Stimulation by Light, and the Response to Electrical Stimulation. This figure shows the variance spectra plotted on the same vertical scale. Not only is the variance spectrum of the response to light larger, it also shows greater peaking at approximately four hz. The spectrum for the response to electric current is flat down to low frequency.

Observations on Filtering of Generator Potential "Noise"

In order to prove that the impulse rate fluctuations are filtered generator potential fluctuations, I had to confirm equation (1) of chapter 4. That equation predicts that the variance spectrum of the impulse rate is the variance spectrum of the generator potential, multiplied by the squared amplitude of the frequency response for the current-to-firing rate process. To verify this prediction required measurement of the variance spectrum of the generator potential, $\phi_G(f)$, the frequency response of the current-to-firing rate process, $S(f)$, and the variance spectrum of the impulse rate, $\phi_N(f)$. The calculation of the variance spectra from data has been described in chapter 3.

The measurement of $S(f)$ is illustrated in Figure 5-4. This figure shows three sample records of the impulse rate from one cell, whose impulse rate was modulated by injected current at three different frequencies: 0.4 hz, 1 hz and 4 hz. The entire frequency response was measured by repeating these measurements at several more frequency points. The amplitude and phase of the response were determined by a least squares fit of a sine and cosine, at the stimulus modulation frequency, to the response. It is clear from the data in Figure 5-4 that low frequencies produce less modulation than higher frequencies; this is a consequence of self-inhibition.

This low frequency cutoff is more clearly illustrated by the graph in Figure 5-5 of the frequency response for the current-to-firing rate mechanism. The logarithms of amplitude and phase are the ordinates and the logarithm of frequency is the abscissa in this graph. The first lobe of the phase shift is a phase lead; at frequencies above 1.5 hz the phase shift changes into a phase lag. The smooth curve drawn through the experimental points is the analytic expression for $S(f)$ which was presented in chapter 4. The features of the predicted and measured frequency response are the same, namely a low frequency cutoff, peak in am-

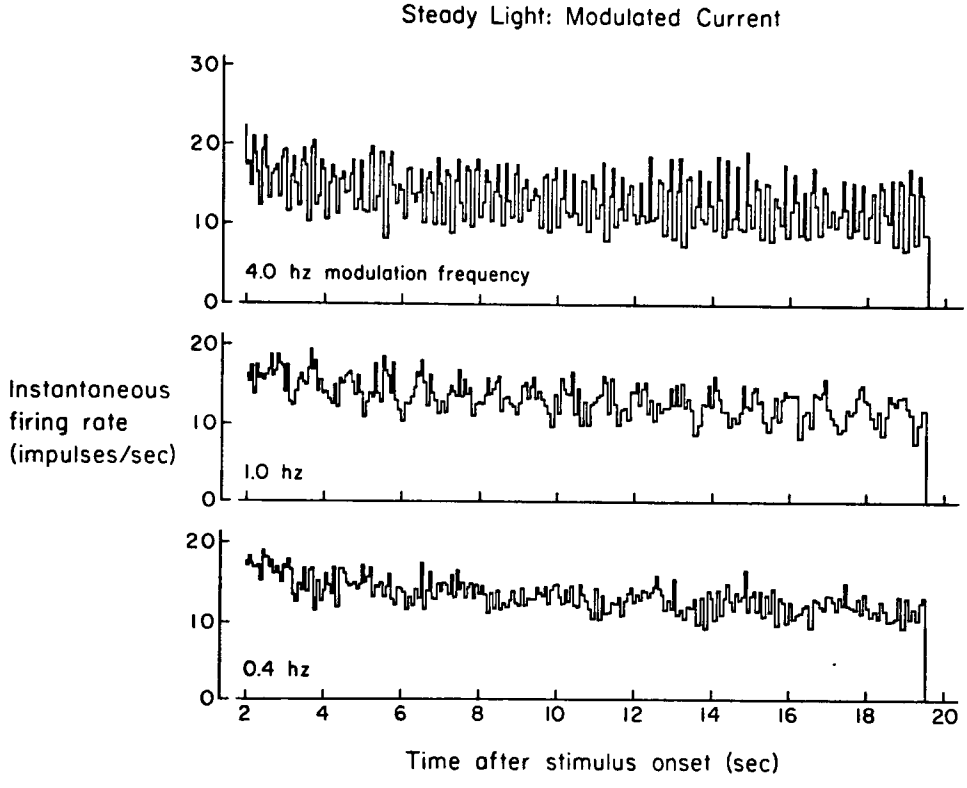

Figure 5-4. Measurement of the Frequency Response for the Current-To-Impulse Rate Mechanism. The response of an eccentric cell to modulated current stimuli is shown. The steady level of firing was set with maintained stimulation by light. The amplitude of the current is the same for the three records, but the modulation frequencies were varied, as shown in the figure.

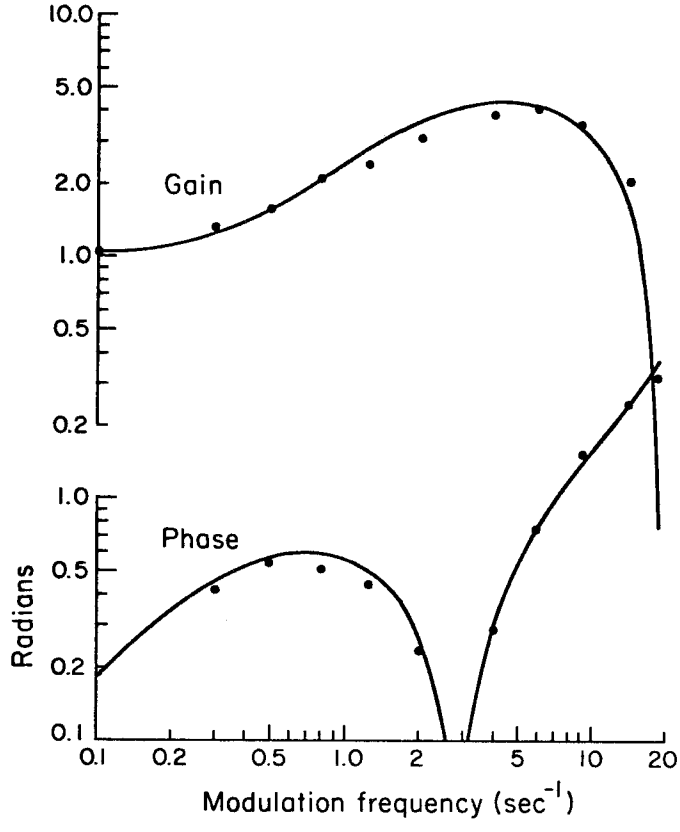

Figure 5-5. The Frequency Response for the Current-To-Firing Rate Mechanism. The amplitude and phase of the response to a whole range of modulated current stimuli are plotted against modulation frequency. The points are experimental; the smooth curve is an analytical fit to the points using the theoretical expression for $S(f)$ which is discussed in the text. The mean firing rate of this cell was 20 adrians.

plitude (gain) at five hertz, and a high frequency cutoff. The theory contains two parameters, the time constant τ_S and the self-inhibitory coefficient K_S. These data were fit with time constants τ_S equal to 0.5 seconds, and a coefficient K_S equal to 3. These are typical values.

Generator Potential "Noise" Causes Neuronal Variability. Spectra for both the generator potential, $\phi_G(f)$, and for the impulse rate, $\phi_N(f)$, were measured in the same cell. Data from such an experiment are shown in Figure 5-6. At the upper left is a graph of ϕ_G, the variance spectrum of the generator potential. Note that, in this cell, the generator potential spectrum shows little peaking. Below ϕ_G is the predicted impulse rate variance spectrum ϕ_N^*. The predicted spectrum is obtained by multiplying each value of the variance spectrum of the generator potential by its appropriate weighting factor -- the squared amplitude of $S(f)$, the frequency response for the current-to-firing rate mechanism. This is the prediction contained in equation (1) of chapter 4. The features introduced by filtering are apparent in the figure. The variance spectrum ϕ_N^* is peaked, with a low frequency and high frequency cutoff on either side of the peak.

The measured variance spectrum of the impulse rate, ϕ_N, is shown on the bottom left of Figure 5-6. It appears to have almost exactly the same shape, and magnitude, as the predicted spectrum ϕ_N^*.

We can estimate the degree of agreement of these two spectra, ϕ_N and ϕ_N^*, by comparing the differences between them with the amount of error inherent in the calculation of spectral estimates from data. As shown in texts on spectral analysis, if the stochastic process has a Gaussian distribution function, each spectral component is a random variable with a chi-squared distribution. The number of degrees of freedom for this chi-square distribution is set by the total amount of data and the degree of frequency resolution in the spectrum (see Jenkins and Watts, 1968; and Welch, 1967). Using this distribution of the spectral components one can calculate a standard error for the variance spectrum. The result is an

Comparison between predictions of filter model and experimental measurements of firing rate variance spectrum and autocorrelation

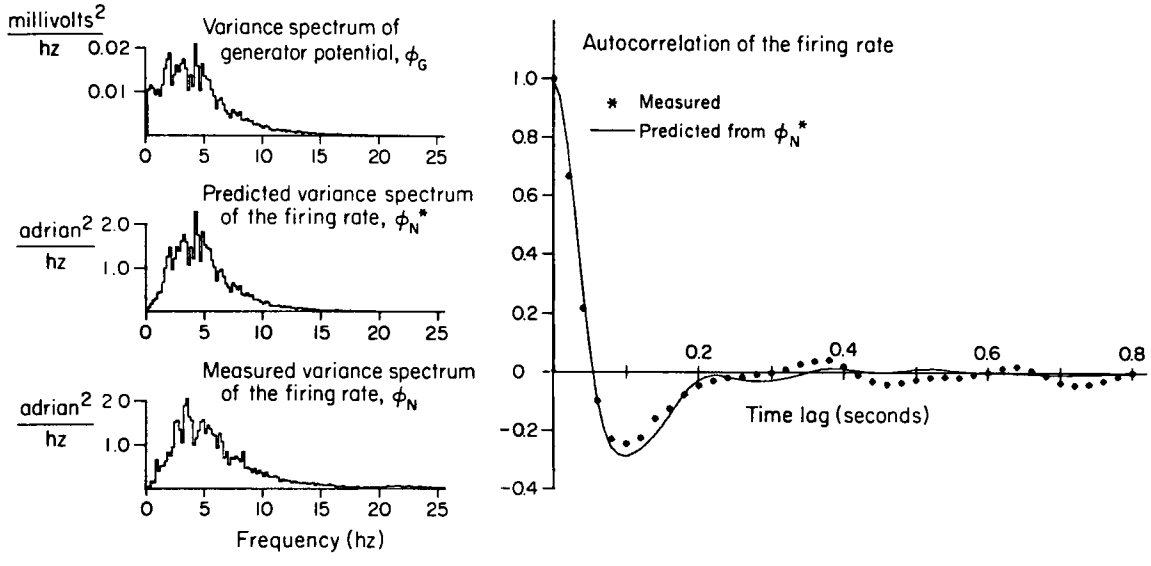

Figure 5-6. Prediction and Measurement of the Variance Spectrum of the Impulse Rate. The test of the hypothesis that generator potential fluctuations cause variability in the impulse rate. Shown in the left hand column are ϕ_G and ϕ_N, the measured generator potential, and impulse rate, variance spectra, respectively. Between them is ϕ_N^*, the predicted spectrum, obtained by multiplying ϕ_G by $|S(f)|^2$, the variance transfer function of the current-to-firing rate mechanism. The autocorrelations, predicted and measured are shown at the right. The average firing rate of this cell was 23 adrians.

approximate standard error of twenty per cent of the magnitude of the spectral component (the standard error depends on the size of the spectral component -- the larger the component, the larger the absolute magnitude of the standard error). The predicted and measured variance spectra, ϕ_N and ϕ_N^*, agree well, within the standard error over most of the frequency range. There is some discrepancy in the high frequency tail, but this is an insignificant amount of the total neuronal variability.

The agreement of the measured variance spectrum of the impulse rate with the predicted spectrum confirms the working hypothesis with which we began. The temporal pattern of variability in the impulse rate originates in the generator potential, and is filtered and therefore shaped by the impulse firing mechanism and self-inhibition.

Predicted and Measured Autocorrelation. The autocorrelation of the impulse rate, for measured data, agrees well with the predicted autocorrelation which is calculated from ϕ_N^*. The two autocorrelation functions, measured and predicted, are shown on the right side of Figure 5-6. As discussed previously, the autocorrelation of the impulse rate can be calculated from the spectrum measures in the frequency domain -- the temporal texture of a random process. Since the variance spectra, ϕ_N and ϕ_N^*, agree within the inherent error of spectral estimation, it is no accident that the predicted and measured autocorrelation functions also correspond very closely to one another.

The Effect of Self-Inhibition on the Magnitude of Variability. It is clear from Figure 5-6 that the current-to-firing rate mechanism strongly affects the shape of the variance spectrum. The impulse rate spectrum is far more peaked than the variance spectrum of the generator potential. The filtering of the generator potential also changes the relative amount of variability in the impulse rate.

Self-inhibition is the main reason why the coefficient of variation of the impulse rate is greater than the coefficient of variation of the generator potential. Self-inhibition determines the shape of $S(f)$, the

frequency response of the current-to-firing rate process. $S(f)$ is the quotient, the relative modulation (or percentage modulation) of the impulse rate divided by the relative modulation of the driving current. Since middle range frequencies are amplified relative to constant or very low frequency stimuli, on account of self-inhibition, $|S(f)|^2$ is larger than 1 over most of the frequency range where the variance spectrum of the generator potential has large values (cf. Figures 5-5 and 5-6). This results in enhancement of these fluctuations relative to the mean -- in other words, a higher coefficient of variation for the impulse rate than for the generator potential.

Variance Spectrum and the Frequency Response, N(f)

Testing equation (3) from chapter 4, the proportionality between the variance spectrum of the impulse rate, ϕ_N , and the squared amplitude of the frequency response for the light-to-firing rate process, $N(f)$, is a straightforward matter. You measure $\phi_N(f)$, and the frequency response $N(f)$, and then compare ϕ_N with $|N(f)|^2$. An experiment in which this was done is shown in Figure 5-7. As before, the autocorrelation of the impulse rate is shown as well as the variance spectrum. The standard error of the spectral components is about twenty five per cent of their magnitude. The predicted (from $|N(f)|^2$) and measured variance spectra agree fairly well within this limit, although there may be a systematic departure in the region, zero to three hertz. This is hardly a significant departure, however. The conclusion from such an experiment is that the variance spectrum is proportional to the squared amplitude of frequency response, $|N(f)|^2$, for many eccentric cells. This is another experimental indication that the linear model for variability in the impulse firing is basically sound. It emphasizes one major implication of that model: that the dynamic response of the neuron, and its steady state fluctuations, are shaped by the same mechanisms and therefore share similar spectral characteristics.

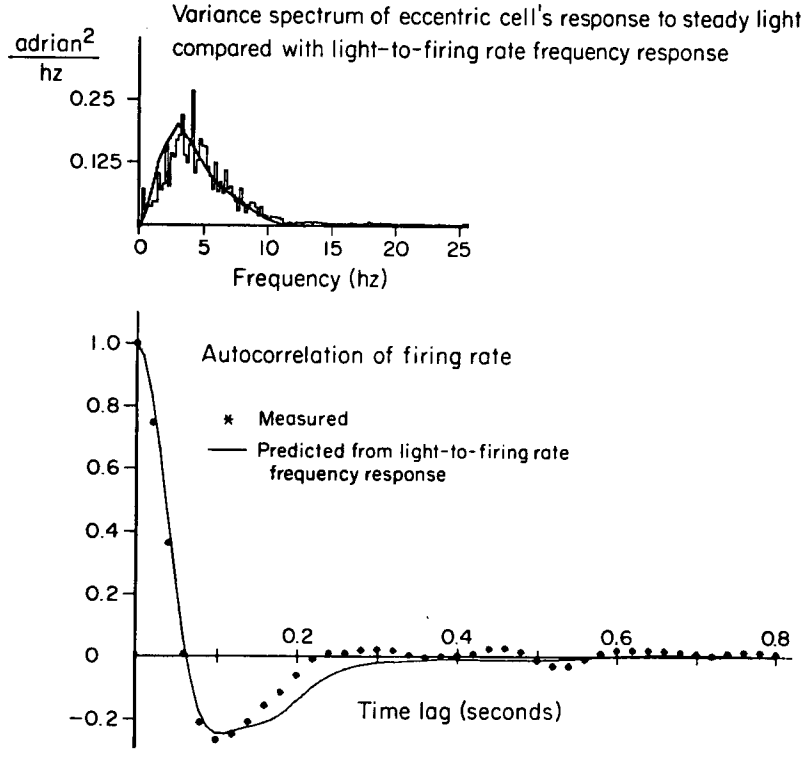

Figure 5-7. Comparison of Variance Spectrum with the Frequency Response of the Light-to-Firing Rate Process. Plotted on the same scale are the squared amplitude of the frequency response, $|N(f)|^2$, and the variance spectrum $\phi_N(f)$. The jagged curve is the variance spectrum (the jaggedness reflecting inherent error in estimating spectral components from data). The smooth curve is the squared amplitude of the frequency response. The squared amplitude of frequency response is plotted on a vertical scale such that the area under the curve will equal the area under the variance spectrum.

Distributions of Impulse Rate and Intervals

To further test the idea that neuronal variability results from fluctuations in the generator potential, I measured the distributions of these quantities and compared their statistical properties. As explained in chapter 4, this statistical measure can provide evidence which is supplementary to the findings from spectral analysis.

Probability density functions for the impulse rate under conditions of steady stimulation by light are well fit by Gaussian functions, of the form $\frac{1}{2\pi\sigma} \exp\left\{-\frac{(n-\bar{n})^2}{2\sigma^2}\right\}$. This finding is important because the distribution of membrane potential deviations is also Gaussian under the same stimulus conditions.

Figure 5-8 shows an impulse rate histogram (estimate of probability density function) and a generator potential histogram for a typical response to a light whose intensity was one thousand times brighter than threshold intensity for maintained impulse firing. Both these histograms approximate Gaussian functions, according to statistical tests on the third and fourth moments. The interval distribution is positively skewed when the impulse rate has a Gaussian distribution, as is expected from the theoretical argument presented in chapter 4.

A marked effect occurred in the statistics of a cell stimulated by electric current, which was allowed to dark adapt for over ten minutes. The statistics of the impulse rate histogram changed very greatly during dark adaptation, an effect which very convincingly reinforces the view that fluctuations in membrane potential cause the observed variability in impulse firing.

When the cell was light adapted the membrane potential fluctuations in the dark were very small and symmetrical about the resting potential; under the same conditions the impulse rate histogram was symmetric and approximately Gaussian in shape. As stated near the beginning of this chapter, the source of the small variability in the firing of a light adapted, current driven eccentric cell has not been investigated. I mention

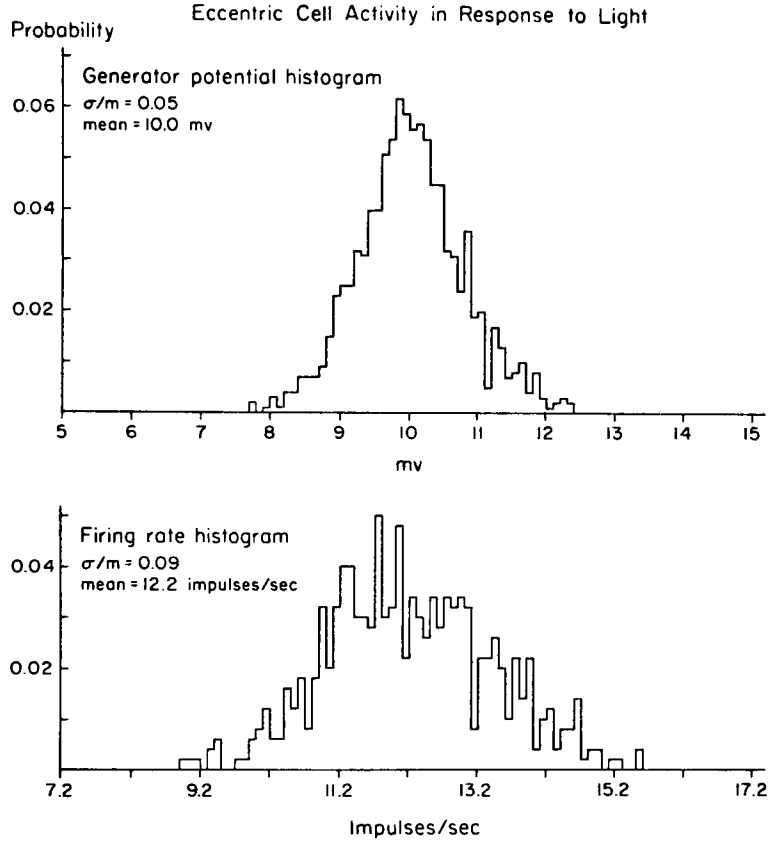

Figure 5-8. Generator Potential Histogram and Firing Rate Histogram for the Response to Steady Light. These two histograms are indistinguishable from Gaussian functions according to tests made on the third and fourth moments. The generator potential histogram appears smoother because more data were used. Both responses were recorded from cells stimulated by a light intensity one hundred to one thousand times brighter than the threshold for steady impulse discharge.

the statistical characteristics of the small variability under these experimental conditions to contrast them with the marked changes which occur during dark adaptation.

During dark adaptation, the striking effect which occurs is an increase in the variance of the impulse rate (previously observed by Ratliff, Hartline and Lange, 1968), and a marked increase in the skewness of the impulse rate distribution. Under the same conditions of dark adaptation, it is well known that the membrane potential distribution changes its character, because of the low rate of appearance of the large, discrete slow potentials mentioned previously (Yeandle, 1957; Adolph, 1964). These discrete events were occurring at the rate of 2/second in the eccentric cell whose impulse rate distribution is graphed in Figure 5-9. The distribution of the membrane potential in an eccentric cell under the same conditions of dark adaptation is shown in the upper graph of Figure 5-9. The skewness of the membrane potential distribution is very obvious. The values of the parameter of skewness, the ratio third moment squared divided by variance cubed, for the histograms of membrane potential and impulse rate, are both about 2. This is very significantly different from the value of zero expected for a symmetrical distribution. Both the membrane potential distribution and the impulse rate distribution are positively skewed; the impulse interval distribution is markedly negatively skewed when the eccentric cell is stimulated by current while dark adapted. The interval distribution is shown in the lowest graph of Figure 5-9.

This marked increase in skewness during dark adaptation, in the probability density functions of both the membrane potential and impulse rate, reinforces even more the idea that random fluctuations in membrane potential underly the major portion of variability in the impulse rate.

Coefficient of Variation During Dark Adaptation

The amount of variability during the course of dark adaptation reveals the importance of generator potential fluctuations on neuronal variability. Further experimental measurements of this effect were made

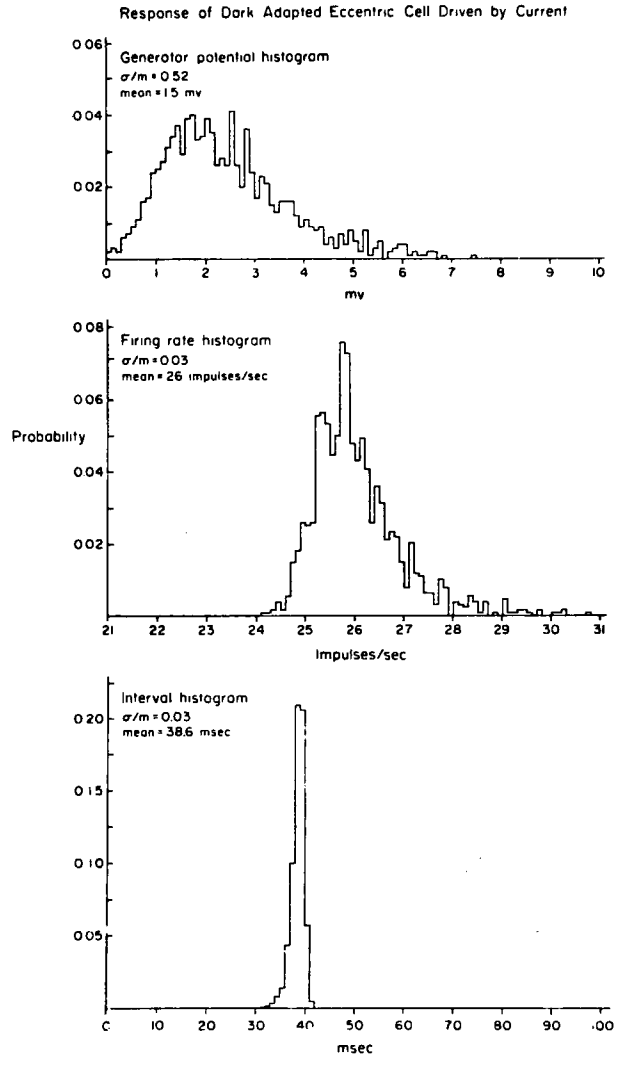

Figure 5-9. Membrane Potential Histogram, Impulse Rate Histogram and Interval Histogram for a Dark Adapted Cell Driven by Injected Current. This figure demonstrates the increase in skewness of the membrane potential, impulse rate and impulse interval in a thoroughly dark adapted cell. The skewness results from the low rate of occurrence of discrete slow potentials, which always tend to depolarize the cell.

in the following way. A light stimulus of a given intensity and twenty seconds duration established a control level of impulse rate, and variance of the impulse rate. An adapting light of an intensity one hundred times brighter than the intensity of the control light stimulus was shone on the photoreceptor for 2 minutes. At intervals of one hundred seconds a test stimulus, identical to the control light stimulus, was applied to the eye. The response changed with time until the cell had adapted back to its former control level.

This experiment is not a perfect measure of the effects of dark adaptation, because of light adaptation by the test stimulus. Nevertheless, it is a useful experiment because it shows that the variability of the firing is reduced when the mean level is reduced by light adaptation. The results are shown in Figure 5-10 as a graph of coefficient of variation vs.time after the adapting flash. During the time the coefficient of variation is recovering to its control value, the mean impulse rate is recovering too. The control value of average firing rate was twelve impulses/second. Immediately after the adapting flash the cell was inexcitable by the test stimulus, and the average impulse rate recovered to its control level with a time course somewhat different from the recovery curve of coefficient of variation.

Reduction in mean level by inhibition will decrease the standard deviation of the impulse rate, by changing the filtering characteristics of the integrate-and-fire mechanism, an effect to be discussed in chapters 8 and 9. However, the magnitude of this kind of reduction of the standard deviation is less than the direct effect of inhibition on the mean rate. As a result the coefficient of variation (standard deviation/mean) will be increased by inhibition, even though the standard deviation is reduced. On the contrary, when the response is reduced because of light adaptation, the standard deviation is reduced even more than the mean, indicating a reduction in the coefficient of variation of the process underlying the neuronal impulse rate, the generator potential. The growth of the average value and standard deviation of the generator potential during the course

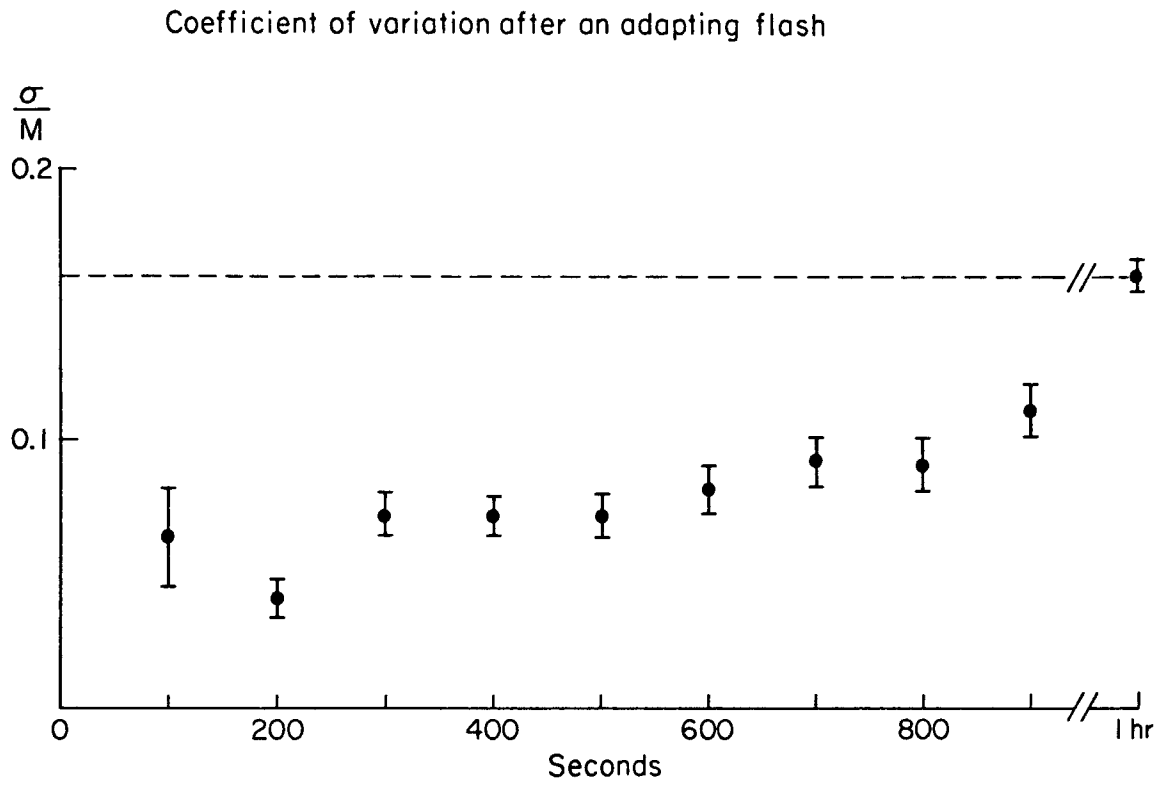

Figure 5-10. The Coefficient of Variation During the Course of Dark Adaptation. Coefficient of variation of the response to a twenty second light stimulus every hundred seconds after a bright adapting flash. Coefficient of variation of the dark adapted cell indicated by the dotted line; this is also the value reached one hour after the adapting flash. Two standard errors around the measurements of the coefficient of variation are indicated by the bars above and below each point.

of dark adaptation, indicated in this experiment on neuronal firing, is consistent with the experiment on dark adaptation by Ratliff, Hartline and Lange (1968), and with experiments on dark adaptation in the Limulus ventral eye (Millecchia and Mauro, 1969a). The dual effect of light adaptation on both the mean level and standard deviation of the generator potential (and therefore indirectly on the impulse rate) is most easily understood in terms of adaptation of the discrete responses of the cell to single photons, a subject investigated by Dodge, Knight and Toyoda (1968a).

"Galloping" and Oscillatory Discharges

Not all Limulus eccentric cells behave in the same manner as the ones discussed above. Most noticeable are cells which "gallop", i.e. cells whose firing rates oscillate in response to a steady stimulus, either light or electric current. Usually the variability of such cells during a steady light stimulus is markedly non-stationary. The impulse rate, in these cells becomes much more variable during prolonged stimulation, finally becoming oscillatory. Deterioration often will make a normal cell become more ragged in its firing until it gallops in response to steady light. And poorly impaled cells will sometimes exhibit galloping in response to steady stimuli.

This is not the only deviation from what is the normal behavior of an eccentric cell. There also seems to be oscillatory activity of some cells in response to very bright lights. These cells do not have the same properties as the galloping cells, for the impulse rate oscillates at a higher rate and with a lower peak to peak oscillation in the impulse rate. While you can pick out a galloping cell by ear, you cannot easily hear these latter high frequency oscillations. The latter type of cell is characterized by alternately large negative and positive serial correlation coefficients between pulse intervals, while the galloping cells have large positive and negative correlation coefficients which are arranged in a more complex sequence: for instance, two large positive correlation coefficients, then two large negative coefficients, and so on.

I think these two particular syndromes are caused by unknown pathologies of the impulse firing mechanism. No aspect of the generator potential of Limulus eccentric cells has been found to account for this kind of oscillatory activity in response to steady light. Since the theory of the impulse firing mechanism which I have used does not take these sorts of complexities into account, the predictions of chapter 4 of this thesis are not applicable to such cells. The oscillatory, markedly non-stationary, cells are a small fraction of Limulus eccentric cells.

Chapter 6

DISCUSSION

Theory of Neuronal Variability

The preceding results confirm the hypothesis that fluctuations of the membrane potential cause the variability of the impulse rate. The amount of variability, and its temporal pattern, result from the filtering of the generator potential by the current-to-firing rate mechanism. This involves two operations on the membrane potential -- temporal integration and self inhibition. These shape the variance spectrum of the impulse rate.

The filtering of generator potential "noise" by the impulse firing system is predictable from a linear model of the eccentric cell. This model has no free parameters; the coefficients and time constants in the model are measurable, and have been measured in these experiments. Therefore, the agreement of predictions and measured data implies the essential soundness of the model in accounting for the source of randomness in the impulse rate. Besides strictly quantitative inferences, there are several qualitative consequences of this neuron model which are observable in the activity of eccentric cells. Examples of this include the effects of dark adaptation on impulse firing elicited by electric current or light.

The reason that modulations of the impulse rate can be analyzed with a linear model in these neurons is that fluctuations in impulse rate are not large compared to the average impulse rate. They are relatively small perturbations around the maintained level of activity. Another factor which influences the degree of agreement between theory and experiment is the relative time course of the underlying voltage fluctuations compared with the firing rate of the cell. In the range of firing rates I studied, the firing rate is rapid compared to the rate of decay of self-inhibitory potentials and compared to the correlation time of the generator potential "noise". The persistence of correlation over several impulse intervals is evidence for the relative speed of impulse firing compared with

underlying correlation times of the membrane potential.

I know of only one other study of neuronal variability in the literature in which predictions from a non-parametric model are compared with data. This is the work of Calvin and Stevens (1968) on spinal motoneurons of the cat. Their neuronal model is similar to the one discussed here, with the exception that instead of integrating the membrane depolarization up to a threshold, their model integrates only the constant level of the depolarization. The fluctuations are not integrated, but instead are added to a linear ramp which is the integral of the constant depolarization. Also they do not include any self-inhibition, or any other neuronal adaptation, in their motoneuron model. A striking difference between motoneurons and eccentric cells is the presence of high frequency components in the membrane potential "noise" of motoneurons. The bandwidth of the motoneuron noise is roughly 40 hz compared to 10 hz or lower in eccentric cells.

The experiments of Calvin and Stevens were performed on spinal cats with no somatosensory stimulation; presumably, the bandwidth of the variance spectrum (or equivalently, the shape of the autocorrelation) of synaptic "noise" could be changed under different experimental conditions. (For instance, descending periodic inputs from the brain might introduce changes in the synaptic "noise"). In any case, under the conditions they used there was zero serial correlation between intervals and their theoretical predictions concerned the shape of the interval distribution. The fact that fluctuations of the membrane potential are slower in Limulus eccentric cells than in cat motoneurons enables you to make predictions about Limulus cells which provide a tighter check on the neuron model, predictions concerning correlation as well as distribution of impulse intervals.

The predominantly negative correlation between intervals in the impulse discharge of eccentric cells resembles the correlation between intervals found by Goldberg et al. (1964) in neurons of the superior

olivary complex (third order auditory neurons). In fact, Geisler and Goldberg (1966) postulate a process similar to self-inhibition in order to explain the negative serial correlation observed by Goldberg et al. (1964).

The negative correlation in the impulse firing of eccentric cell extends over two to four impulse intervals. This indicates that there is some persistent underlying process causing the correlation. This result alone is sufficient to rule out a first order Markov process as the cause of variability. If the impulse firing were a Markov process (see Feller, 1957; Jenkins and Watts, 1968) it would "forget" everything which occurred before the previous pulse interval; this loss of memory would lead to an oscillatory set of serial correlation coefficients, if the first serial correlation coefficient were negative. A Markov model which predicts zero correlation between pulse intervals, has been proposed by Junge and Moore (1966) for Aplysia neurons. Such a model could not explain the major portion of variability in Limulus eccentric cells.

The quantitative model for neuronal firing, which I have used to account for variability in eccentric cell activity, can be extended to yield general conclusions about neuronal variability. The theory presented here for Limulus cells can be expressed in analytic form and the qualitative effects of varying the properties of the generator potential, temporal summation, and self-inhibition can be understood without computer simulations. Many neuron models require Monte Carlo methods to investigate the effect of varying parameters on fluctuations in impulse firing (Stein, 1967; Moore et al., 1966).

Conclusions

Periodicities. One generally applicable conclusion from the model is that periodicities in the underlying generator potential will be reflected in the variance spectrum (or, equivalently, in the autocorrelation) of the impulse rate. This kind of result is also indicated for cells of the cat

dorsal spino-cerebellar tract by Walloe's work (Walloe, 1968).

Inhibition. A second general prediction from this model is that any negative feedback like self-inhibition will tend to increase the relative variability, measured by the coefficient of variation (standard deviation/mean). This is because a negative feedback must reduce the effect of the maintained level of excitation compared to the effects of rapid fluctuations of excitation. This is strikingly illustrated by Limulus eccentric cells in which the coefficient of variation of the impulse rate is several times larger than the coefficient of variation of the generator potential.

This conclusion can be extended to include all kinds of inhibition, not merely self-inhibition, but the problem is subtle. I have investigated the effects of inhibition on variability and will present those results in Part II.

Adaptation. On the other hand, adaptation in size of the quantal responses of the Limulus eccentric cell, or adaptation of individual excitatory synaptic potentials, will reduce the coefficient of variation of the firing rate. This has already been shown by Stein (1967) for a computer model and inferred by H.B. Barlow and Levick (1969) from a neuron model very similar to ours. The Poisson scaler model of Barlow and Levick can be viewed as an integrate-and-fire device with a Poisson process as input. This means that synaptic potentials (or quantal responses) are assumed to be brief compared to impulse intervals, and are assumed to occur purely randomly in time. The interval distribution for such a model will depend on the ratio of the threshold for firing to the integral of a single synaptic potential (the number of quanta per spike). In fact, if we call this ratio S, the interval probability density function will be a gamma probability density of order $S-1$ of the form $\frac{1}{\tau(S-1)!}\left(\frac{t}{\tau}\right)^{S-1}e^{-t/\tau}$, with coefficient of variation $S^{-1/2}$. Barlow and Levick call S the quantum/spike ratio in their study of variability in retinal ganglion cells of the cat.

Diminution of unit synaptic potential size will increase S, other things being equal. This will tend to make firing more regular; in fact as the parameter S of a gamma density becomes larger the density function approaches a Gaussian probability density and its coefficient of variation decreases. In my experiment on light and dark adaptation in the Limulus eye, the same qualitative effect was present, namely, a shift to greater regularity of firing when quantal responses were diminished in size by light adaptation.

Such a simple version of the integrate-and-fire model will not explain all the complexities of variability and correlation in the retinal ganglion cells which Barlow and Levick studied, or in Limulus eccentric cells, or most other neurons. Self-inhibitory negative feedbacks at earlier stages in the nervous system will tend to increase the coefficient of variation in the firing rate of a neuron at a later stage in the nervous system. This will decrease the value of the apparent "quantum to spike ratio" in such a neuron. Barlow and Levick observed just this sort of effect in their experiments, when inhibition from the periphery of a receptive field increased the coefficient of variation of the firing in a retinal ganglion cell. With such a simple neuronal model they could not deal with problems like the correlation of impulse intervals, nor the magnitude of the effects of adaptation and inhibition on neuronal variability. These are the sort of more detailed, quantitative problems I have attempted to solve in this study of variability in eccentric cells.

Using the methods described here, one can understand the fluctuations in neuronal firing as resulting from temporal integration of excitatory and inhibitory synaptic potentials which are occurring randomly in time. From this vantage point the variability in neuronal activity is one example of the general case of filtered shot noise, a fundamental subject of the theory of stochastic processes.

PART II

THE EFFECTS OF NEURONAL INTERACTION ON VARIABILITY

PART II

INTRODUCTION

I have shown in Part I that, for Limulus eccentric cells, stimulated by spots of light which act as purely excitatory stimuli, the variability of neuronal discharge is caused by fluctuations of the generator potential in the eccentric cell. These generator potential fluctuations result from the inherent randomness of the arrival and absorption of photons.

As is the case in many other neurons, an eccentric cell can also be influenced by neuronal interaction; illumination of neighboring ommatidia in the Limulus eye causes inhibition of the impulse discharge of an eccentric cell (Hartline, Ratliff and Miller, 1963). This lateral inhibition is similar to postsynaptic inhibition in other nervous systems (Purple, 1964; Eccles, 1964; Kandel and Wachtel, 1968). The effects of inhibitory interaction on randomness in the impulse firing of the Limulus cells should be similar to the effects of inhibition on other neurons.

In Part II of the thesis, I will present results concerning the effects of lateral inhibition on randomness in impulse firing of eccentric cells. Because the interaction of excitatory and inhibitory influences within Limulus eccentric cells resembles integrative interaction in neurons of more complex nervous systems, the results presented here should be, to some extent, applicable to those neurons too. The time course, size, and rate of occurrence of excitatory and inhibitory postsynaptic potentials are very important in determining the properties of variability in impulse firing. These factors which influence variability will differ from animal to animal, and from cell to cell within the same animal. For this reason, it is obvious that details of the statistical properties of the activity of Limulus visual sensory neurons need not be identical to the characteristics of nerve cells performing

different functions in other animals. Nevertheless, there should be general usefulness to the methods of analysis, and the qualitative and quantitative conclusions, of this research on the stochastic component of neuronal response resulting from neuronal interaction.

Chapter 7

EXPERIMENTAL METHODS

Recording

These experiments were done mainly on single nerve fiber preparations from the horseshoe crab optic nerve. Techniques for Limulus optic nerve fiber recording have been described previously in this thesis (Chapter 2). In addition, one type of experiment was done with intracellular recording from an eccentric cell body. For this experiment I used the same technique and equipment for intracellular recording described in Chapter 2.

Experiments were also done on multiple fiber responses to light. For these experiments, dissection of the optic nerve stopped before the isolation of a single fiber. The activity of several nerve fibers was thereby recorded. A standard narrow pulse was produced for each nerve impulse recorded, with the use of pulse generator (Tektronix 161 unit). Coincidences were rare under the conditions used: total dead time of the pulse generator of 0.5 millisecond and pulse rates less than 200 adrians on the average. The pulses were fed to a four stage, single time constant (6 msec.) filter. This was done to restrict the bandwidth of the multiple fiber signal, so that it was less than the sampling rate of subsequent equi-spaced time samples. This procedure prevented distortion due to beating between the sampling rate and high frequency components in the multiple fiber signal. The smoothed multiple fiber voltage was sampled and stored in the CDC 160-A computer in the same way as, for instance, measurements of the generator potential (described in chapter 2); via the use of periodic samples by an a/d converter and a computer program which acquired and stored the samples for subsequent analysis.

Stimulus

For one part of this investigation, antidromic electrical stimulation of the optic nerve was used to produce lateral inhibition on a single fiber whose activity was monitored. This is a technique pioneered by Tomita (1958). The experimental method was very similar to that used by Lange (1965) in his study on the step response of lateral inhibition. The optic nerve was stimulated in air with a bipolar electrode made out of platinum wire. Brief pulses from a pulse generator (Tektronix 161) were passed through an isolation transformer and thence to the stimulating electrodes. The electric shocks produce volleys of antidromically conducted nerve impulses in most of the optic nerve fibers. Standard supramaximal shock values were 5 volts for 0.5 msec. The rate of supramaximal shocks was varied to produce larger or smaller amounts of inhibition.

A typical experiment proceeded as follows. A response of a single unit to a twenty second light stimulus was recorded. Then after two minutes the response of the same unit to an identical light stimulus was recorded while the steady antidromic electrical shocks were being produced. The alternating sequence, first control, then inhibited firing, was repeated five to ten times in order to obtain sufficient data.

In other experiments I measure the effect of naturally evoked lateral inhibition, i.e. lateral inhibition produced by neighboring spots of light. For these experiments the light stimulus on the test receptor was provided by a small single optical wave guide as described in chapter 2. At a nearby region of the horseshoe crab eye a bundle of light guides was aligned to stimulate a group of receptors. I attempted to place this larger inhibitory spot in order to get the maximum inhibitory effect. The inhibitory light was turned on at the same moment as the test light. On alternate runs the inhibitory light was left off, so that again there was a sequence, first control, then inhibited activity. This stimulus procedure was useful in case there was any long term drift in the preparation, since alternate runs as well as averages over all the runs could be compared.

Timing of stimuli was controlled by the programmed timer discussed in Chapter 2. Measurement of nerve impulse intervals, computation of impulse rate from pulse intervals, calculation of variance spectra -- all were performed as previously described (chapter 2).

Chapter 8

THEORETICAL BACKGROUND

As mentioned before, there is a fairly comprehensive mathematical model for the operation of Limulus eccentric cells. This model is based on the response of the cell to time-varying modulations of stimuli around their steady state level. A schematic diagram of the model is shown in Figure 8-1. The different component processes which determine the cell's response are labeled in the block diagram. These are: GENERATOR POTENTIAL, Frequency Modulation (FM), SELF INHIBITION, and, in addition, LATERAL INHIBITION. The first three components and their effects on firing rate variability have been discussed before (Chapter 4). In this section I will present the expected effects of lateral inhibition on the stochastic component of neural response. Then we can compare the observed results of experiment with these theoretical predictions.

Eccentric Cell Model

First, I will recapitulate the idea of the neuronal model which was discussed in Chapter 4. This is a review of how the eccentric cell functions, with reference to the block diagram of the model. The eccentric cell fires nerve impulses when the membrane of the cell is sufficiently depolarized. The membrane potential which influences the impulse firing site is labeled Σ in the block diagram; this represents the idea that it is a summing point for excitatory and inhibitory influences which are acting upon the cell. Depolarization of the membrane causes an impulse firing mechanism, labeled FM, to fire impulses at a rate proportional to the level of the depolarization. The behavior of the impulse firing mechanism to time-varying depolarization suggests that this process behaves as if it were integrating the membrane potential (or current through the membrane) until the integral exceeds a threshold at which time an impulse is fired.

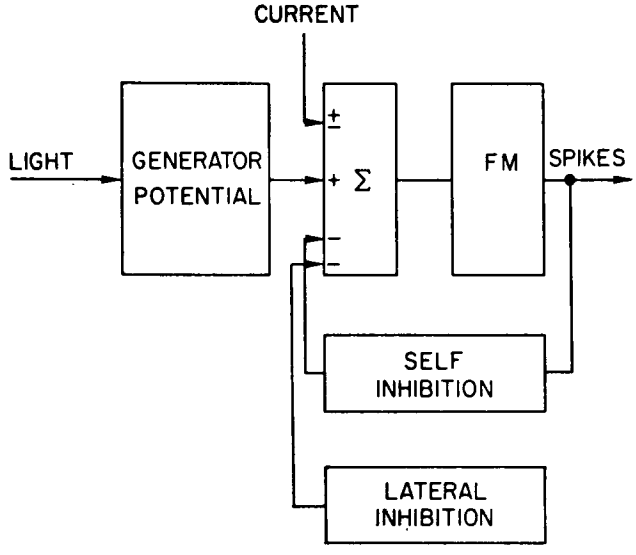

Figure 8-1. Model of Eccentric Cell with Lateral Inhibition. This is the same model as in Figure 4-1, with the addition of LATERAL INHIBITION which acts as another negative signal at the summing point. This figure taken from Dodge, Knight and Toyoda (1968b).

After each nerve impulse a single inhibitory synaptic potential is summed with the membrane potential, which reduces the level of depolarization. This is the phenomenon called self-inhibition, and is so labeled in the schematic diagram of Figure 8-1. The integrate-and-fire mechanism, and self-inhibition, shape the impulse firing response of the cell to any stimulation which affects the membrane potential, be it excitation by light or electric current, or inhibition from neighboring eccentric cells.

There are two external natural stimuli which can affect the membrane potential of the eccentric cell. The first is stimulation of the ommatidial photoreceptor by light. The many microscopic steps which lead to production of the membrane depolarization from photon absorption are included under the heading, GENERATOR POTENTIAL. The effect of fluctuations of the generator potential on neuronal variability has been extensively discussed in Part I. The second naturally occurring influence on the membrane potential is lateral inhibition.

Lateral inhibition of a given cell's activity is produced by the firing of nerve impulses by neighboring eccentric cells in the Limulus compound eye. Dodge, Knight and Toyoda (1968b) showed that the inhibitory synaptic potential resulting from a single nerve impulse in an inhibitory nerve fiber is biphasic, with a brief depolarizing phase and a prolonged inhibitory hyperpolarization. The time constant for decay of the lateral inhibitory synaptic potential is about one third of a second, as opposed to about one half a second for decay of a self-inhibitory synaptic potential. The unit lateral inhibitory postsynaptic potential can be considered to be the impulse response of the lateral inhibitory synapse. Toyoda measured both the impulse response and frequency response of the lateral inhibitory synapse (which are related to each other by the Fourier transform). The two functions are shown in Figure 8-2. The temporal characteristics of lateral inhibition play an important part in determining its effect on neuronal variability, as will be shown in the ensuing discussion.

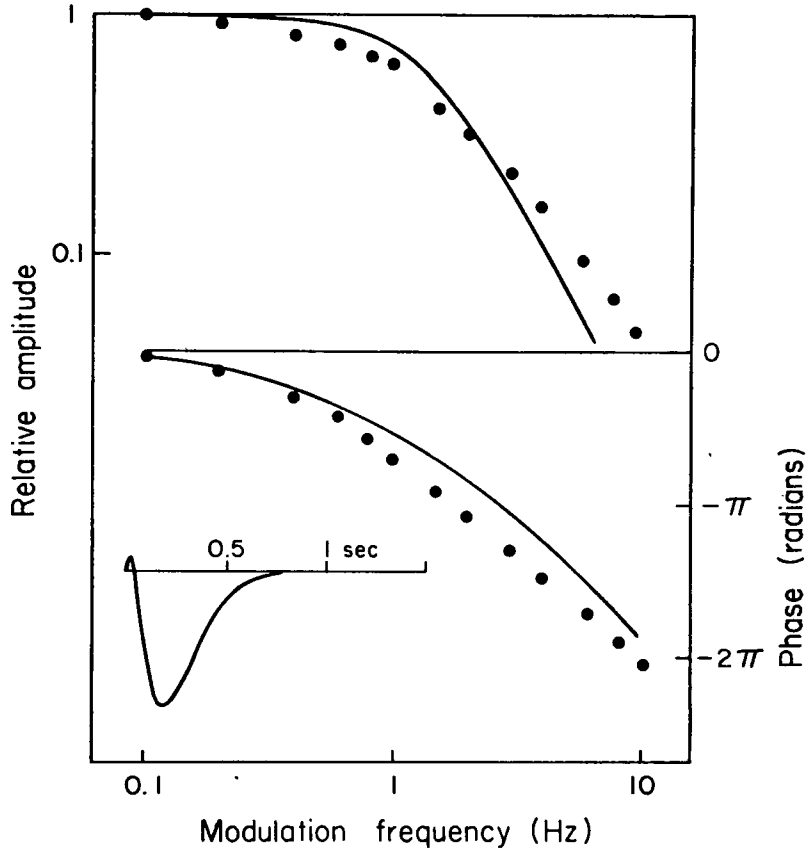

Figure 8-2. Lateral Inhibition - Frequency Response and Impulse Response. This shows the amplitude and phase of the frequency response of the lateral inhibitory synapse. The points were measured by imposing sinusoidal variations in the firing rate of fibers in the optic nerve and measuring the amplitude and phase of the lateral inhibitory potential. The smooth curve is a similar frequency response measured indirectly by observing modulations of the firing rate in response to modulated firing of inhibitory fibers in the optic nerve. The insert is the impulse response, the Fourier transform of the measured frequency response. This figure is adapted from Dodge, Knight and Toyoda (1968b).

Analogue Simulation

The effects of mixed excitation and inhibition are complex. To simulate these effects analogue eccentric cells have been designed by F.A. Dodge and constructed by the Rockefeller University Electronics Shop. The neuronal analogues can be used for imitating the behavior of Limulus eccentric cells in response to a variety of stimuli. They have been extremely useful in the study of variability in the firing rate.

These electronic devices conform to the block diagram model of the eccentric cell shown in Figure 8-1. There is a section of bandpass filters corresponding to the generator potential mechanism at the input of the analogue. The analogue possesses a summing point (Σ) which is the output of an operational amplifier. This summing amplifier has as inputs the "Generator Potential" section, the "Current" input, "Self Inhibition" and "Lateral Inhibition". The "Current" input receives continuous external voltages. The "Self Inhibition" input to the summing point is a negative, decaying, exponential for each pulse the analogue fires as a result of stimulation. The "Lateral Inhibition" input to the summing amplifier is a filtered pulse train from external pulse sources, for instance from other analogue eccentric cells.

The output of the summing operational amplifier is fed into a voltage-to-frequency converter which is an integrator circuit in series with a monostable, fast recovery, multivibrator. The output of the multivibrator is the impulse output of the analogue; these are the pulses which are also fed back through the "Self Inhibition" network to the summing amplifier, or to the "Lateral Inhibition" network of other analogue eccentric cells.

The strength of self inhibition and lateral inhibition is set by potentiometers which determine how much inhibition each impulse exerts.

Variance-Firing Rate Relation

The primary effect of inhibition is to lower the mean firing rate by reducing the average level of membrane depolarization. Such a change in the average rate of firing will affect the variance of the impulse rate. This can be viewed in two ways, in the time domain and the frequency domain. You can consider that the length of an interval between nerve impulses is an averaging interval; fluctuations of the membrane potential which are rapid enough to be averaged out during the pulse interval will have only a small effect on pulse firing variability -- the longer the interval, the more high frequency components will be averaged out. An alternative way of considering the same effect is to view the impulse firing mechanism as a filter which has a high frequency cutoff set by the mean firing rate. For instance, as the impulse rate decreases, the band-pass of the filter is narrowed, and, consequently, higher frequency components are filtered out from the impulse rate. Although the latter approach has some limitations, it has proved to be useful for obtaining analytical predictions of the effect of mean firing rate on firing variability.

The view of an integrate-and-fire mechanism as a linear filter must be applied with caution because of the phenomenon of side-bands or aliasing. These terms refer to the appearance of difference frequency components in the firing rate spectrum when the firing rate is modulated at frequencies which exceed half the mean firing rate (cf. Lange, 1965). As will be shown, aliasing does not affect the filter theory of the impulse firing mechanism, because it is an empirical fact that the side band components do not contribute much variance to impulse rate fluctuations in eccentric cells.

In order to compute the effect of changing the average impulse rate, we must consider the filtering action of the current-to-firing rate mechanism. This involves the contributions of the integrate-and-fire mechanism and self-inhibition. As previously mentioned in chapter 4, the frequency response for the overall process is

$$S\left(\frac{\omega}{2\pi}\right) = \frac{(1+K_s)\left(B\left(\frac{\omega}{2\pi}\right)\right)}{\left\{1+K_s\left[1 - \frac{(1/\tau_s f_o)(1-e^{-i\omega/f_o})}{(e^{1/\tau_s f_o}-1)(1-e^{-(\frac{1}{\tau_s}+i\omega)/f_o})}\right]\right\}}$$

$\omega = 2\pi f$

$S(f)$ depends on the mean firing rate f_o, and the self inhibitory coefficient K_s and time constant τ_s. $B(f)$ is the frequency response of the integrate-and-fire device and, as has been shown before, it also depends on f_o.

$$B(f) = \frac{1-e^{-2\pi i f/f_o}}{2\pi i f/f_o} = \frac{1-e^{-i\omega/f_o}}{i\omega/f_o}$$

The dependence of $S(f)$ on f_o is quite complex; however, I have been able to simplify the analytic expression for $S(f)$ by means of an approximation.

If we assume that $\tau_s f_o >> 1$, which is true over a useful range of the response of eccentric cells, then $e^{1/\tau_s f_o} \cong 1 + \frac{1}{\tau_s f_o}$ and we can write

$$S(f) = \frac{(1+K_s)(B(f))}{1 + K_s\left[1 - \frac{1-e^{-i\omega/f_o}}{1-e^{-\frac{1}{\tau_s f_o}}e^{-i\omega/f_o}}\right]}$$

$$1 - \frac{1-e^{i\omega/f_o}}{1-e^{-1/\tau_s f_o}e^{-i\omega/f_o}} \cong \frac{\omega/f_o}{\omega\tau_s(e^{i\omega/f_o}-1)}$$

$$\Rightarrow S(f) \cong \frac{(1+K_s)(B(f))}{1 + \frac{K_s}{1+B(-f)2\pi i f\tau_s}}$$

154923

In fact, $S(f)$ can be further approximated to yield

$$S(f) \approx \left(\frac{1 + K_s}{1 + \frac{K_s}{1 + 2\pi i f \tau_s}} \right) B(f)$$

where the dependence on the mean firing rate is entirely contained in $B(f)$. That (2) is a good approximation for $S(f)$ is shown in Figure 8-3. $S(f)$ is computed for nominal values of K_s and τ_s, and two values for f_o: 10 adrians (impulses/second) and 20 adrians. The amplitude and phase of the complex valued frequency response $S(f)$ are shown. The approximation for $S(f)$ based on equation (2) is plotted as points (+) on the solid curve. The latter is computed from the exact expression (1). The approximation is plotted as points rather than as a continuous curve because the approximation is good enough that if the curves were plotted for both the approximation and the full expression they would almost entirely coincide. What this approximation ignores is the discrete nature of self-inhibition, the fact that self-inhibitory potentials are phased to the firing of nerve impulses. That it is a good approximation for typical eccentric cell parameter values tells us that the self-inhibitory potentials are long enough that we can safely ignore the discreteness of self-inhibition at moderate firing rates.

The approximate expression for the frequency response is a product of two parts: $B(f)$ which depends on the mean firing rate, and a function (which I have called $I(f)$ in chapter 4) which does not depend on the average impulse rate. Therefore, the approximation allows us to predict the effect of changes in the mean rate on the stochastic component of impulse firing, in terms of the single function $B(f)$.

We can do this by considering the variance spectrum of the impulse rate, $\phi_N(f)$. As shown previously, the impulse rate

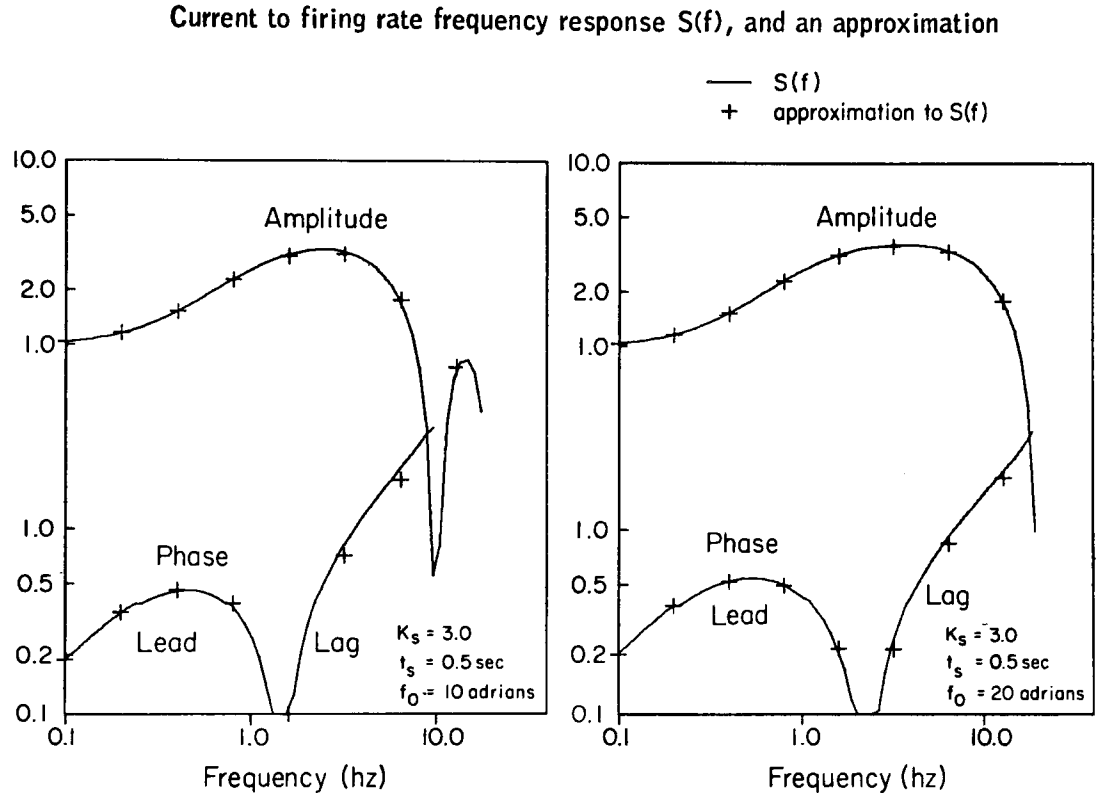

Figure 8-3. $S(f)$ and a Continuous Approximation. The theoretical current-to-firing rate frequency response is plotted as a continuous curve on log-log coordinates against frequency. A continuous approximation to $S(f)$, ignoring the discrete nature of the self-inhibitory hyperpolarizations, is plotted as crosses at several points on the curve. Values of the parameters are shown in the figure; K_S is the self-inhibitory coefficient, τ_S is the self-inhibitory time constant, f_o is the mean firing rate.

variance spectrum, $\phi_N(f)$, is produced by filtering the variance spectrum of the generator potential $\phi_G(f)$ through the current-to-firing rate mechanism. This is expressed in the following equation.

$$\phi_N(f) = |S(f)|^2 \cdot \phi_G(f)$$

Suppose the generator potential variance spectrum, $\phi_G(f)$, <u>remains the same</u> but the mean firing rate is changed. Call the original variance spectrum of the firing rate $\phi_{N1}(f)$, and the variance spectrum after the rate has been changed $\phi_{N2}(f)$. Using the approximation of equation (2) and the same notation as for the spectra, $B_1(f)$ for the original firing rate and $B_2(f)$ for the changed firing rate, we obtain the following expression.

$$\frac{\phi_{N2}(f)}{\phi_{N1}(f)} = \frac{|B_2(f)|^2}{|B_1(f)|^2}$$

or

$$\phi_{N2}(f) = \phi_{N1}(f) \cdot \frac{|B_2(f)|^2}{|B_1(f)|^2}$$

The variance can be calculated by integrating the variance spectrum with respect to frequency, f.

There is some difficulty with the application of equation (3). The denominator of the right hand side of that equation, $|B_1(f)|^2$ equals zero at $(f_a)_1$. This can make the variance, as calculated from (3), appear infinite if $\phi_{N1}(f)$ does not equal zero at $(f_a)_1$. It is perfectly legitimate to omit these spurious infinities in the calculation of the change in variance with firing rate.

Using equation (3), we can calculate the change in variance with average impulse rate. Given $\phi_{N1}(f)$ at a particular average firing

rate we can predict, from this linear model with a continuous approximation for self-inhibition, the variance, and shape of the variance spectrum, for any other mean firing rate. In practice, it is best to choose $(f_o)_1$ to be high, and calculate variance for lower mean impulse rates. The curve relating variance with the average impulse rate is shown in Figure 8-4. The variance increases monotonically but non-linearly with mean firing rate.

To check whether this method of calculating the variance-firing rate relation is theoretically correct, I simulated the problem with one of the neuronal analogues which have been discussed before. The generator potential variance spectrum $\phi_G(f)$ for the neuronal analogue was held the same while the firing rate was varied by varying a constant voltage which was added to the noisy voltage at the summing point of the analogue. The variance and variance spectrum were computed from the impulse rate produced by the analogue. The points marked with an x in Figure 8-4 are the values of the variance of the impulse rate at different average impulse rates. The analytically calculated curve for the variance-firing rate relation fits the simulation rather well; this indicates that the assumptions used for the calculation (linear filtering, continuous self-inhibition) are sufficiently applicable to enable us to calculate the effects of mean impulse rate on the variance of the impulse rate.

It is also interesting to consider the effect on the coefficient of variation of changes in average impulse rate. This relation is shown also in the graph of Figure 8-4. The curve is derived from the variance-firing rate curve and the points, marked with open circles, are computed for the same data from the neuronal analogue. While the variance decreases with decreasing impulse rate, it decreases more slowly than the mean rate: this results in a net increase in the fraction, standard deviation divided by the mean, which is the coefficient of variation of the impulse rate. This implies the conclusion that noise-free inhibition will decrease the variance of neural firing, while increasing the coefficient of variation.

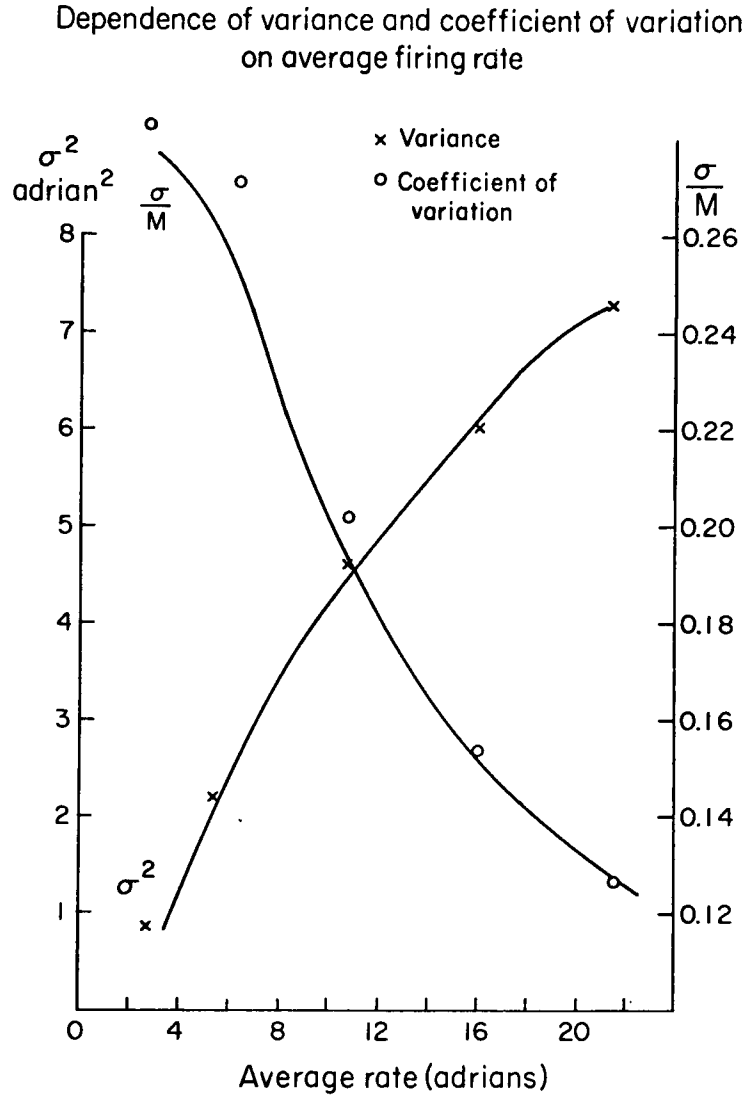

Figure 8-4. Variance (σ^2) and Coefficient of Variation (σ/m) as Functions of Mean Firing Rate. Variances at different firing rates of eccentric cell analogue are denoted X. The smooth curve for variance is calculated by filtering the firing rate spectrum at the average firing rate 16.1 adrians, according to the theory presented in the text. The coefficient of variation points, marked o, are calculated from the variance points, and the coefficient of variation curve from the variance curve. It is important to note the slope of these curves: positive for the variance, negative for the coefficient of variation.

While this conclusion is derived from theoretical calculation for a particular neural model, it may be generally applicable.

Lateral Inhibition As A Noise Source

Besides its effect on the average impulse rate, lateral inhibition must add some extra randomness to the membrane potential of the eccentric cell. This is because, during natural stimulation by light, a group of inhibitory cells fire nerve impulses asynchronously and to some extent randomly in time. The summed inhibitory synaptic potential fluctuates because of this effect. This inhibitory synaptic noise should be independent of the generator potential, so the variances of the two fluctuating components should add.

The characteristics of the summed inhibitory synaptic potential should depend on two factors: statistical properties of the occurrences of nerve impulses in inhibitory neurons, and the time course of the lateral inhibitory synaptic potentials.

The Point Process Underlying Lateral Inhibition. The point process which underlies the summed synaptic potential is a superposition of the impulse trains from each of the nerve fibers which have a synaptic effect. You can construct the superposed pulse train in the following manner. Whenever a pulse occurs on any of the converging presynaptic nerve fibers, assign a pulse to the superposed pulse train. Another way of looking at it is to consider the superimposed pulse train as the electrical record obtained by recording from all the presynaptic nerve fibers with the same electrode (with pulses recorded monophasically).

The variance spectrum of a pulse train (not the firing rate) is an important statistical measure for understanding the relation between the pulse train, a stochastic point process, and the noisy voltage produced by filtering the point process. The variance spectra for the pulse train of a single eccentric cell and for the superposition of many such pulse trains are shown in Figure 8-5. Because the firing of the cell is

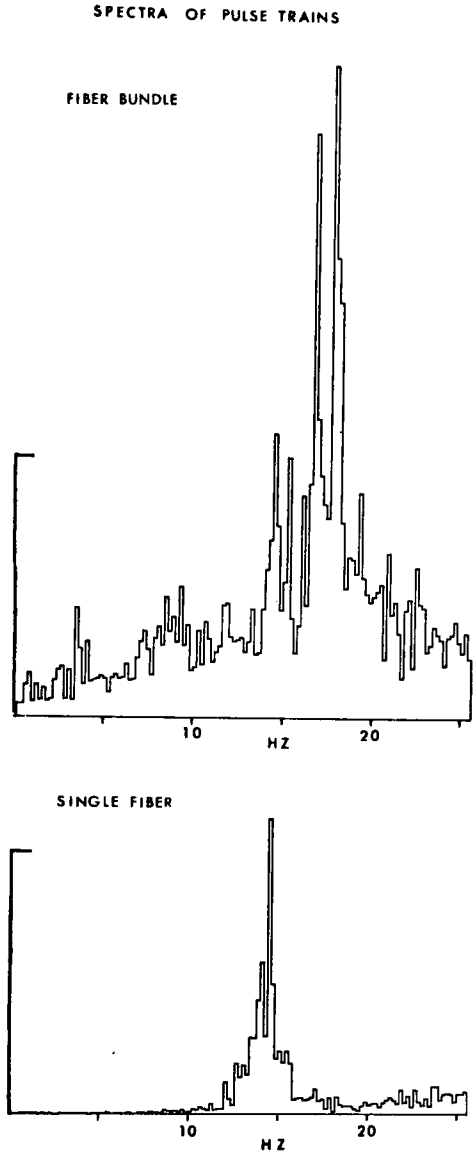

Figure 8-5. Variance Spectrum of Single Fiber's Pulse Train and for Multiple Fiber Pulse Train. This figure shows how peaking in the multiple fiber pulse train arises from regularity in the firing of individual nerve fibers. The single fiber, the spectrum of whose pulse train is shown in the lower graph, contributes to the firing of the fiber bundle. Therefore, the peak at 14.5 hz observed in the fiber bundle spectrum is contributed by the single fiber from the lower figure. Peaks at 7, 15.5, 17 and 18 hz presumably come from several other, regularly firing, single fibers.

fairly regular, with a coefficient of variation of only 0.15, the spectrum for the pulse train of the single fiber is peaked around a frequency equal to the mean firing rate. For the superposed point process, the spectrum is the sum of the spectra of the pulse trains from the individual fibers. There are peaks at frequencies equal to the mean rates of the fibers, and their harmonics, and wide band noise on account of the small variability in neuronal firing.

The response of the single fiber was recorded on one electrode and the multiple fiber firing was recorded on another electrode. The activity of the single fiber was also recorded on the electrode which recorded multiple fiber firing. So, in this case, you can see the spectrum of the pulse train of a single nerve fiber by itself and after superposition with several other pulse trains. The presence of the same peak in the variance spectrum of the superposed pulse trains as in the single fiber spectrum conforms to the theoretical expectation that superposition of pulse trains results in superposition of their variance spectra.

We can predict that the variance spectrum of the superimposed pulse train for Limulus nerve fibers will have peaks at the average firing rates of the individual fibers, and at higher harmonics of these average rates. It will therefore differ from a Poisson point process whose variance spectrum is a constant with frequency, i.e. white noise. This spectral peaking occurs in other nervous systems, e.g. the cat spinal cord (Wallø, 1968). It is a consequence of the regularity of presynaptic nerve impulse firing.

The Lateral Inhibitory Synapse as a Filter. The departure from purely random arrival of presynaptic nerve impulses has a major effect on the summed postsynaptic potential. The inhibitory potential, like all summed synaptic potentials, can be viewed as a filtered shot noise. The shots are the presynaptic nerve impulses and the filter is the synapse; the unit inhibitory postsynaptic potential is the impulse response of the synaptic filter. The shape of a typical lateral inhibitory postsynaptic

potential is shown in Figure 8-2; also shown in this figure is the frequency response of the lateral inhibitory synapse. The low pass characteristic of this filter tends to reduce high frequency periodic components in the summed inhibitory potential. As a result the summed inhibitory potential exhibits smaller fluctuations than it would if it were produced by filtering a Poisson point process through the same low pass filter.

This reduction in noise as a result of filtering out high frequency periodicities is illustrated in Figure 8-6. At the top of the figure two variance spectra are shown, one for a pulse train which is the superposition of several regularly firing nerve cells, the other for a Poisson pulse train of the same intensity (mean arrival rate of pulses) produced by a photomultiplier tube. Both have been passed through a filter with a high frequency cutoff around 12 hz. The variances of the two filtered shot noises produced in this manner are equal. The filter was wide enough not to significantly attenuate the periodic component of the multiple fiber point process. In the second row of this figure are spectra of the same two point processes filtered through a low pass filter with the same frequency response as a typical lateral inhibitory synapse (i.e. it had a frequency response like that shown in Figure 8-2). Samples from the simulated synaptic potentials produced in this way are illustrated in the bottom row of the figure. A striking difference is apparent between the amount of noise in the filtered multiple fiber spectrum and the filtered Poisson spectrum. Because there is much less variance at low frequencies in the multiple fiber pulse train compared to the amount at the peak, filtering the pulse train through a synapse which passes only low frequencies results in a large reduction in size of fluctuations. For the purely random pulse train, the variance is as great at low as at high frequencies and so the low frequency filtering does not reduce the variance as much.

Another consequence of the low pass character of the lateral inhibitory synapse is that whatever inhibitory fluctuations there are must be very low frequency fluctuations. So we expect to see additional low fre-

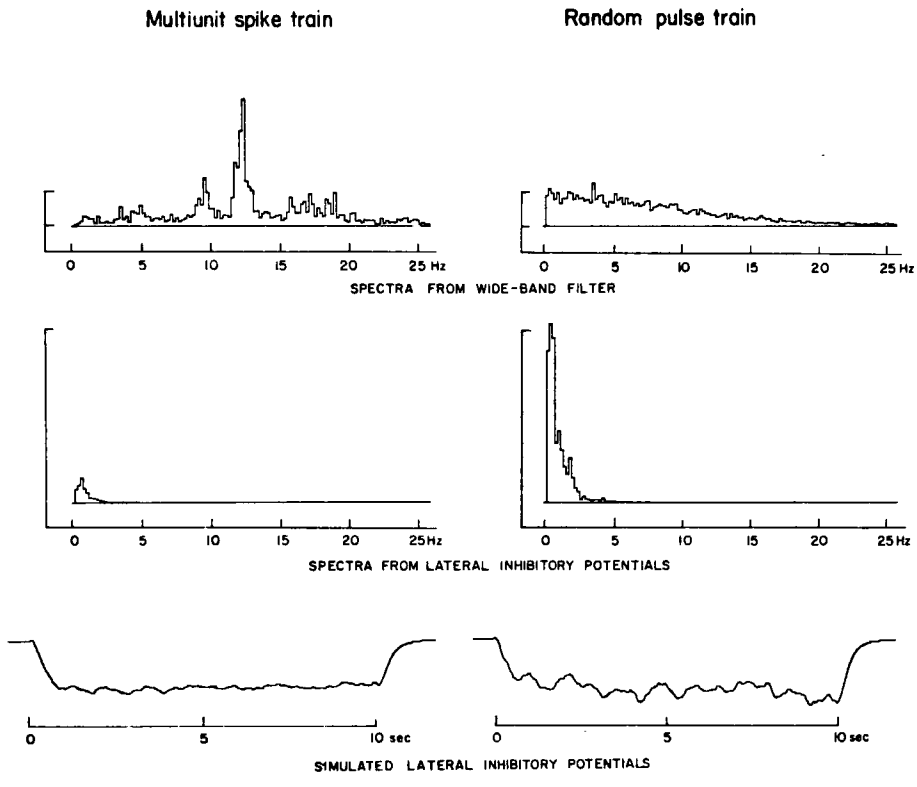

Figure 8-6. Filtered Multiple Fiber and Poisson Pulse Trains. Top two variance spectra are from pulse trains filtered through a wide band filter (time constant 6 msec). Below these are, respectively, the spectra and sample time function for the same two pulse trains filtered through a simulated inhibitory synapse. The vertical scale marks for the upper and lower spectra are the same.

quency components in the impulse rate variance spectrum in an eccentric cell which is influenced by lateral inhibition. If the lateral inhibitory synaptic potential should happen to be fast enough, and the average firing rates of the presynaptic, inhibitory nerve fibers were low enough, the periodic components in the inhibitory potential would significantly increase the variance of the impulse rate in the inhibited cell. But in the circumstances illustrated in Figure 8-6 the stochastic component added by lateral inhibition would be quite small and the major effect of inhibition would be exerted by its effect on the average impulse rate of the inhibited eccentric cell.

We can get definite predictions for this complicated phenomenon, the effect of inhibitory interaction on neuronal variability, by using the neuronal analogue of the eccentric cell. Typical neuronal firing in response to purely excitatory stimuli can be simulated (as described above). Then a good imitation of naturally occurring lateral inhibition can be produced by feeding into the inhibitory synapse a multiple fiber pulse train actually recorded from a Limulus eye.

The results of this analogue experiment are summarized in the impulse rate variance spectra of Figure 8-7. The control spectrum, characteristic of the firing which results from purely excitatory stimuli, shows the low frequency cutoff imposed by self-inhibition and the high frequency cutoff resulting from the inegrate-and-fire mechanism. The inhibited impulse rate spectrum shows an increase in the size of low-frequency components and a lower high frequency cutoff as a result of the reduction of average firing rate. If our model is correct, the same kind of change in the pattern of neuronal randomness should be observed in Limulus eccentric cells which are inhibited by light-evoked lateral inhibition. The observations of these effects are presented in the next chapter.

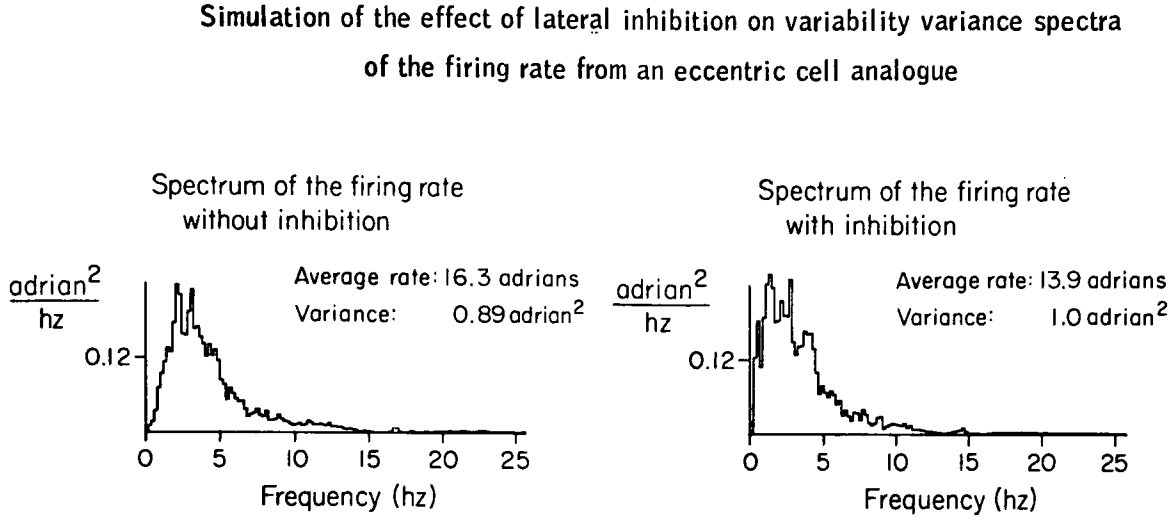

Figure 8-7. Control and Inhibited Variance Spectra - Prediction from Analogue Model. The variance spectrum of the inhibited cell has larger low frequency components in the variance, and a more abrupt high frequency cutoff because of the reduction in average firing rate. These spectra were calculated from data produced by the eccentric cell analogue.

Chapter 9

RESULTS

Effect of Reduction in Average Firing Rate

Inhibition produced by antidromic electrical stimulation reduces the variance of the impulse firing rate. When the antidromic electric shock rate is high enough, i.e. greater than 10/sec., the steady state summed inhibitory potential ought to be practically constant, with very small ripple at the shock rate. Therefore, the change in variance with "antidromic inhibition" should occur because of the effect on variance of changing the average impulse firing rate.

The data from such an experiment are displayed in Figure 9-1. Two sample records of impulse rate are shown: the lower record is control firing in response to a purely excitatory light stimulus, the upper record is firing in response to the same light stimulus while the cell is also undergoing steady inhibition elicited by antidromic electric shock of the optic nerve.

The variance of the antidromically inhibited firing rate is 60% of the variance of the control firing rate. This drop in variance is associated with a reduction in average impulse rate of 5.2 adrians. The magnitude of the variance reduction predicted by the filter model for the impulse firing mechanism is 59% of control. The agreement, both qualitatively and quantitatively, of the mathematical model with this experimental result is strong support for the theory.

What seems at first a simpler and more straightforward method for controlling the firing rate, namely d.c. current injection into the cell through a microelectrode, has proved to have more complicated effects than antidromic inhibition. This seems to occur because current injected at the cell soma level affects the nearby photoreceptor membrane while the inhibitory synaptic potential, which occurs at a point far from the photoreceptor, does not. The inhibitory potential occurs at the point of synaptic contact

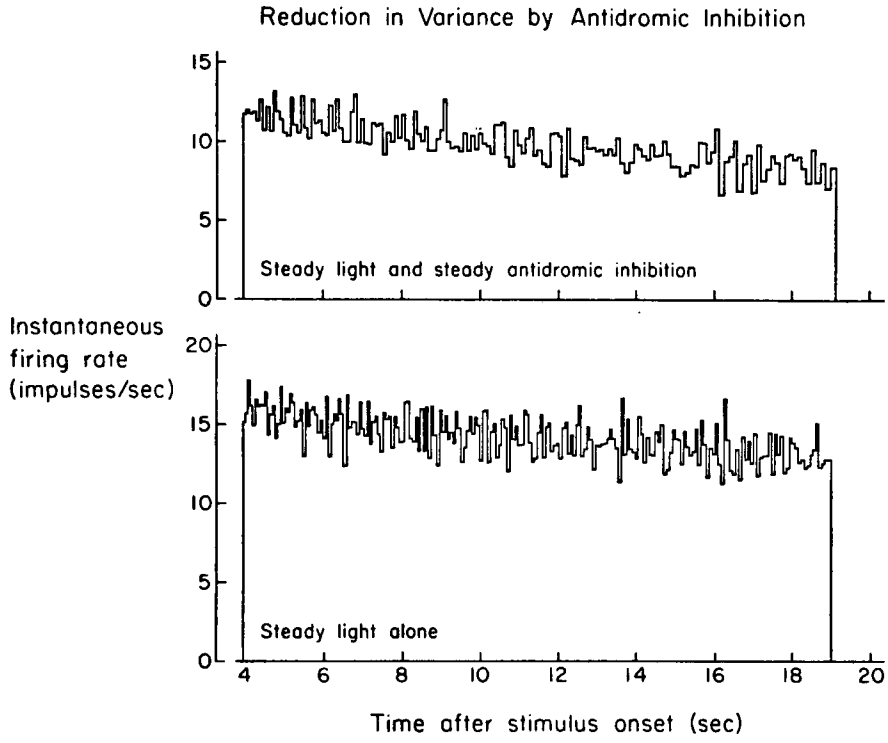

Figure 9-1. Data from the Experiment with Steady Inhibition Produced by Antidromic Electric Stimulation of the Optic Nerve. The lower record is a sample record from the response of the cell to excitation by light. The upper record is obtained by using the same excitatory stimulus while stimulating the optic nerve at a fixed rate of twenty per second to produce steady inhibition. The samples of data shown are the maintained component of the responses, the first four seconds of each responses having been omitted from the figure.

between eccentric cells, which point is close to the impulse firing mechanism and far from the cell soma and photoreceptor membrane (Purple, 1964).

It is a consistent finding that injected current has an effect on the variance of the firing rate which is the inverse of its effect on the average firing rate. For instance, a step of hyperpolarizing current will reduce the average firing rate in the response to a steady light. However, the variance of the firing increases under these conditions. This is just the opposite of what we would predict if the mean firing rate were the only factor affecting the variability of the firing rate.

However, it is possible to measure an effect of injected current on the generator potential. In one of the experiments which dealt with the effect of injected current on the firing rate, this measurement was accomplished. The experiment shows that the injected current influences the variance of the firing rate through its action on generator potential fluctuations. Depolarizing current reduces the variance, while hyperpolarization increases the variance of generator potential fluctuations. Quantitative aspects of this phenomenon are graphed in Figure 9-2. Plotted against current strength are firing rate variance and generator potential variance.

Such an effect of steady polarization on the generator potential should be expected since the generator potential seems to be caused by a light-triggered conductance increase. Nevertheless, these results underscore the importance of regarding the mathematical model of the eccentric cell only as a first approximation to the complexity of the living neuron. Under conditions of modulation around a steady state it is a perfectly adequate model. This experiment shows that steady state change in one of the parameters which determine the state of the cell can affect fluctuations of the firing rate in a nonlinear fashion. It also reveals another limitation of the simplified neural model -- the simple model is a lumped parameter model which does not take into account the

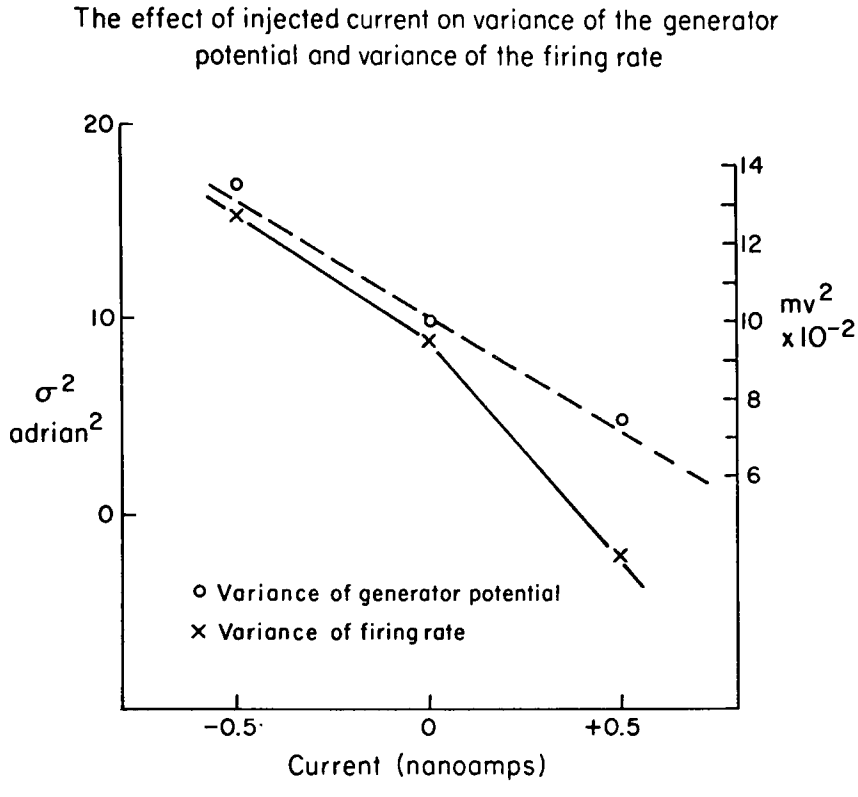

Figure 9-2. Variance of Firing Rate and Generator Potential as a Function of Injected Electric Current. The increase of variance with hyperpolarization and the decrease of variance with depolarization is clear, for both the generator potential, o, and the firing rate, x. The two vertical scales have been chosen to emphasize the similarity of the effect on generator potential and firing rate.

cable properties of the eccentric cell (a subject investigated by Purple, 1964; and Purple and Dodge, 1965). Since injected d.c. current exerts a complex influence on firing rate variability, I think the best experimental method for control of the firing rate alone is the use of antidromic electric shock applied to the optic nerve. The results of such experiments, described above, indicate that firing rate variance will change in the same direction as average firing rate, other things being equal.

Lateral Inhibition Produced By Light

Lateral inhibition produced by stimulating a neighboring group of receptors with light has a more complex effect than a mere reduction in average firing rate. A data record from an experiment which demonstrates this is shown in Figure 9-3. The firing rate of a Limulus optic nerve fiber is shown. At time zero a small light illuminates the test receptor. At four seconds a large spot of light stimulates a neighboring group of receptors and the test cell is inhibited by their activity. Both the pattern and magnitude of the cell firing rate variability is changed by the light-evoked inhibition. In this cell the variance of the firing actually increased while the cell was being inhibited.

The nature of the effects produced by lateral inhibition can be seen by examination of firing rate variance spectra. As discussed before, the shape of such a spectrum informs you about the pattern of firing rate randomness, and the area under the spectrum measures the total variance of the firing rate. Firing rate spectra for control and inhibited firing are shown in Figure 9-4 for two cells. The experiment was the standard paradigm for demonstration of naturally evoked lateral inhibition: a test light spot stimulated a single ommatidium and an inhibitory spot stimulated a neighboring group of ommatidia. The change in the shape of the variance spectra because of the presence of lateral inhibition is very much in agreement with the theoretical predictions advanced in chapter 8; to see this, compare Figure 9-4 with Figure 8-7.

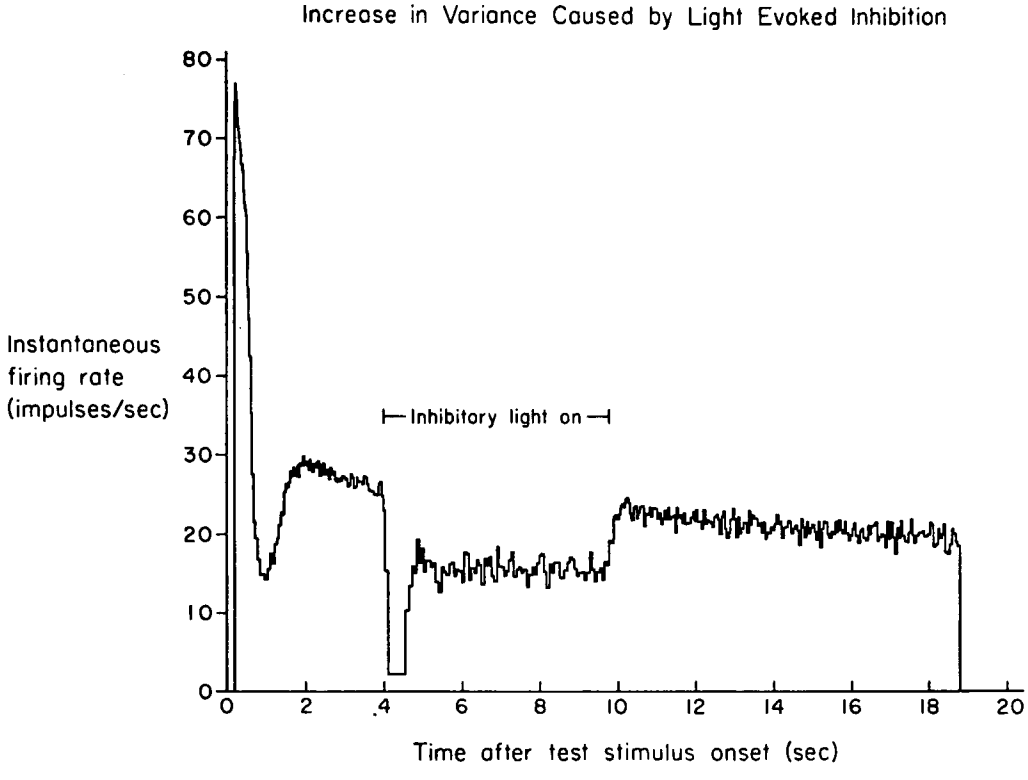

Figure 9-3. Lateral Inhibition Produced by Illumination of Neighboring Receptors. Shown is the response of an eccentric cell to excitatory stimulation by light, of nineteen second duration, and a superimposed inhibitory flash, of six second duration and starting four seconds after the onset of the excitatory stimulus. The variance of the maintained response is increased by the presence of inhibition (0.8 adrian^2 without inhibition, 1.2 adrian^2 with inhibition).

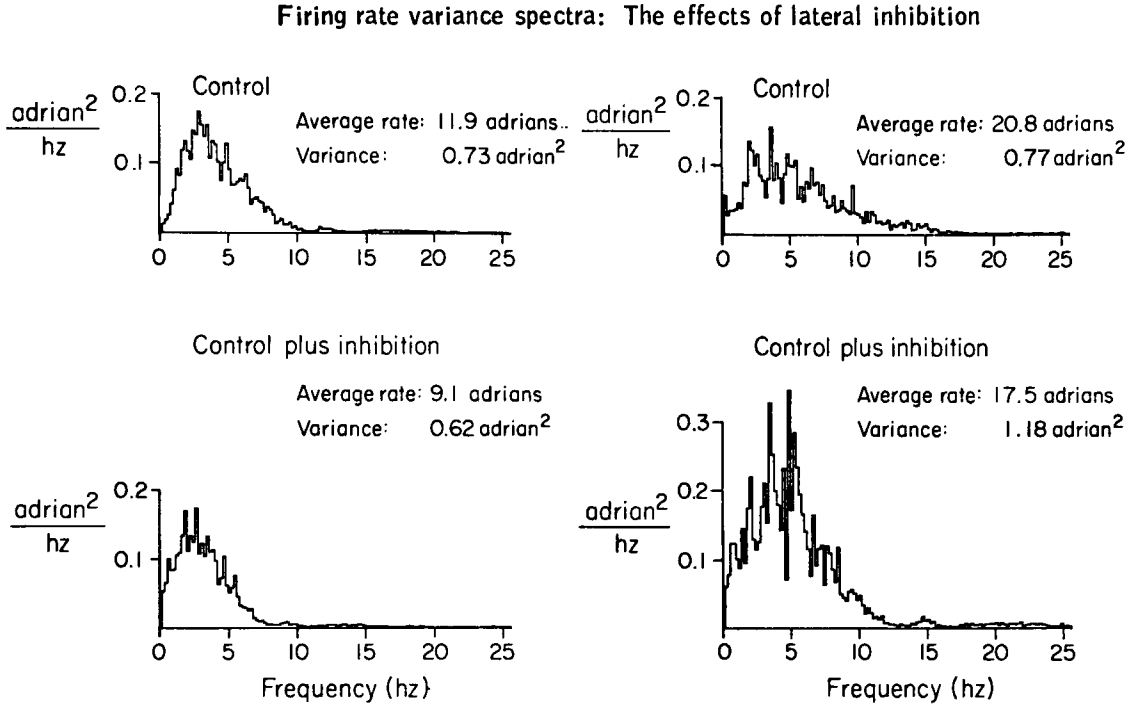

Figure 9-4. Firing Rate Spectra for Control and Inhibited Firing. Variance spectra are shown for two different cells. The Control spectra are from response of each cell to a purely excitatory stimulus (small steady light). The spectra labeled Control plus Inhibition are the response of the cell to the excitatory stimulus presented simultaneously with stimulus which evoked lateral inhibition (large neighboring spot of light). The inhibition leads to the presence of larger low frequency components in the spectrum and a more abrupt high frequency cutoff.

There is an apparent contradiction in the data from these two experiments, since in one case the variance increased during inhibition, and in the other it decreased during inhibition. This occurs because the naturally evoked inhibition produces two opposing influences on the variance. As discussed in Theoretical Background (Chapter 8), lateral inhibition tends to decrease variance by its reduction in the mean firing rate, and increase variance by adding an additional noise source to the membrane potential. These two opposing influences can sometimes result in a net increase in variance though more often the balance is on the side of a reduction in firing rate variance. Since these effects take place at opposite ends of the firing rate variance spectrum, they are clear to see in the spectra of Figure 9-4.

In both of these experiments, reduction of the average firing rate by inhibition (lengthening the average interval) tends to reduce the total variance by causing a filtering out of higher frequency components. In opposition to this effect, the added noise from inhibition should augment low frequency components in the membrane potential and these should be transmitted to the firing rate fluctuations. The presence of larger low frequency components in the inhibited firing rate variance spectra, compared to control firing rate spectra, is evident on inspection of Figure 9-4. The larger amount of variance added at the low frequency end of the impulse rate spectrum for the cell on the right hand side of the figure, and the wider bandwidth of the additional variance, are not completely explained by the experimental measurements I have been able to make. A conjecture which might explain the facts is that the average firing rates of the inhibitory nerve fibers was lower and the lateral inhibitory synaptic potentials decayed more rapidly than in the experiment on the left side of the figure. Most of my experiments on this particular topic were done with small spots, approximately 4 ommatidial diameters, and the intensities of the inhibitory spots were as bright as, or brighter than, the test spot. Under these conditions, the results most often resembled those depicted on the left hand side of Figure 9-4. With larger, dimmer inhibitory spots the

results should be significantly different from results obtained from small, bright spots, since the average firing rates of the inhibitory nerve fibers ought to be an important variable in determining how much "noise" lateral inhibition adds to the membrane potential (cf. Theoretical Background, Chapter 8). I have not yet done conclusive experiments to test this expectation.

The Relation Between Variance Spectrum And The Frequency Response N(f)

In chapter 5, proportionality was demonstrated between the variance spectrum of the impulse rate $\phi_N(f)$ and the squared amplitude of the light-to-firing rate frequency response $N(f)$. As explained in chapter 4, the frequency response $N(f)$ is determined from experiments on the neuronal response to sinusoidally modulated light. It is interesting to see how lateral inhibition affects the relation between sinusoidal flicker response and the variance spectrum of steady state fluctuations.

Figure 9-5 shows the results of an experiment designed to measure this effect. Lateral inhibition has clearly reduced the similarity between frequency response and variance spectrum. The variance spectrum of the firing of a single cell in response to a large spot of steady light intensity is shown. On the same scale is the squared amplitude of the response to sinusoidal modulation of the large spot of light. (A large spot was used to provide a substantial amount of lateral inhibition). The squared amplitude of the frequency response showed very marked peaking under these conditions of large spot illumination; this is the amplification phenomenon reported and explained by Ratliff, Knight et al. (1968, 1969). The frequency response with large spot illumination shows a steeper low frequency cutoff and greater peaking than with small spot illumination because lateral inhibition subtracts from the low frequency modulated response. However, because of a delay in the onset of the inhibition, it tends to enhance the modulated response at the peak frequency of the frequency response.

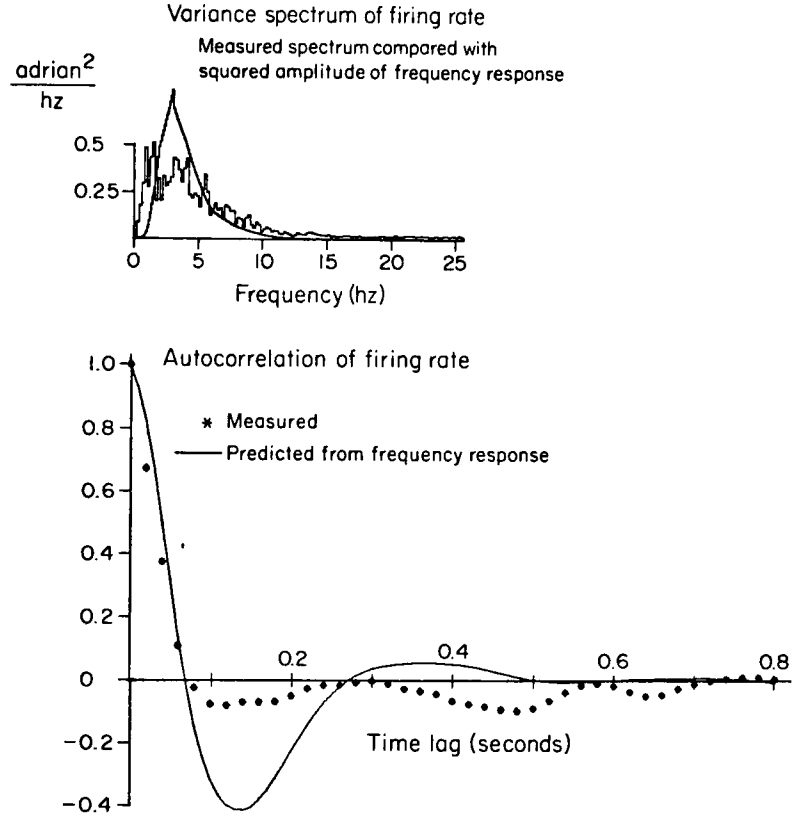

Figure 9-5. The relation between frequency response of the light-to-firing rate process and the variance spectrum: the effect of lateral inhibition. The frequency response of the impulse rate to large spot of light, sinusoidally modulated in intensity, is compared with the variance spectrum of the maintained firing to the same large spot of light at a constant intensity. The deviation between prediction and measurement is obviously large and significant at low frequencies, and at the peak frequency of the frequency response. Compare this with Figure 5-7.

The variance spectrum of the firing rate exhibits its characteristic features under the influence of lateral inhibition. In contrast to the spectral pattern of variability with small spot illumination, the spectrum is almost flat down to very low frequencies. The large spot produced a large inhibitory effect on the firing rate. This added substantial components to the low frequency end of the impulse rate spectrum, since lateral inhibition is a source of low frequency "noise" in the membrane potential. The variance spectrum of the impulse rate and $N(f)$ did not agree at all under stimulus conditions which produced a large inhibitory effect. What this means is that, in terms of the impulse rate, lateral inhibition reduces the signal-to-noise ratio* for low frequency modulated stimuli while maintaining, or even increasing, the signal-to-noise ratio for stimuli at the "tuning" frequency, the peak frequency of the frequency response. In the frequency response, lateral inhibition subtracts at low frequencies while, in the variance spectrum, it adds at low frequencies. A somewhat different situation occurs in the effect of lateral inhibition on the signal-to-noise ratio at the peak frequency of the frequency response. Lateral inhibition increases the magnitude of both $\phi_N(f)$ and $|N(f)|^2$ -- but produces a proportionally greater increase in $|N(f)|^2$.

---

* I am using the term signal-to-noise ratio in an unconventional way. By signal-to-noise ratio at a given modulation frequency f , I mean the ratio $|N(f)|/(\phi_N(f))^{1/2}$. This is the signal-to-noise ratio of the signal plus noise passed through a filter optimally tuned to the frequency f ; it is a measure of the optimal performance of which a system is capable. The usual definition of signal-to-noise ratio is, of course $|N(f)|/(\int_0^\infty \phi_N(f)df)^{1/2}$

Chapter 10

DISCUSSION

The Summed Lateral Inhibitory Synaptic Potential

The results of the experiments reported here show that fluctuations in the impulse rate of Limulus eccentric cells can be understood in terms of a linear neuron model. This mathematical model is a generalization of the Hartline-Ratliff equations to the case of time-varying excitation and inhibition. Using the method of spectral analysis, and applying it to the filtering of noise, you can calculate with reasonable accuracy the observed effects of excitatory and inhibitory stimuli on randomness in the firing rate. In Part I I have shown how this approach accounts for variability caused by purely excitatory stimuli. In this part of the thesis, I have extended the same theory to the case of mixed excitation and inhibition.

Inhibition, as theoretically predicted, tends to lower variance of the impulse rate by reduction of average impulse rate; at the same time, lateral inhibition tends to increase the variance by adding additional low frequency fluctuations to the membrane potential of the neuron. These competing effects more often result in a net decrease of firing rate variance. The coefficient of variation of the impulse rate, the standard deviation/mean of the impulse rate, is invariably increased by the introduction of lateral inhibition.

Given the shape of the firing rate variance spectrum for a purely excitatory stimulus, I can predict how much variance will be lost because of the reduction in firing rate resulting from lateral inhibition. Then the difference between the change in observed variance produced by naturally evoked inhibition and the variance calculated for "noise free" inhibition will yield an estimate of the added noise from the lateral inhibitory input. Since this noise will usually be confined to the very low end of the spectrum, you can assume that it will be filtered by the impulse coding mechanism to the same degree as the constant component of inhibition. The

square root of the difference between the two variances will be an estimate of the lateral inhibitory standard deviation. In this way I have calculated estimates of the coefficient of variation of the lateral inhibitory potential and compared its value with predictions based on simulations performed on the eccentric cell analogue. These calculations and the value from the simulation for the coefficient of variation of the summed inhibitory potential are given in Table 1. As is clear, lateral inhibition has a fairly small coefficient of variation. This is a result of the long duration of the lateral inhibitory synaptic potential and small size of that potential.

Comparison With Other Models

The qualitative findings of this entire investigation on eccentric cell firing should be useful in studying variability of other neurons. I think it is particularly important that even "noise-free" inhibition, whose only direct action is to lower the average impulse rate, will increase the coefficient of variation of the impulse rate. Noise from the random arrival of inhibitory potentials will add even more to the increase of relative variability.

There are several neuronal models in the literature which contain similar notions about the sources of neuronal variability as the eccentric cell model presented here (Stein, 1967; Gerstein and Mandelbrot, 1964; Geisler and Goldberg, 1966; Calvin and Stevens, 1968). Such models include the assumption that noise in the membrane potential, probably due to randomly arriving synaptic potentials, causes the randomness in neural firing. They differ somewhat in degree, not in kind, from models which involve triggering single impulses off presynaptic pulses arriving on several convergent channels -- the pooling models of Bishop *et al.* (1964), and ten Hoopen (1965). All of these models possess the same property that I mentioned above, namely that inhibition will tend to make the firing relatively more variable, other things being equal.

Table 1

Coefficient of Variation of the Lateral Inhibitory Potential

Analogue	Experiments
0.12	0.0
	0.14
	0.22
	0.28

These values for the coefficient of variation of the lateral inhibitory potential were calculated as follows. The variance, predicted from a variance-firing rate curve like Figure 8-4, was subtracted from the variance observed in the inhibited firing. This should be the variance added by the summed lateral inhibitory synaptic potential. Dividing the square root of this variance by the average reduction in the impulse rate produced by inhibition yields the coefficient of variation of the lateral inhibitory potential.

The "Analogue" value was calculated from the summed lateral inhibitory potential obtained by putting a multiple fiber pulse train into the neuronal analogue described in Chapter 8.

Gerstein-Mandelbrot Model. Let me support this assertion with reference to one particular neuron model, the one dimensional Gerstein-Mandelbrot model. As discussed in Chapter 1, Gerstein and Mandelbrot proposed that variability in neural impulse firing reflects the random bombardment of excitatory and inhibitory synaptic potentials on the neuron. In their model, Gerstein and Mandelbrot assume that synaptic potentials are very brief, that they are integrated up to a threshold, and that each individual synaptic potential is small so that many are required to sum up to the firing threshold. From the Gerstein-Mandelbrot model, the authors derived a probability density function for nerve impulse intervals, which is,

$$P(t) = K t^{-3/2} \exp\{-a/t - bt\}$$

K is a normalization constant. The parameter a measures the height of the threshold relative to the single synaptic potential, and the parameter b measures the difference between the rate of occurrence of excitatory synaptic potentials and the rate of occurrence of inhibitory synaptic potentials, i.e. the net rate of drift towards threshold. In order to understand the effects of introduction of additional inhibition into a neuron, one needs to be able to calculate the coefficient of variation of the Gerstein-Mandelbrot model. This reduces to the problem of calculating the first and second moments for the probability density function derived from the model. This problem, solved with the help of Bruce Knight, is treated in Appendix II.

The results of the calculations of Appendix II show that the coefficient of variation of the Gerstein-Mandelbrot model is $(4ab)^{-1/4}$. If a is kept constant, and b is decreased by introduction of more inhibition, the coefficient of variation will be increased. The quantitative dependence of coefficient of variation on inhibition is not the same for the Gerstein-Mandelbrot model as for the Limulus eccentric cell;

for instance, the Gerstein-Mandelbrot model assumes identical time constants for excitation and inhibition and the departure from this condition in the Limulus cells has significant effects on variability. Nevertheless, it is instructive to note that postsynaptic inhibition should have the same qualitative effect, an increase of the coefficient of variation, for two such different neural models as the Gerstein-Mandelbrot model and the Limulus eccentric cell linear model.

Since these models were devised to account for impulse firing data, the same conclusion can be generalized with caution to nerve cells. Inhibition will tend to make maintained neuronal discharge relatively more random than it would be without inhibition.

Although this conclusion is implicit in many of the theories of neuronal mechanisms, it has not been emphasized in previous discussions of this subject. The increased randomness due to postsynaptic inhibition may be a price the nervous system has to pay for the increased discriminability and tuning, both spatial and temporal, provided by inhibition (Ratliff, 1965; Ratliff et al., 1969).

However, randomness introduced by inhibition also may serve to mask signals which are not important physiologically. For instance, lateral inhibition in Limulus eccentric cells decreases the signal-to-noise ratio (as defined in the last chapter) for low frequency flicker. On the other hand it tends to maintain or increase the signal-to-noise ratio at the peak frequency of the frequency response. The Limulus eye is sharply tuned to a modulation frequency of approximately three hertz while the fluctuations introduced by inhibition are mainly concentrated in the frequency range from zero to one hertz. So, while variability may be designed into the Limulus nervous system, it still may not degrade the transmission of signals which are physiologically important. This may be a design principle in other nervous systems.

APPENDIX I

Removal of Slow Trends

In the statistical analysis of experimental data, there is often the problem of separating rapid fluctuations from very slow variations. This problem may arise in two ways. There may be a simple non-stationarity of the mean, due to linear drifts or slow oscillation of the mean value which can be described by deterministic functions. Alternatively, there may be stochastic linear drifts or slow oscillations. In either case, estimation of the variance and other such statistical measures may be distorted by the presence of these slow trends.

In my experiments this problem has been solved by editing the low frequency components of the variance spectrum from 0.2 to 0.3 hz, when it appeared that these components made the spectrum abnormally large at low frequency (see also, Shapley, 1969). Lanczos (1956) called this technique "smoothing in the large". (In his case, the slow component was desired and the higher frequency "noise" was removed; in the statistical case the situation is reversed and it is the "smooth" component which is removed so that the "noise" may be analyzed). The editing of the low frequency portion of the variance spectrum was done by extrapolating the spectrum from the region of one hertz down to two tenths of a hertz. For pulse rate spectra from eccentric cells, the extrapolation was sometimes easy, since there was theoretical support for the idea that the very low frequency components were small (Chapter 4). If the spectrum had low frequency components which were not expected to be very small, extrapolation of the spectrum to very low frequency involved some judgment about the relative size of the very slow components in the random process under study. This may sound somewhat inexact, but there is no completely exact method for dealing with very slow stochastic components.

Piecewise smoothing has been used by others to remove very low frequency components from random neural data (Firth, 1966; Ratliff, Hartline

and Lange, 1968). This involves calculation of a smoothed value by means of a moving average and subtraction of the fluctuation data from the smoothed value. This procedure acts as a filter on the data, removing low frequency components. The extent of filtering depends on the number of data points used in computing the moving average. For neuronal pulse rate data, it also depends on the mean pulse rate. Piecewise smoothing may remove low frequency components whether or not they are components of the process under study. In the study of Ratliff et al. (1968) moving average smoothing probably did not distort the low frequency components significantly, because typically the low frequency components in the variance spectrum of eccentric cells are small.

However, in Firth's study of crayfish stretch receptor neurons, he concluded there was a significant negative correlation between adjacent intervals in the steady firing of these cells. The observed negative correlation was an artifact of his smoothing procedure, which filtered out low frequency components and thereby introduced an artifactual negative correlation. I have investigated the maintained firing of crayfish stretch receptor using the technique of "smoothing in the large" and found no negative correlation in the firing of these cells. The variance spectrum of the impulse rate is flat down to very low frequency.

While piecewise smoothing will remove trend, it may also remove low frequency components of the process under study. Therefore, it should be used with prudence and a proper appreciation of the pitfalls involved. The use of spectral analysis for the problem of "detrending" is much safer, since it gives a relatively clear indication if there are noticeably large very low frequency components, and a relatively conservative method for estimating the proper contribution of very low frequency components to the variance spectrum.

Finally, I should add that most often in this investigation there was no need to remove low frequency trend. By inspection of the spectrum one could see no abnormally large low frequency components in the variance

spectrum. Under such circumstances, piecewise smoothing would have altered the low frequency portion of the spectrum; this procedure would have been an unnecessary distortion of the data. The avoidance of this error was made possible through the use of spectral analysis.

APPENDIX II

Moments of the Distribution Calculated From the Gerstein-Mandelbrot Model

(With the assistance of Bruce Knight)

The interval density function derived from the Gerstein-Mandelbrot one dimensional neural model, a random walk with drift in the diffusion limit, is,

$$P(t) = K\, t^{-3/2} \exp\left\{ -\frac{a}{t} - bt \right\}$$

This is equation (10) in the paper of Gerstein and Mandelbrot (1964). In order to calculate the moments of this density function e.g. $\overline{t}$, $\overline{t^2}$, $\overline{t^3}$... we have to evaluate integrals of the form

$$K \int_0^\infty dt \;\; t^{n-1/2} \exp\left\{ -\frac{a}{t} - bt \right\}$$

where $n = 0$ for the calculation of $\overline{t}$, $n = 1$ for calculation of $\overline{t^2}$, etc.

The problem is made more tractable by introduction of a parameter γ such that $t = \gamma\tau$ and $\gamma = \sqrt{a/b}$. Then, $a/t + bt = a/\gamma\tau + b\gamma\tau$

$= \sqrt{ab}\left(\frac{1}{\tau} + \tau\right)$. Also, let $\frac{z}{2} = \sqrt{ab}$

The integrals for calculation of the moments then become of the form

$$K\, \gamma^{n+1/2} \int_0^\infty d\tau \;\; \tau^{n-1/2} \exp\left\{ -\frac{z}{2}\left(\frac{1}{\tau} + \tau\right) \right\}$$

In particular we want to calculate this integral for $n = 0$, and $n = 1$, in order to obtain the first and second moments of the interval density function.

It is possible to show, using the substitution $\zeta = \frac{1}{\tau}$ that

$$\int_0^\infty d\tau \;\; \tau^{n-1/2} \exp\left\{-\frac{z}{2}\left(\frac{1}{\tau}+\tau\right)\right\} = \int_0^\infty d\tau \;\; \tau^{-n-3/2} \exp\left\{-\frac{z}{2}\left(\frac{1}{\tau}+\tau\right)\right\}$$

or, if we say $F_n = \int_0^\infty d\tau \;\; \tau^{n-1/2} \exp\left\{-\frac{z}{2}\left(\tau+\frac{1}{\tau}\right)\right\}$

then $F_n = F_{-n-1}$

and in particular, for $n = 0$

$$K \int_0^\infty d\tau \;\; \tau^{-1/2} \exp\left\{-\frac{z}{2}\left(\frac{1}{\tau}+\tau\right)\right\} = K \int_0^\infty d\tau \; \tau^{-3/2} \exp\left\{-\frac{z}{2}\left(\frac{1}{\tau}+\tau\right)\right\}$$

This implies that $\bar{t} = \gamma = \left(\frac{a}{b}\right)^{1/2}$. This result is derived from the fact that the calculation of the first moment differs from the normalization integral ($n = -1$) only by an extra factor of γ before the integral.

In order to calculate the second moment, $\overline{t^2}$, we must obtain a little deeper understanding of these integrals. By differentiating with respect to z it is possible to establish the identity

$$F_{n+1} = -2F_n' - F_{n-1}$$

where $F_n = \int_0^\infty d\tau \;\; \tau^{n-1/2} \exp\left\{-\frac{z}{2}\left(\frac{1}{\tau}+\tau\right)\right\}$

It is also possible to show that $F_0(z) = \sqrt{2\pi}\, e^{-z}/\sqrt{z}$

and to calculate from the above identity $F_1(z) = \frac{\sqrt{2\pi}}{\sqrt{z}}\, e^{-z}\left(1+\frac{1}{z}\right)$

This leads finally to the conclusion that

$$\overline{t^2} = \gamma^2\left(1+\frac{1}{z}\right)$$

where $z = 2\sqrt{ab}$ or

$$\overline{t^2} = \frac{a}{b}\left(1+\frac{1}{2\sqrt{ab}}\right)$$

The variance of the intervals is then

$$\sigma^2 = \overline{t^2} - \bar{t}^2$$
$$= \gamma^2\left(1 + \frac{1}{z}\right) - \gamma^2$$
$$= \gamma^2/z$$
$$= \frac{1}{2}\,\frac{a^{1/2}}{b^{3/2}}$$

and the coefficient of variation $\sigma/\bar{t}$ is

$$\frac{(\sigma^2)^{1/2}}{\gamma} = \frac{1}{(4ab)^{1/4}}$$

As Gerstein and Mandelbrot pointed out in their paper, when $b = 0$, i.e. when there is no net drift to threshold because inhibition on the average balances out excitation, the moments become infinite. A consequence they did not explore is the divergence of the coefficient of variation as net drift approaches zero.

BIBLIOGRAPHY

Adolph, A. 1964: Spontaneous Slow Potential Fluctuations in the Limulus Photoreceptor, J. Gen. Physiol., 48, 297-322.

Barlow, H.B., and Levick, W.R. 1969: Changes in the Maintained Discharge with Adaptation Level in the Cat Retina, J. Physiol., 202, 699-718.

Barlow, R. 1967: Inhibitory Fields in the Limulus Lateral Eye, Thesis, The Rockefeller University.

Barlow, R. 1969: Inhibitory Fields in the Limulus Lateral Eye, J. Gen. Physiol., 54, 383-396.

Bartlett, M.S. 1955: An Introduction to Stochastic Processes, Cambridge University Press, Cambridge.

Behrens, M., and Wulff, V. 1965: Light Initiated Responses of Retinula and Eccentric Cells of the Limulus Lateral Eye, J. Gen. Physiol., 48, 1081-1093.

Bicking, L.A. 1965: Some Quantitative Studies on Retinal Ganglion Cells, Thesis, Johns Hopkins University.

Biscoe, T.J., and Taylor, A. 1962: Irregularity of Discharge of Carotid Body Chemoreceptors, J. Physiol., 163, 4P-6P.

Bishop, P.O., Levick, W.R., and Williams, W.O. 1964: Statistical Analysis of the Dark Discharge of Lateral Geniculate Neurones, J. Physiol., 170, 598-612

Blackman, R.B., and Tukey, J.W. 1958: The Measurement of Power Spectra, Dover, New York.

Borsellino, A., Poppele, R., and Terzuolo, C. 1965: Transfer Functions of the Slowly Adapting Stretch Receptor Organ of Crustacea, Cold Spring Harbor Symp. Quant. Biol., 30, 581-586.

Buller, A., Nicholls, J., and Ström, G. 1953: Spontaneous Fluctuation in Excitability in the Muscle Spindle of the Frog, J. Physiol., 122, 409-418.

Bullock, T.H., and Horridge, G.A. 1965: Structure and Function of the Nervous Systems of Invertebrates, W.H. Freeman, San Francisco.

Burns, B.D. 1968: The Uncertain Nervous System, Arnold, London.

Calvin, W.H., and Stevens, C.F. 1968: Synaptic Noise and Other Sources of Randomness in Motoneuron Interspike Intervals, J. Neurophysiol., 31, 574-587.

Cooley, J., Lewis, P.A.W., and Welch, P.D. 1967: Historical Notes on the Fast Fourier Transform, IEEE Trans. on Audio and Electroacoustics, AU-15, 76-79.

Cox, D.R., and Lewis, P.A.W. 1966: The Statistical Analysis of Series of Events, Methuen, London.

Dodge, F.A. 1968: Excitation and Inhibition in the Eye of Limulus, in Optical Data Processing by Organisms and Machines, "Enrico Fermi", Varenna - in press.

Dodge, F.A., Knight, B.W., and Toyoda, J. 1968a: Voltage Noise in Limulus Visual Cells, Science, 160, 88-90.

Dodge, F.A., Knight, B.W., and Toyoda, J. 1968b: How the Horseshoe Crab Eye Processes Optical Data, IBM Research, RC 2248 (#11117).

Eccles, J.C. 1964: The Physiology of Synapses, Academic Press, New York.

Feller, W. 1957: An Introduction to Probability Theory and Its Applications, Wiley, New York.

Firth, D.R. 1966: Interspike Interval Fluctuations in the Crayfish Stretch Receptor, Biophysical J., 6, 201-216.

Fuortes, M.G.F. 1959: Initiation of Impulses in Visual Cells, J. Physiol., 148, 14.

Geisler, C.D., and Goldberg, J. 1966: A Stochastic Model of the Repetitive Activity of Neurons, Biophysical J., 6, 53-70.

Gerstein, G.L., and Mandelbrot, B. 1964: Random Walk Models for the Spike Activity of a Single Neuron, Biophysical J., 4, 41-68.

Goldberg, J., Adrian, H., and Smith, F. 1964: Response of Neurons in the Superior Olivary Complex of Cat to Acoustic Stimuli of Long Duration, J. Neurophysiol., 27, 706-749.

Harmon, L.D., and Lewis, E.R. 1966: Neural Modeling, Physiol. Rev., 46, 513-591.

Hartline, H.K., and Graham, C.H. 1932: Nerve Impulses from Single Receptors in the Eye, J. Cell. Comp. Physiol., 1, 277-295.

Hartline, H.K., and McDonald, P.R. 1947: Light and Dark Adaptation of Single Photoreceptor Elements in the Eye of Limulus, J. Cell. Comp. Physiol., 30, 225-253.

Hartline, H.K., and Ratliff, F. 1957: Inhibitory Interaction of Receptor Units in the Eye of Limulus, J. Gen. Physiol., 40, 357-376.

Hartline, H.K., Wagner, H., and MacNichol, E.F. 1952: The Peripheral Origin of Nervous Activity in the Visual System, Cold Spring Harbor Symp. Quant. Biol., 17, 125-141.

Jenkins, G., and Watts, D. 1968: Spectral Analysis and its Applications, Holden-Day, San Francisco.

Junge, D., and Moore, G. 1966: Interspike-Interval Fluctuations in Aplysia Pacemaker Neurons, Biophysical J., 6, 411-434.

Kandel, E., and Wachtel, H. 1968: The Functional Organization of Neural Aggregates in Aplysia, in Physiological and Biochemical Aspects of Nervous Integration, F.D. Carlson, Ed., Prentice-Hall, New Jersey.

Katz, B. 1939: Electric Excitation of Nerve: A Review, Oxford Univ. Press, London.

Kiang, N. 1965: Discharge Patterns of Single Fibers in the Cat's Auditory Nerve, M.I.T. Press, Cambridge, Mass.

Knight, B. 1969: Frequency Response for Sampling Integrator and for Voltage to Frequency Converter, in Systems Analysis in Neurophysiology. (Notes from conference held at Brainerd, Minn., June 1969).

Lanczos, C. 1956: Applied Analysis, Prentice-Hall, New York.

Lange, D. 1965: Dynamics of Inhibitory Interactions in the Eye of Limulus: Experimental and Theoretical Studies, Thesis, The Rockefeller Institute.

Lange, D., Hartline, H.K., and Ratliff, F. 1966: The Dynamics of Lateral Inhibition in the Compound Eye of Limulus, in The Functional Organization of the Compound Eye, C.G. Bernhard, Ed., Pergamon Press, New York.

MacNichol, E.F. 1956: Visual Receptors as Biological Transducers, in Molecular Structure and Functional Activity of Nerve Cells, Amer. Inst. Biol. Sci. publication # 1.

Millecchia, R., and Mauro, A. 1969a: The Ventral Photoreceptor Cells of Limulus. II. The Basic Photoresponse, J. Gen. Physiol., 54, 310-330.

Millecchia, R., and Mauro, A. 1969b: The Ventral Photoreceptors of Limulus. III. A Voltage Clamp Study. J. Gen. Physiol., 54, 331-351.

Moore, G.P., Perkel, D., and Segundo, J. 1966: Statistical Analysis and Functional Interpretation of Neuronal Spike Data, Ann. Rev. of Physiol., 28, 493-522.

Parzen, E. 1962: Stochastic Processes, Holden-Day, San Francisco.

Purple, R., 1964: The Integration of Excitatory and Inhibitory Influences in the Eccentric Cell of the Eye of Limulus, Thesis, The Rockefeller Institute.

Purple, R., and Dodge, F.A. 1965: The Interaction of Excitation and Inhibition in the Eccentric Cell in the Eye of Limulus, Cold Spring Harbor Symp. Quant. Biol., 30, 529-537.

Ratliff, F. 1965: Mach Bands: Quantitative Studies on Neural Networks in the Retina, Holden-Day, San Francisco.

Ratliff, F., Hartline, H.K., and Lange, D. 1968: Variability of Interspike Intervals in Optic Nerve Fibers of Limulus: Effect of Light and Dark Adaptation. Proc. Nat. Acad. Sci., 60, 464-469.

Ratliff, F., Hartline, H.K., and Miller, W.H. 1963: Spatial and Temporal Aspects of Retinal Inhibitory Interaction, J. Opt. Soc. Am., 53, 110-120.

Ratliff, F., Knight, B.W., and Graham, N. 1969: On Tuning and Amplification by Lateral Inhibition, Proc. Nat. Acad. Sci., 62, 733-740.

Ratliff, F., Knight, B.W., Toyoda, J., and Hartline, H.K. 1967: Enhancement of Flicker by Lateral Inhibition, Science, 158, 392-393.

Rice, S.O. 1944: Mathematical Analysis of Random Noise, Bell Tel. J., 23, 282.

Schoenfeld, R.L., and Milkman, N. 1964: Digital Computers in the Biological Laboratory, Science, 146, 190-198.

Shannon, C.E., and Weaver, W. 1949: The Mathematical Theory of Communication, Univ. of Illinois Press, Urbana.

Shapley, R. 1969: Fluctuations in the Response to Light of Visual Neurones in Limulus, Nature, 221, 437-440.

Stein, R.B. 1967: Some Models of Neuronal Variability, Biophysical J., 7, 37-68.

Stein, R.B., and Matthews, P.B.C. 1965: Differences in Variability of Discharge Frequency Between Primary and Secondary Muscle Spindle Afferent Endings of the Cat, Nature, 208, 1217-1218.

Stevens, C.F. 1964a: A Quantitative Theory of Neural Interaction: Theoretical and Experimental Investigations, Thesis, The Rockefeller Institute.

Stevens, C.F. 1964b: Letter to the Editor, Biophysical J., 4, 417-419.

Tomita, T. 1958: Mechanism of Lateral Inhibition in the Eye of Limulus, J. Neurophysiol., 21, 419-429.

Verveen, A.A., and Derksen, H.E. 1965: Fluctuations in the Membrane Potential of Axons and the Problem of Coding, Kybernetik, 2, 152-160.

Wallø e, L. 1968: Transfer of Signals Through a Second Order Sensory Neuron, Thesis, University of Oslo.

Waterman, T.H., and Wiersma, C.A.G. 1954: The Functional Relation Between Retinal Cells and Optic Nerve in Limulus, J. Exp. Zool., 126, 59-86.

Welch, P.D. 1967: The Use of Fast Fourier Transform for the Estimation of Power Spectra: A Method Based on Time Averaging Over Short, Modified Periodograms, IEEE Trans. on Audio and Electroacoustics, AU-15, 70-73.

Werner, G., and Mountcastle, V.B. 1965: Neural Activity in Mechanoreceptive Cutaneous Afferents: Stimulus-Response Relations, Weber Functions, and Information Transmission, J. Neurophysiol., 28, 359-397.

Wolbarsht, M., and Yeandle, S. 1967: Visual Processes in the Limulus Eye, Ann. Rev. Physiol., 29, 513-542.

Yeandle, S. 1957: Studies on the Slow Potential and the Effects of Cations on the Electrical Responses of the Limulus Ommatidium (With an Appendix on the Quantal Nature of the Slow Potential), Thesis, Johns Hopkins University.